CRANFIELD UNIVERSITY

Philani Ncube

Tertiary treatment of wastewater using multimedia filtration for solids removal

School of Water, Energy and Environment (SWEE)
Research Degree

PhD
Academic Year: 2012 - 2015

Supervisor: Prof. Peter Jarvis
Dr Marc Pidou
November 2015

CRANFIELD UNIVERSITY

School of Water, Energy and Environment (SWEE)
Research Degree

PhD

Academic Year 2012 - 2015

Philani Ncube

Tertiary treatment of wastewater using multimedia filtration for solids removal

Supervisor: Prof. Peter Jarvis
Dr Marc Pidou
November 2015

This thesis is submitted in partial fulfilment of the requirements for the degree of PhD

ABSTRACT

The tightening of wastewater discharge standards for environmental protection and the increasing requirements for wastewater reuse have pushed for further tertiary treatment of wastewater to remove pollutants including suspended solids. This thesis explores the process science behind the removal of suspended solids from wastewater secondary effluent with the aim of improving the process for high quality effluent and efficient operation. Treatment plants receive diurnal flows and wastewater quality which challenges the production of a consistent compliant quality which meets reuse or discharge standards to receiving water bodies. A pilot-scale quadruple media filter was operated at the Cranfield Sewage Works to investigate the removal of suspended solids from secondary treated wastewater effluent under controlled and variable hydraulic loading rate, solids concentration and different wastewater characteristics. To measure the solids removal and operational performance of the filter, total suspended solids, turbidity, particle size analysis, zeta potential, headloss and temperature were measured under different operational conditions such as wastewater hydraulic loading rate, pH, solids concentration and filter depth.

The media materials were examined to determine how they could be used to improve process performance and yield improved predictions in the application of filter models. A new method was developed for measuring the sphericity of media grains which improves the application of filter theory models to irregular shaped media grains. The method measured accurately the sphericity of glass spheres as 1.01 ± 0.02; the determined sphericity values correlated well with the measured headloss through filter media beds. The organic matter in the wastewater masked the media surface charge characteristics through coating on the media surface. Aggregation and deposition of wastewater solids was found to be most efficient near neutral pH. Adjustment of operational conditions were also explored. The solids removal efficiency of the filter varied inversely with an increase in hydraulic loading rate. However, multiple media layers reduced the negative impact of increased hydraulic loading rate and moderated headloss development. Particle retention was predominantly in the first 0.1 m depth of the

filter, with further increases in filter depth producing marginal performance improvements whilst the headloss developed more quickly, reducing filter run times and wastewater throughput. While the specific deposit increased with rising influent concentration, the solids removal efficiency reduced. Thus, for an increase in the influent solids concentration of 10 mgL^{-1}, the specific deposit increased by a factor of 1.2 while the removal efficiency decreased by an average factor of 0.9. Thus, the effluent deteriorates with increase in influent concentration while the filter holds more solids.

Keywords:

Wastewater, depth filtration, granular media, porous media, multimedia, surface charge, zeta potential, particle size, shape, aggregation, deposition, hydraulic loading rate, flowrate, pressure drop, headloss, digital image processing (DIP), tertiary, secondary effluent, suspended solids, concentration

ACKNOWLEDGEMENTS

Firstly, a massive thanks to Peter Jarvis for being a fantastic supervisor throughout my research. Thanks also to Marc Pidou for pushing me the extra mile since joining the team. The expertise and guidance you both gave me was unparalleled.

I'm grateful for the funding from EPSRC and Bluewater Bio Ltd, and most of all the invaluable input and time Dr Garry Hoyland, Dr Caroline Xun Huo and Richard Harnett gave to this project.

I am thankful to the pilot hall and laboratory staff which was my home away from home, all your support is well appreciated.

I would like to offer my gratitude to all those I have not mentioned who have helped me throughout this project.

I feel truly privileged for having had this opportunity to study at a late stage of my life and for everything it has provided me and the great people I have meet in pursuit of this expedition, thank you all.

Most of all, thanks to my family for bearing with me during this period.

TABLE OF CONTENTS

LIST OF FIGURES

LIST OF TABLES

LIST OF EQUATIONS

LIST OF ABBREVIATIONS

APHA	American Public Health Association
ASTM	American Society for Testing and Materials
AWWA	American water works association
BOD	Biological oxygen demand
CMOS	Complementary metal oxide semiconductor
COD	Chemical oxygen demand
DIP	Digital image processing
DLVO	Derjaguin-Landau-Verwey-Overbeek
EDL	Electric double layer
ES	Effective size
GAC	Granular activated carbon
HLR	Hydraulic loading rate
IEP	Isoelectric point
M	Molar
NTU	Nephelometric Turbidity Unit
NHL	Normalised Headloss
PSD	Particle size distribution
pzc	Point of zero charge
RT Model	Rajagopalan and Tien (1976) Model
STW	Sewage Treatment Works
TE Model	Tufenkji and Elimelech (2004) Model
TSS	Total suspended solids
UC	Uniformity coefficient
WEP	Water Environment Federation

Yao Model	Yao et al. (1971) Model
ZP	Zeta potential
2D	2 Dimensions
3D	3 Dimensions

LIST OF NOTATIONS

A	Polygon Area
A_{eq}	Equivalent area
A_i	Area of i^{th} particle
C	Effluent concentration
C_0	Influent concentration
D	Diffusivity
d10, d50, d90	Particle diameter of 10^{th}, 50^{th}, 90^{th} percentile size
d_{eq}	Equivalent diameter
d_p	Suspension particle diameter
d_m	filter media diameter
d_{min}	Minimum diameter
d_{mean}	Mean diameter
d_{max}	Maximum diameter
$d_{rms.d}$	Root mean square deviation
F_f	Frictional force
F_{Hydro}	hydrodynamic drag force
F_l	hydrodynamic lifting force
F_T	Net tangential force
F_{DL}	Double layer force
F_v	London van der Waals force
H	Hamaker constant
K_0	Carman shape factor
$K_0(L_e/L)$	Kozeny-Carman constant
K_p	Coefficient of permeability

κ_k	Kozeny coefficient
k_l	Coefficient of lifting force
k_f	Coefficient of sliding friction
L	Filter depth
L_e/L	Tortuosity factor
M	Total mass of n particles
n	Number of particles
P	Perimeter
Re	Reynolds number
S(= A/V)	specific surface area, where A is the total surface of grains and V is bulk volume of the filter bed
S_F	Shape factor
p	$(1-\varepsilon)^{1/3}$
w	$2-3p+3p^5-2p^6$
A_s	$2(1-p^5)/w$
u	filtration flow velocity
α	Attachment efficiency
δ	Particle-media separation distance
ε_0	Clean bed porosity
ε	Filter bed porosity
η	Transport coefficient
κ	Debye reciprocal double layer thickness
λ	Filter coefficient
Λ	Thickness determinant
μ	Dynamic viscosity
v	Kinematic viscosity

ξ	Zeta potential
ξ_g	Media zeta potential
ξ_p	Particle zeta potential
π	pi
ρ	Water density
σ	Bulk specific deposit
ψ	Filter media sphericity
ϵ_0	Permittivity of free space
ϵ_r	Relative permittivity

1 Introduction

1.1 Background

Increased environmental awareness has driven improvements in the quality of treated wastewater before it is discharged into receiving waters or reused. Implementation of tighter discharge standards from regulatory bodies such as the Environment Agency in England and Wales, and the increased requirement for wastewater reuse, requires higher quality treated wastewater, including better removal of suspended solids (Hamoda, Al-Ghusain and Al-Jasem, 2004; te Poele *et al.*, 2005; Michael *et al.*, 2015). The high solid concentration in wastewater secondary effluent challenges conventional sand filters as it results in rapid development of a terminal headloss (Aronino *et al.*, 2009). As an alternative, multimedia configurations using two, three or even four layers of different sized media (such as sand, anthracite, alumina and magnetite) delay the onset of limiting headloss, improving the filtration of secondary wastewater effluent (Monk, 1987).

Perception has softened on treated wastewater, it is no longer viewed as a disposal material into rivers and oceans, but an invaluable resource to alleviate water scarcity in arid and semi-arid regions and to augment natural fresh water bodies (Hamoda, Al-Ghusain and Al-Jasem, 2004). There are many wastewater reuses including agricultural and landscape irrigation such as irrigation of golf courses or public parks (De Leon *et al.*, 1986; Adin and Elimelech, 1989; Hamoda, Al-Ghusain and Al-Jasem, 2004; Michael *et al.*, 2015), direct potable water supply after extensive treatment (te Poele *et al.*, 2005), renewable resource such as in groundwater recharge (Hamoda, Al-Ghusain and Al-Jasem, 2004), bridging water supply-demand deficit through non-potable urban use such as toilet flushing or industrial cooling (Paul and Blunt, 2012), indirect potable reuse of treated wastewater through discharge to an environmental buffer such as discharge to rivers, dams or aquifers (Michael *et al.*, 2015).

This drive for safe reuse of treated wastewater effluent has substantially increased interest in granular media tertiary filtration to achieve quality and

productivity because of its potential and simplicity. Tertiary filtration is needed to meet appropriate standards or regulatory directives required to ensure that public and environmental health are maintained, by removing contaminants and microbes breaking through conventional treatment (te Poele *et al.*, 2005; Scherrenberg *et al.*, 2011; Michael *et al.*, 2015). Granular media filtration has a proven historical application in drinking water systems, however, the organic content and high suspended solids concentrations challenges tertiary filters (Vigneswaran and Mazumdar, 1984; Cleasby and Lodgsdon, 1990).

Researchers have found that tertiary filtration may be ineffective, operationally challenging or used increased amounts of backwash water due to a high backwash frequency (West, Rachwal and Cox, 1979; Vigneswaran and Mazumdar, 1984; Horan and Lowe, 2007). Challenges include achieving a high quality effluent and an economic throughput before reaching limiting headloss where backwash becomes necessary (Williams *et al.*, 2007). The feasibility of tertiary treatment depends on the media used, typically larger media than is used in drinking water filters, suitable filter bed depth with small headloss and loading rate to achieving a large throughput of acceptable quality (Maxwell *et al.*, 1977; Evers, Nichols and Koleini, 1985; Boller and Kavanaugh, 1995; Williams *et al.*, 2007).

The process and outcome of media filtration is influenced by the media materials and properties (Boller and Kavanaugh, 1995). Sand media used to be filter material of choice but of late, there has been some innovative filter materials in use such as multimedia with materials such as anthracite, magnetite, alumina crushed glass, garnet or ilmenite (Horan and Lowe, 2007) . Media materials are characterised by grain size distribution, shape, specific gravity, voidage/porosity and hardness. The media size determines the filtrate quality, and together with the specific gravity are important on backwash hydrodynamics and media stratification. Small grains provide small pore spaces leading to better solids capture and filtrate quality, however the small throughput achievable and high headloss make the operation with very small media uneconomic (Boller and Kavanaugh, 1995). Large grains have fewer large pore spaces allowing deeper

penetration of solids however particulate capture is less efficient resulting in low filtrate quality but has a low initial headloss allowing for long run times throughout (Boller and Kavanaugh, 1995).

Apart from the bulk physical properties of the media, the grain surface physicochemical properties are important for suspension particle transport and attachment, (Boller and Kavanaugh, 1995). Experiments performed by Ho et al (2011) for the removal of chemical contaminants from clean water system using sand and GAC of similar effective size showed that GAC was capable of removing more contaminants than sand. Coagulants such as alum or ferric chloride are used to alter the surface charge properties of both the media and suspension particles such that aggregation and deposition are improved (De Leon *et al.*, 1986; Kim and Lawler, 2006).

In this research, a commercial quadruple filter was investigated to understand the potential of the filter in the removal of solids of different surface characteristics. By utilising the different characteristics of media, the filter had media size decreasing in the direction of flow (with typically large grains at the top and small grains at the bottom). Such a media configuration gives the filter a tapered void; ensuring large particulates have a higher chance of being retained first and smaller ones progressively down in the filter, distributing particulates more evenly throughout the depth of the filter. This delays the build-up of headloss, enabling the filter to run longer. The different media material of a multimedia filter has distinct surface characteristics and hence potential to target contaminants of different properties (Boller and Kavanaugh, 1995). However, the types of particles removed by different media materials in a mono-media or multimedia configuration are not well understood, particularly in wastewater applications. Operating the filter on wastewater secondary effluent exposes it to significant amounts of inorganic and organic material, where such materials may coat on media surface altering the removal characteristics (Jackson, 1980; Ho *et al.*, 2011).

It was the purpose of this research to investigate the role of each media material and understand how the combined media configuration improves the effluent

quality in multimedia filtration systems. The experiments enable a deeper understanding of media material physicochemical properties, the contribution of each media layer and the effect of changes in filter operation characteristics to the overall filtration process. Improved media characterisation provides better information on contaminant removal; operational characterisation will inform on the conditions needed to achieve the desired filtrate quality and maximise water production.

The completion of this thesis aims to provide contributions to knowledge through the following ways:

a) Improve on the methods of characterising filter media materials hence enhancing the design and prediction of performance using filter theory.
b) Understand the impact of filter media and suspension solids surface characteristics on the filter performance and removal of contaminants.
c) The significance of wastewater solid concentration on filter performance and the optimisation of filter depth, the findings would be incorporated into the design of wastewater filters.
d) Determine the impact of high filtration rate on the filter effluent quality. The filter throughput can be optimised with the knowledge of filtrate quality and operational conditions such as headloss development.

1.2 Research Aims and Objectives

The research outcome will provide a deeper knowledge of media material physical and physicochemical properties; the impact of wastewater organic matter on the filtration process. Informed media characterisation will enable improved prediction of contaminant removal, achievement of desired filtrate quality by informed filter design and operation such as the hydrodynamics to maximise water production. The following aims and objectives were used to achieve the desired outcomes.

The aims of the research were to:

a) Characterise granular filtration media material properties and in turn understand the process science behind the removal of solids from wastewater treatment secondary effluent.
b) Understand the interaction between the flowrate, bed depth, solid concentration and headloss in filter columns of multimedia configurations.

The objectives were as follows:

i. Determine the properties of the filter media used in the quadruple media filter and investigate how they affect the filtrate quality.
ii. Determine how the surface charge of suspension wastewater solids and filter bed media affect the solids removal achievable in the quadruple filter.
iii. Evaluate the solid removal efficiency of a quadruple filter and illustrate how it relates to the flowrate, bed depth and solid concentration.
iv. Determine the variation of headloss with media properties, flowrate, bed depth, and deposition of solids.

1.3 Thesis Plan

The research sections were structured into chapters formatted as papers for publication in scientific journals. One paper has been published, another has been submitted and the other two are in preparation. The papers were written by the first author, Philani Ncube, and edited by Professor Peter Jarvis and Dr. Marc Pidou. Specific technical advice was sought from Professor Bruce Jefferson and Professor Tom Stephenson on zeta potential and filtration modelling in two of the chapters (3 and 5). The pilot filter was designed, constructed and operated by Philani Ncube. All laboratory work was undertaken by Philani Ncube. The connectivity and relationships between the thesis chapters is shown in Table 1.1.

Chapter 1 is the introduction to thesis. It lays out the background of the research, aims and objectives of the research and the structure of the thesis.

Chapter 2 (Paper 1) discusses the measurement of media physical properties and the challenges. The media shape of irregular shaped grains, usually quantified as sphericity, was determined to be a challenging media property that needed further investigation. The focus of the chapter was to introduce a more accurate and reliable method of determining media sphericity. With the aim to improved accuracy in the measurement of media sphericity and yield reliable results on application to current filter models.

Chapter 3 (Paper 2) explored the effects of changing pH on media and wastewater characteristics. The media and wastewater surface charges were studied by measuring the zeta potentials at different pH, and how it affected aggregation and deposition during filtration. The paper has been accepted by Water Research with moderate revision, titled as “Consequences of pH change on wastewater filtration using a multimedia filter”. The chapter focused on how the presence of organic matter in wastewater altered the media surface characteristics and hence deposition of wastewater solids.

Chapter 4 (Paper 4) investigated how the filter depth and the change in influent wastewater concentration affected filter performance. The chapter is in preparation for publication. The paper focuses on where solids removal mainly

occurs in the filter and hence develops recommendations for how filters can be designed shallower than current filter while achieving the desired effluent quality.

Chapter 5 (Paper 3) explored operational conditions of the filter, mainly the effect of hydraulic loading rate on the performance of a filter. The chapter has been published in Water Research (Ncube, P., Pidou, M., Stephenson, T., Jefferson, B., Jarvis, P., 2016. The effect of high hydraulic loading rate on the removal efficiency of a quadruple media filter for tertiary wastewater treatment. Water Research. 107, 102–112.)

Chapter 6 is the overall discussion of the thesis.

Chapter 7 provides a summary of key conclusions of the thesis and further work.

The table outlining the chapter and paper plan is as below (Table 1.1).

Table 1.1 : The chapter and paper plan with the respective titles of the thesis

Chapter	Paper	Objectives	Title
1			Introduction
2	1	i	Measurement of filter media particle characteristics: challenges with irregularly shaped objects
3	2	ii	Consequences of pH change on wastewater filtration using a multimedia filter
4	3	iii, iv	The impact of filter bed depth and solids loading using a multimedia filter.
5	4	iii, iv	The effect of high hydraulic loading rate on the removal efficiency of a quadruple media filter for tertiary wastewater treatment
6		i, ii, iii, iv	Thesis Discussions
7		i, ii, iii, iv	Conclusions and Further work

References

Adin, A. and Elimelech, M. (1989) 'Particle Filtration for Wastewater Irrigation', *Journal of Irrigation and Drainage Engineering*, 115(3), pp. 474–487. .

Aronino, R., Dlugy, C., Arkhangelsky, E., Shandalov, S., Oron, G., Brenner, A. and Gitis, V. (2009) 'Removal of viruses from surface water and secondary effluents by sand filtration', *Water Research*. 43(1), pp. 87–96.

Boller, M. A. and Kavanaugh, M. C. (1995) 'Particle characteristics and headloss increase in granular media filtration', *Water Research*, 29(4), pp. 1139–1149.

Cleasby, J. L. and Lodgsdon, G. S. (1990) 'Granular Bed and Precoat Filtration', in Pontius, F. W. (ed.) *AWWA Water Quality and Treatment*. 4th edn. American Water Works Association, p. 8.1.

Evers, D. K., Nichols, W. R. and Koleini, H. K. (1985) 'Advanced filtration techniques for the reclamation of sewage works effluent', in *Environmental Engineering, Proceedings of the 1985 Specialty Conference*. Boston: Environmental Engineering, p. 947.

Hamoda, M. F., Al-Ghusain, I. and Al-Jasem, D. M. (2004) 'Application of Granular Media Filtration in Wastewater Reclamation and Reuse', *Journal of Environmental Science and Health, Part A*, 39(2), pp. 385–395. .

Ho, L., Grasset, C., Hoefel, D., Dixon, M. B., Leusch, F. D. L., Newcombe, G., Saint, C. P. and Brookes, J. D. (2011) 'Assessing granular media filtration for the removal of chemical contaminants from wastewater', *Water Research*. 45(11), pp. 3461–3472.

Horan, N. J. and Lowe, M. (2007) 'Full-scale trials of recycled glass as tertiary filter medium for wastewater treatment', *Water Research*, 41(1), pp. 253–259.

Jackson, G. E. (1980) 'Granular media filtration in water and wastewater treatment, Part 1', *CRC Critical Reviews in Environmental Control*, 11(1), p. 339.

Kim, J. and Lawler, D. F. (2006) 'Aspects of particle attachment in filtration', *Water Science and Technology: Water Supply*, 6(4), pp. 125–134.

De Leon, R., Singh, S. N., Rose, J. B., Mullinax, R. L., Musial, C. E., Kutz, S. M., Sinclair, N. A. and Gerba, C. P. (1986) 'Microorganism removal from wastewater by rapid mixed media filtration', *Water Research*, 20(5), pp. 583–587.

Maxwell, M. J., Work, S. W., Linstedt, K. D. and Bennett, E. R. (1977) 'Making optimum use of filter media in wastewater filtration', *Water Sewage Works*, 124(12), pp.56–61.

Michael, I., Michael, C., Duan, X., He, X., Dionysiou, D. D., Mills, M. A. and Fatta-Kassinos, D. (2015) 'Dissolved effluent organic matter: Characteristics and potential implications in wastewater treatment and reuse applications', *Water Research*, 77, pp. 213–248.

Monk, R. D. (1987) 'Design Options for Water Filtration', *Journal - American Water Works Association*, 79(9), pp. 93–106.

Ncube, P., Pidou, M., Stephenson, T., Jefferson, B. and Jarvis, P. (2016) 'The effect of high hydraulic loading rate on the removal efficiency of a quadruple media filter for tertiary wastewater treatment', *Water Research*, 107, pp 102-112

Paul, J. D. and Blunt, M. J. (2012) 'Wastewater filtration and re-use: an alternative water source for London.', *Science of the Total Environment*, 437, pp. 173–184.

te Poele, S., Menkveld, W., Boom, J. and van Bragt, W. (2005) 'Effluent treatment by multi-media filtration, microfiltration and ultrafiltration: Results of a pilot investigation at WWTP Hoek van Holland', *Water Science and Technology, 52(4) pp. 99-105*.

Rajagopalan, R. and Tien, C. (1976) 'Trajectory analysis of deep-bed filtration with the sphere-in-cell porous media model', *AIChE Journal*, 22(3), pp. 523–533.

Scherrenberg, S. M., Postma, P., Neef, R., Menkveld, H. W. H., Bechger, M. and van der Graaf, J. H. J. M. (2011) 'Experiences on dual media filtration of WWTP effluent', *Water Science and Technology*, 63(10). pp. 2462-9.

Tufenkji, N. and Elimelech, M. (2004) ‘Correlation Equation for Predicting Single-Collector Efficiency in Physicochemical Filtration in Saturated Porous Media’, *Environmental Science and Technology*, 38(2), pp. 529–536.

Vigneswaran, S. and Mazumdar, B. (1984) ‘Intermixing of media in dual media filters’, *Effluent & Water Treatment Journal*, 24(9), pp. 341–345.

West, J., Rachwal, A. J. and Cox, G. C. (1979) ‘Experiences with high rate tertiary treatment filtration in the Thames Water Authority’, *Journal of the Institution of Water Engineers and Scientists*, 33 pp. 45–63.

Williams, G. J., Sheikh, B., Holden, R. B., Kouretas, T. J. and Nelson, K. L. (2007) ‘The impact of increased loading rate on granular media, rapid depth filtration of wastewater’, *Water Research*, 41(19), pp. 4535–4545.

Yao, K., Habibian, M. T. and O’Melia, C. R. (1971) ‘Water and Waste Water Filtration: Concepts and Applications’, *Environmental Science & Technology*, 5(11), pp. 1105–1112.

2 Measurement of filter media particle characteristics: Challenges with irregularly shaped objects

Philani Ncube, Marc Pidou, Peter Jarvis

Cranfield Water Science Institute, Cranfield University, Cranfield, MK43 0AL, UK

Abstract

The shape of particles in processes such as granular media filtration in water treatment applications play a key role in performance effectiveness. In many cases, particles are characterised by a sphericity factor that measures how similar the particle is to a sphere. In practical terms, sphericity is a shape parameter that influences the headloss during filtration, the behaviour of the media during fluidisation and the solids removal characteristics of filters. However, the media used for filtration and the suspension particles are difficult to characterise due to their irregular shape and structure. The aim of this research was to compare alternative determinations of sphericity and propose a new more accurate method for the determination of sphericity of granular filter media. The different approaches yielded different values of sphericity. The new method proposed in this study, calibrated using spherical glass beads, yielded sphericity values that were used to accurately correlate the measured headloss through the different media filters. The implication from this work is that improved accuracy in measuring sphericity will improve application of filter theory models to irregularly shaped media grains.

Keywords

Particle size, particle shape; media properties; pressure drop; digital image analysis; digital image processing; filtration

2.1 Introduction

The process effectiveness of granular media filtration is determined by the media, suspension properties and hydraulics (Boller and Kavanaugh, 1995). Filter media are loose aggregates characterised by particle size distribution, particle shape, specific gravity and porosity, while dispersed suspension particles are mostly described by size and concentration in filtration processes. These media properties are important in describing the filtration system, modelling and optimisation of the filtration process (Carter and Yan, 2005); however there are complications with practical determination of some of these parameters such as media shape and size (Cavarretta, O'Sullivan and Coop, 2009). The media porosity characteristics are also important. For example, particle size distribution and shape dictate the media packing arrangement, hence the resulting bed porosity (Boller and Kavanaugh, 1995; Li *et al.*, 2012), and the process removal efficiency (Polakowski *et al.*, 2014). In addition, media bed porosity also affects the hydrodynamics during the filter cycle and the backwash process (Boller and Kavanaugh, 1995; Soyer and Akgiray, 2009; Haarhoff and Vessal, 2010; Slavik, Jehmlich and Uhl, 2013).

As an example of how particle properties influence the filtration process, angular media results in high bed porosity but results in a convoluted flow path through the filter bed. In addition, angular media has a charge concentration on the angular edges of the particle resulting in more attraction of charged particles at these points (Suthaker, Smith and Stanley, 1995). Shape also has a direct impact on how the filter media particle size distribution is determined using methods such as sieve analysis and optical methods (Jarvis, Jefferson and Parsons, 2005; Crittenden *et al.*, 2012; Polakowski *et al.*, 2014). Optimisation of processes such as filtration rely on shape quantification of the media. However, the complication of practically determining particle shape means that approximations and estimations of shape are usually made (Carter and Yan, 2005; Cavarretta, O'Sullivan and Coop, 2009).

Shape is widely quantified based on a particle's similarity to a circle or sphere. In filtration and many engineering processes, sphericity is the more applicable

descriptor of shape for process design and modelling as the models consider the particles under consideration to be 3-dimensional structures. Wadell (1935) defined sphericity of a particle as the “ratio of surface area of a sphere of same volume as a particle to the surface area of the particle”. This definition is now commonly referred to as true sphericity. A perfect sphere has a sphericity value of 1 while other shapes will have values between 0 and 1. The sphericity of regular shapes can be calculated from the true sphericity definition, but for irregular shapes like filter media, the surface area is variable and difficult to measure (Siwiec, 2007). Because of this difficulty, various approximate methods are in common use, including digital image processing (DIP), fluidisation, pressure drop methods and correlation with porosity.

Traditional sphericity quantification was based on visual comparison of media to images on charts and assigning a corresponding value (Sneed and Folk, 1958). DIP is an improvement on the traditional method, being quicker and less subjective (Carter and Yan, 2010). However use of 2D images to infer 3D shape information in DIP limits the accuracy of the method (Mora and Kwan, 2000; Cavarretta, O’Sullivan and Coop, 2009). Cavarretta *et al.* (2009) demonstrated analytically that the use of 2D projections to characterise the shape of 3D particles has associated limitations. For example, the nonconformity broadens as the particle flatness increases. This is because DIP relies on random orientation of the particles in the image. However, during sample preparation, particles favour orientation on a surface (such as a microscope slide) in the most stable manner, typically the flattest surface of the particle resulting in non-random orientation of the particle (Rodriguez, Edeskär and Knutsson, 2013; Polakowski *et al.*, 2014). However, new microscopes have improved techniques which use different focal points to capture multiple images to construct 3D shape of particles, providing room to devise software to calculate sphericity.

Another common method for sphericity determination involves measuring the pressure drop across a clean filter bed and applying established headloss correlations (Kozeny-Carmen or Ergun expression) to determine the particle sphericity (Akgiray and Saatçi, 2001; Siwiec, 2007). Haarhoff and Vessal (2010)

used a falling head method on a clean filter bed and approximated the sphericity using a numerical method to solve the Ergun headloss expression. Other methods have determined sphericity by correlating to porosity measurement (Yu and Standish, 1993; Zou, R.P. Yu, 1996) or have measured backwash flow velocity at incipient fluidisation and then evaluated the resulting correlations (Wen and Yu, 1966; Cleasby and Fan, 1981; Richardson and Zaki, 1997). Fluidised bed correlations were proposed by Dharmarajah and Cleasby (1986), and have been improved by Soyer and Akgiray (2009). The incipient fluidisation method is, however, not practical for real filter media as particles are not of uniform size and hence fluidise at different velocities.

Reliable determination of media shape is important because it is a major parameter that controls particle capture in the filtration process. For example it has been shown that particle retention is controlled by the particle's shape, as it affects flow hydrodynamics, the particle transport and is a determinant of the active surface area which affects the process rate (Boller and Kavanaugh, 1995).

Sphericity is therefore of absolute importance in the process of filtration. It is determined by approximate methods, but there is no comparison or agreed measurement technique and practical formulation to quantify particle sphericity (Blott and Pye, 2008). This research compares different methods of sphericity measurement and develops a new method that better aligns to applications in filtration. The new method improves on the 2D DIP methods by introducing third dimensionality through the incorporation of the 3D feature, the 3D equivalent diameter.

2.2 Materials and Methods

2.2.1 Digital Image Processing

The DIP approach used a combination of light microscopy to magnify the image and a mounted complementary metal oxide semiconductor (CMOS) camera to capture the image followed by processing using imaging software (Image Pro Premier, Media Cybernetics). The light microscope was operated to produce a suitable magnification, focus and light intensity to obtain a good contrast between

the object and the background needed for image processing. Prior to image capture, a graticule was used to make a pixel to length calibration for the imaging analysis. During the image acquisition process, 3D objects were captured as planner images (2D objects). The captured images were analysed for minimum, mean and maximum dimension and the area of individual objects. In this study diameter is used loosely in place of dimensions of irregular objects. 724-836 images were captured to obtain a representative sample size. This was above the recommendation given in the British Standards for particle sizing, which suggests a minimum of 625 particles to provide a representative sample for particle size determination (BS3406, 1963).

2.2.2 Sphericity Determination

The image measurements from the DIP software were used to calculate sphericity from various formulations found in the literature and including the new method introduced in this study (Table 2-1). Among these methods the Sneed and Folk (1958) is not dimensionally correct. The DIP methods use 2D measurement of dimensions, perimeter and area on planar images while the new method incorporates a 3D equivalent area.

The new method proposed in this paper (Table 2-1) compensates for the loss of 3D information during image capture through use of a physically determined 3D equivalent area (A_{eq}). The 3D equivalent area is calculated from the 3D equivalent diameter, a filter media size parameter useful in filtration models. The equivalent diameter is a volume attribute determined by measuring the mass of a counted number of grains, followed by calculation of the equivalent volume and diameter. Thus, for a media grain of mass (M) and density (ρ), the equivalent volume (V), $V=M/\rho$ and the equivalent diameter (d) of the sphere can be calculated from ($V=\pi d^3/6$). Hence the equivalent area ($A_{eq}=\pi d^2/4$) is an attribute of volumetric particles. For a sphere, the projected area is proportional to its surface area. However, for an irregular object, the projected area deviates from its surface area and the more non-spherical the object, the greater the deviation. This deviation between the projected area and the equivalent area was utilised to calculate the sphericity of the irregularly shaped object in the new method.

Table 2-1 Literature 2D expressions for determining sphericity by DIP formulations and the new method.

Method	Expression	Description
Sneed and Folk (1958)	$\psi = \sqrt{d_{\min}} \Big/ \sqrt[3]{d_{\max} \times d_{mean}}$	d_{min}, d_{mean} and d_{max} are minimum, mean and maximum diameters respectively
Sympatec (2015)	$\psi = 2\sqrt{\pi A} \Big/ P$	A is the area and P is the perimeter of particle
Liao *et al.*(2010)	$S_F = d_{rms.d} \Big/ d_{mean}$ $\psi = 1 - S_F$	S_F is the shape factor and $d_{rms.d}$ is the root mean square deviation
Cho *et al.*(2006)	$\psi = d_{\min} \Big/ d_{\max}$	d_{min} and d_{max} are the minimum and maximum diameters
Mora and Kwan (2000)	$\Lambda = M \Big/ \rho_p \sum_{i=1}^{n} \left(d_{mean} \times A\right)_i$ $\psi = \sqrt[3]{\Lambda \left(d_{mean} / d_{\max}\right)^2}$	M is the total mass of the n particles, ρ_p is the density of particles, Λ is a thickness determinant, d_{max} and d_{mean} are maximum and mean dimensions respectively. Λ re-introduces the 3D information
New Method	$\psi = nA_{eq} \Big/ \sum_{i=1}^{n} A_i$	A_{eq} is a 3D equivalent area and A_i is the area of each particle as determined by digital image analysis

In the new method, the sum of 3D equivalent area of particles was compared to the sum of their projected area as determined by DIP to get sphericity. DIP systems measure the 2D projected area very accurately, while the equivalent area preserves 3D information and hence the sphericity values calculated with the new method are expected to be more reliable. Glass spheres of diameter 0.52 mm were used to validate the new method through the measurement of sphericity and offer a comparison of the different literature method based on what would be regarded as a true sphere.

2.2.3 Media characterisation

The PSD of the media used in a commercial quadruple media filter (FilterClear, Bluewater Bio Ltd) was determined using sieve analysis (American Society for Testing and Materials, ASTM C136-2006). The filter media were respectively anthracite, flint, alumina and magnetite. The sieve analysis technique sizes the media grains through their ability to pass through the sieve openings or be restricted from passage through a set of different mesh sizes. The specific gravity was determined using a standard method (APHA, AWWA and WEF, 2005) by comparison of the weight of the media to the weight of an equal volume of water. The loose bed porosity was determined using a standard method as the volume proportion of all void spaces to the total volume of the bed (ASTM C1252-2006).

2.2.4 Headloss

An established clean bed headloss expression was used to calculate the sphericity of media grains from empirical data using filter column apparatus. The filter media at a depth of 100 mm was backwashed in an acrylic perspex column of 74 mm internal diameter and 700 mm height and allowed to settle while gradually reducing the flow rate. The columns were fitted with pressure transducers (PN2026, IMF Electronic Ltd, Germany) at the top and bottom of the media bed, 100 mm apart, to measure the pressure drop across the filter bed when tap water was passed through the media at a fixed flow rate of 25 mh^{-1} by means of a peristaltic pump (620 Industrial LoadSure, Watson Marlow, UK). An air trap was secured on the pump output pipe to dampen the flow pulse. The clean bed headloss measurements were at a temperature of 20 ^{0}C. The Kozeny-Carman equation was applied using the media parameters (equivalent diameter and porosity) to calculate the sphericity as a missing variable. The Kozeny-Carmen correlation was appropriate for these flow conditions since the Reynolds numbers of 2-11 were calculated for flow through all the media used which falls within the laminar flow regime.

2.3 Results and Discussion

2.3.1 Media Sphericity

Since measurement of true sphericity as defined by Wadell (1935) is complicated by the measurement of surface area of irregularly shaped filter grains, the various formulations discussed in section 2.2 were evaluated for sphericity of filter media. The sphericity of media materials was measured using the new method as 0.69 ± 0.02, 0.59 ± 0.02, 0.66 ± 0.01, 0.72 ± 0.07 and 1.01 ± 0.02 for anthracite, flint, alumina, magnetite and glass spheres, respectively (Table 2-2). These values compare to some extent to visual observation of the media (Figure 2-1). Comparison of the media in Figure 2-1 to the sphericity chart (Appendix A) shows how difficult the determination through visual observation could produce variability in judgements. As a practical exercise three researchers produced different values on comparing the filter images to charts. This showed that visual observation is subjective and unreliable as it depends on an individual's experience and judgement. Systematic determination of sphericity is more favourable (Carter and Yan, 2010). The sphericity of the glass sphere standards was measured as 1.01 ± 0.02 showing good validation of the new method at measuring sphericity with high accuracy.

The values obtained from the proposed new method were compared with those obtained from the literature sphericity measurement terms. The DIP methods determined sphericity for anthracite, flint, alumina and magnetite in the range 0.54 – 0.86, 0.51 – 0.78, 0.60 – 0.80 and 0.59 – 0.81 respectively (Table 2-2). As these values indicate, there was some variance among the different methods in the measurement of sphericity of the same sets of media samples. Measurement of sphericity of the glass spheres was used as a measure of accuracy of the various techniques. The literature methods measured the sphericity of glass spheres to be slightly less than the expected value of 1. The Sneed and Folk (1958) and Sympatec methods had the highest degree of accuracy, resulting in a sphericity value of 0.97, followed by the Cho *et al.* (2006) method at 0.95, then Liao *et al.* (2010) at 0.90 and lastly Mora and Kwan (2000) at 0.85. Deviations in sphericity values are all inherent in the assumptions made in deriving the respective

algorithm. These methods were expected to converge for true spheres. Deviation was expected on irregular media grains since the different methods assume particles to have random orientation on a microscope slide for image capture, but in reality, they would lie on the stable flat position. Additionally, the failure to capture the particle thickness introduces a technical inaccuracy in DIP methods for shape characterisation since a planar image is processed by software (Mora and Kwan, 2000).

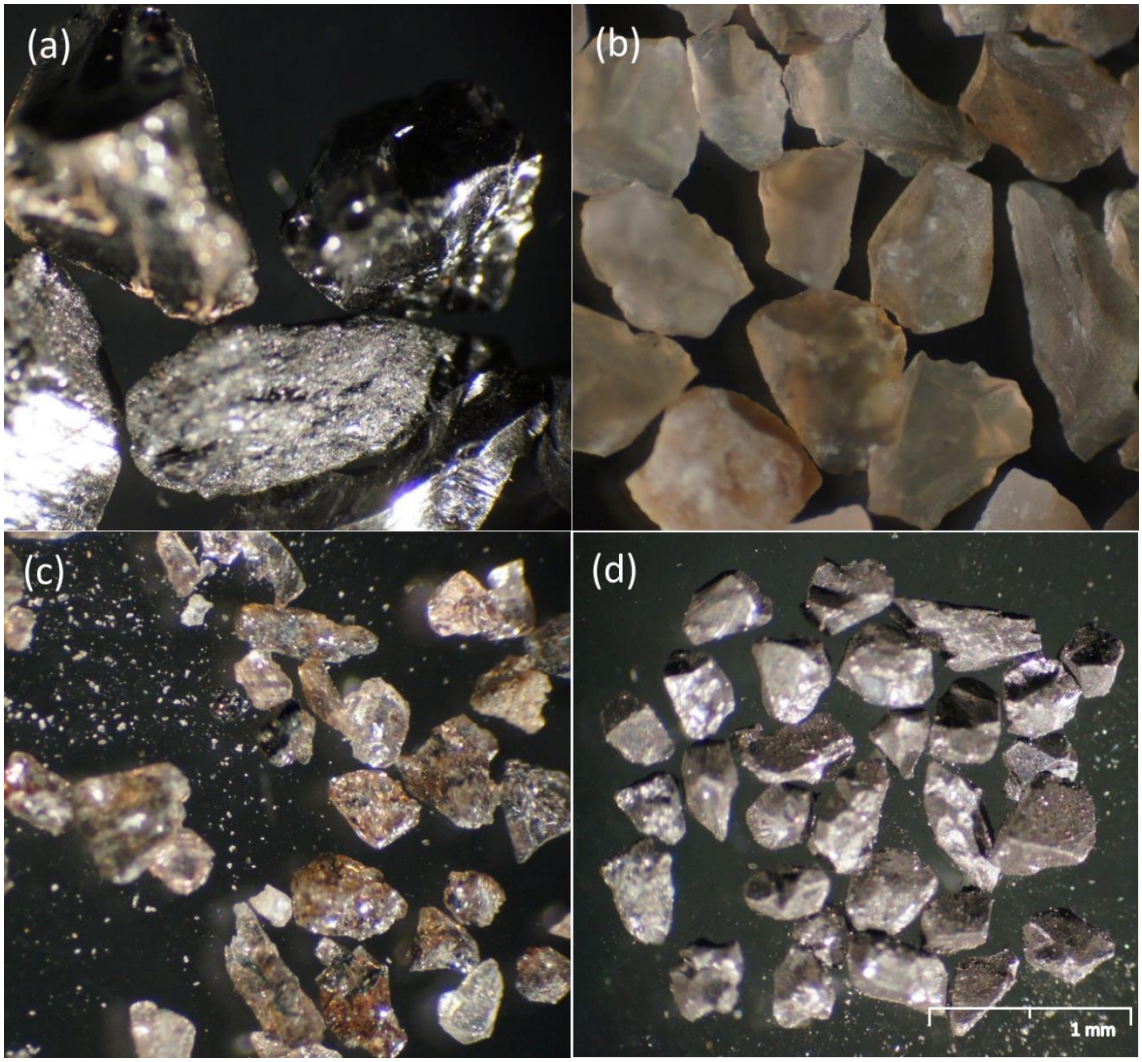

Figure 2-1: Images of media grains used visual observation and for the determination of sphericity. The media names were (a) anthracite, (b) flint, (c) alumina and (d) magnetite.

The headloss method was also used to determine the sphericity of the media materials and the glass spheres (Table 2-2). The headloss method was based on the hydrodynamics through the media bed, an approach that was different to the physical shape characterisation of other methods, but was a real reflection of the flow dynamics around the porous media in the filter. The sphericity of glass spheres was measured by the headloss method as 0.82 ± 0.01 which was 18% lower than the expected value of 1. The headloss method depends on the flow resistance of water around the media. There are, however, stagnation regions of flow around media and hence reduced surface area between flowing water and media material. These factors may introduce some deviation on the physical shape of media.

Table 2-2: Media sphericity values determined by the different methods.

	Anthracite	**Flint**	**Alumina**	**Magnetite**	**Glass Spheres**
Sneed and Folk (1958)	0.78 ± 0.08	0.78 ± 0.08	0.80± 0.07	0.80 ± 0.07	0.97 ± 0.03
Sympatec	0.86 ± 0.04	0.77 ± 0.1	0.64 ± 0.1	0.76 ± 0.1	0.97 ± 0.03
Liao *et al.*. (2010)	0.70 ± 0.1	0.68 ± 0.2	0.75 ± 0.1	0.73 ± 0.1	0.90 ± 0.07
Cho *et al.* (2006)	0.61 ± 0.1	0.61 ± 0.1	0.64 ± 0.1	0.65 ± 0.1	0.95 ± 0.06
Mora and Kwan (2000)	0.58 ± 0.04	0.51 ± 0.04	0.60 ± 0.03	0.59 ± 0.04	0.85 ± 0.02
New Method	**0.69 ± 0.02**	**0.59 ± 0.02**	**0.66 ± 0.01**	**0.72 ± 0.07**	**1.01 ± 0.02**
Number of grains used	751	795	724	836	775
Headloss Method	0.54 ± 0.03	0.66 ± 0.04	0.60 ± 0.02	0.81 ± 0.02	0.82 ± 0.01

2.3.2 Media Characteristics

Additional media characteristics are important for determining a complete media and filter bed description and are required for modelling filtration and design of

filters. These media characteristics include grain size, bed porosity and specific gravity. The volume based 3D equivalent diameter for the media were determined for anthracite as 1.59 ± 0.03 mm, flint as 0. 67 ± 0. 02 mm, alumina as 0. 68 ± 0. 01 mm and magnetite as 0. 41 ± 0. 08 mm (Table 2-3). The glass sphere standards were supplied as diameter 0.50 ± 0. 01 mm and were measured with good accuracy as 0. 52 ± 0. 01 mm 3D equivalent diameter.

The cumulative PSD for the filter media anthracite, flint, alumina and magnetite was determined using sieve analysis. Sieve analysis is the industry standard for particle sizing of loose aggregates. It separates particles based on their smallest orientation that can pass through a set of decreasing sized sieves. Anthracite was measured as the largest particle with a d_{50} particle size of 1.62 mm (UC = 1.57), followed by flint with a d_{50} of 0.72 mm (UC = 1.44), alumina d_{50} of 0.66 mm (UC = 1.14), while magnetite was the smallest media with a d_{50} of 0.38 mm (UC = 1.55) (Figure 2-2a and Table 2-3a). Among the three sets of diameter measurement, the 3D equivalent diameter is preferred in filter modelling as particles are assumed to be spherical in models, the same concept is used to calculate the 3D equivalent diameter. Since the difference between 3D equivalent diameter and sieve analysis d_{50} size is small, the sieve analysis value may be used if the 3D equivalent diameter is not measured.

DIP is an emerging particle sizing technique, it uses software to measure diameter in different orientations, giving the PSD by means of the minimum, median or longest axis of particle. The DIP measured the anthracite d_{50} as 1.54 mm (UC = 1.42), flint d_{50} as 0.70 mm (UC = 1.43), alumina d_{50} as 0.68 mm (UC = 1.20) and magnetite d_{50} as 0.40 mm (UC = 1.36) based on the minimum diameter (Figure 2-2b and Table 2-3). The d_{50} sizes measured by sieve analysis and the minimum axis diameter from the DIP were very similar. This is because sieve analysis, separated particles based on their smallest dimensions through a sieve opening which is similar to DIP technique based on the minimum axis of the particle. The diameter on the minimum axis obtained by DIP corresponded to the smallest orientation of particles selected in sieve analysis. DIP has the advantage of being quick and less labour intensive than sieve analysis. However,

DIP has less frequently been used for sizing filter media because of the reliability sieve analysis has offered the industry over years, hence becoming a common standard method.

Commercial filter media are commonly specified by the sieve analysis d_{10} size, known as the effective size (ES) and the range of the media sizes, called the uniformity coefficient (UC), calculated as d_{60}/d_{10}. The ES is used as it specifies by number the smaller media in the filter bed, which has a greater collector surface area, and impact on headloss through the filter bed. The UC measures the spread of media size, where a value of 1 represents a uniformly sized media, with increasing values representing more poly-dispersed media. A wider spread of media size is representative of varying collector surface which will characterise a filter with varying filter coefficient with depth.

The loose bed porosity was determined as 0.510 ± 0.001, 0.517 ± 0.002, 0.546 ± 0.001, 0.471 ± 0.002 and 0.417 ± 0.002 for anthracite, flint, alumina, magnetite and glass spheres respectively (Table 2-3). The glass spheres had the lowest measured porosity. This was an unsurprising result given that these particles are close to being true spheres. Theoretical porosity values for spheres have been calculated as ranging from 0.259 (compacted bed) to 0.476 (loose bed) based on either hexagonal (compact) or square (loose) packing of spheres in the filter bed (Siwiec, 2007).

A larger porosity value is an indication of more angular shaped media. This is because porosity is a function of particle shape, with no size dependence, hence it is sometimes used to facilitate particle shape characterisation (Yu and Standish, 1993). In terms of the porosity, the media can be ranked in order of highest to lowest from: glass spheres, magnetite, anthracite, flint and alumina. The porosity ranking in this study closely matched the order of the sphericities measured by the new method developed in this study. The exception was for alumina, which showed none conformity in many of the measurements. The deviation in alumina sphericity determination may be due to its structure. It was composed of crystalline aggregates and had variations in shape, introducing inconsistencies in the measurement of the media grain dimensions.

Porosity is an important characteristic of a filter bed since solids are packed in the voids during filtration (Boller and Kavanaugh, 1995) and filling of these voids with solids increases flow resistance through a filter, thus increasing headloss through the filter bed (Stevenson, 1997). Backwashing of a media filter leaves a loosely packed media bed. Alumina was found to have the highest porosity, thus alumina had the greatest capacity for retained solids storage. The structure of the filter can be reflected by the change in void space from top to bottom. The voidage defined as volume of voids over volume of media grains and calculated from porosity ε, as ε/(1-ε), for anthracite (1.0), flint (1.1), alumina (1.2) and magnetite (0.9). The voidage shows the quadruple filter tapers on the lower magnetite layer enabling the filter to capture small particles as the flow path comes closer to the collectors.

The media characteristic important for stratification of media materials as separate layers is the specific gravity, determined for anthracite, flint, alumina and magnetite as respectively 1.41 ± 0.01, 2.59 ± 0.01, 3.92 ± 0.01 and 5.10 ± 0.01 (Table 2-3). Magnetite had the highest specific gravity (most dense) while anthracite had the lowest value (least dense). The media stratified based on both the different media sizes measured earlier and the specific gravity. After fluidisation, the media settles at different rates based on Stokes law (laminar settling) as fluidising flow is reduced (Crittenden *et al.*, 2012), facilitating stratification. On this same basis, the media was layered as anthracite, flint, alumina and magnetite from top to bottom. Some degree of intermixing occurs on the media interfaces particularly between small media from the bottom layer and larger media of the upper layer. The combination of media particle size distribution, shape and specific gravity are all fundamental in the design and operation of the quadruple media filter. The next section illustrates the use of media characteristics as used in a headloss model to predict and compare to measured headloss through media in filters.

2.3.3 Filter headloss Validation

The Kozeny-Carmen equation was used with the sphericities, 3D equivalent diameter and porosity as determined previously (Table 2-2 and Table 2-3), to calculate the headloss through filters made of the respective media for comparison with the measured starting bed headloss. The sphericity determined by the headloss method was not used as that would have been the reversal of the determination. The sphericity determined by the new method calculated the headloss for the anthracite, flint, alumina, magnetite and glass spheres filter beds as 192, 1336, 850, 3956 and 2116 Pa respectively which were a good match to the measured headloss of 209, 1214, 1300, 3945 and 2161 Pa except for alumina, where the headloss was higher than that calculated (Figure 2-3).

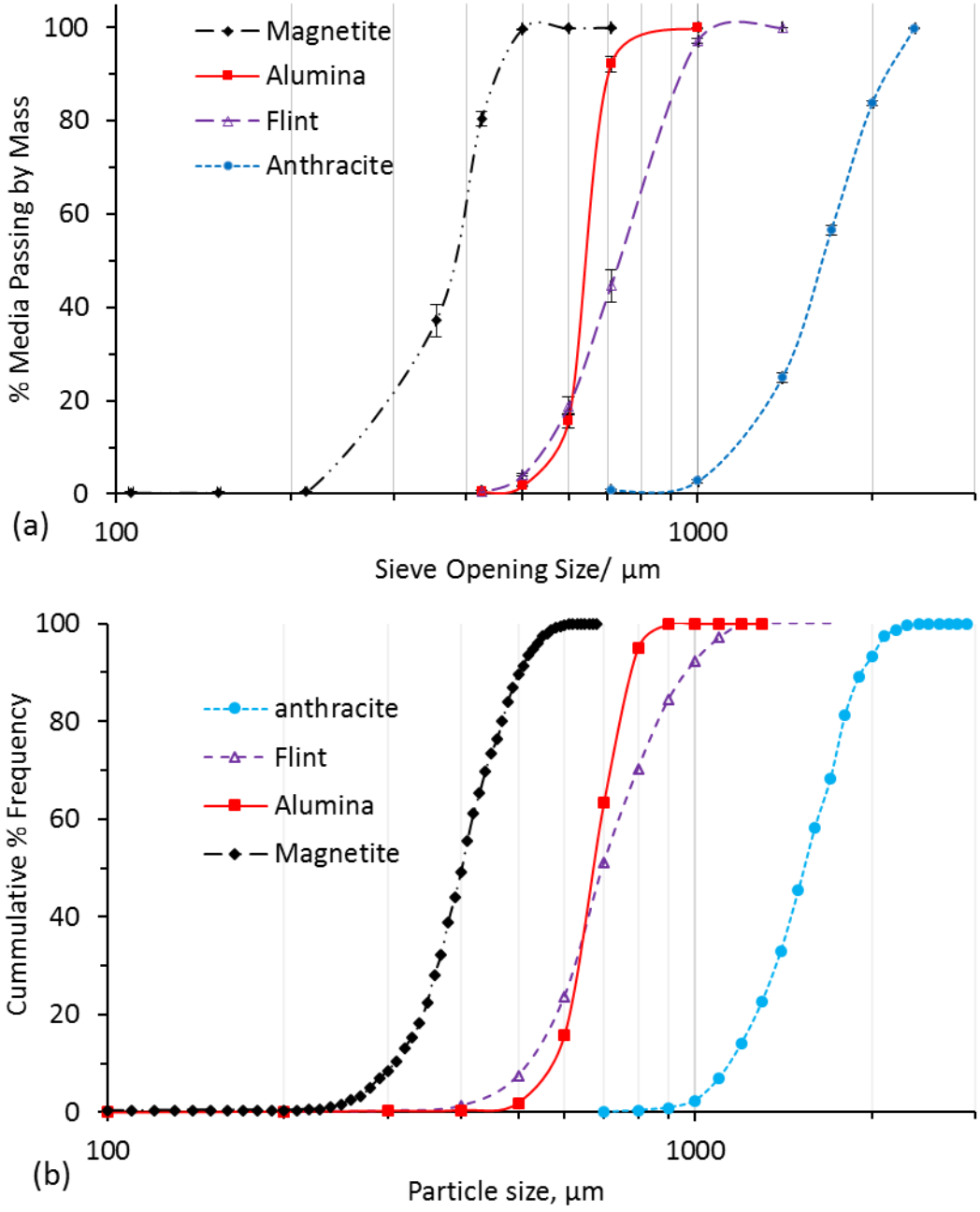

Figure 2-2 (a) Cumulative media mass particle size distribution determined by sieve analysis and (b) Cumulative frequency media particle size distribution determined by DIP.

Table 2-3: Characterisation of filter media grains used for sphericity determination.

		Anthracite	Flint	Alumina	Magnetite	Glass Spheres
d_{eq} /mm	Mean	1.59 ± 0. 03	0. 67 ± 0. 02	0. 68 ± 0. 01	0. 41 ± 0. 08	0. 52 ± 0. 01
	Count	1037	1182	1547	1827	1874
Porosity (ε)		0.510 ± 0.001	0.517 ± 0.002	0.546 ± 0.001	0.471 ± 0.002	0.417 ± 0.002
Specific Gravity		1.41 ± 0.01	2.59 ± 0.01	3.92 ± 0.01	5.10 ± 0.01	2.49 ± 0.01
Particle Size/ mm (Sieve Analysis)	d_{10}	1.09	0.54	0.59	0.25	-
	d_{50}	1.62	0.72	0.66	0.38	-
	d_{90}	2.03	0.95	0.71	0.46	-
	UC	1.57	1.44	1.14	1.55	-
DIP particle size (mean), mm*	d_{10}	1.55	0.70	0.75	0.41	0.44
	d_{50}	1.96	0.89	0.84	0.50	0.52
	d_{90}	2.34	1.20	0.95	0.60	0.59
	UC	1.31	1.35	1.15	1.27	1.21
DIP particle size (min)/ mm*	d_{10}	1.14	0.52	0.58	0.31	0.43
	d_{50}	1.54	0.70	0.68	0.40	0.51
	d_{90}	1.92	0.96	0.77	0.50	0.58
	UC	1.42	1.43	1.20	1.36	1.22
*Number of particles		751	795	724	836	775

*Number of particles analysed for DIP particle size.

The match of correlated headloss using the new method sphericity to the measured headloss further confirmed the accuracy of this method. Therefore, the sphericities of the method introduced in this study can be reliably applied to filtration models. The headloss through the alumina media was not closely matched by all methods. This was thought to be due to inaccuracies in the measurement of alumina sphericity which was used in the calculation of headloss.

By deduction based on the headloss calculation, alumina was less spherical than determined by the sphericity methods. The Mora and Kwan (2000) methods measured the lowest sphericity compared to the other methods and the calculated alumina headloss was closest to the measured. The differences in calculated and measured headloss illustrate the importance of an accurate determination of sphericity. Filter models assume spherical particles, while the sphericity in the formulation quantifies the deviation. Hence high accuracy in the sphericity improved the prediction from the models. The close match in headloss calculated from the 3D equivalent diameter and the new method sphericity validates the method as accurate.

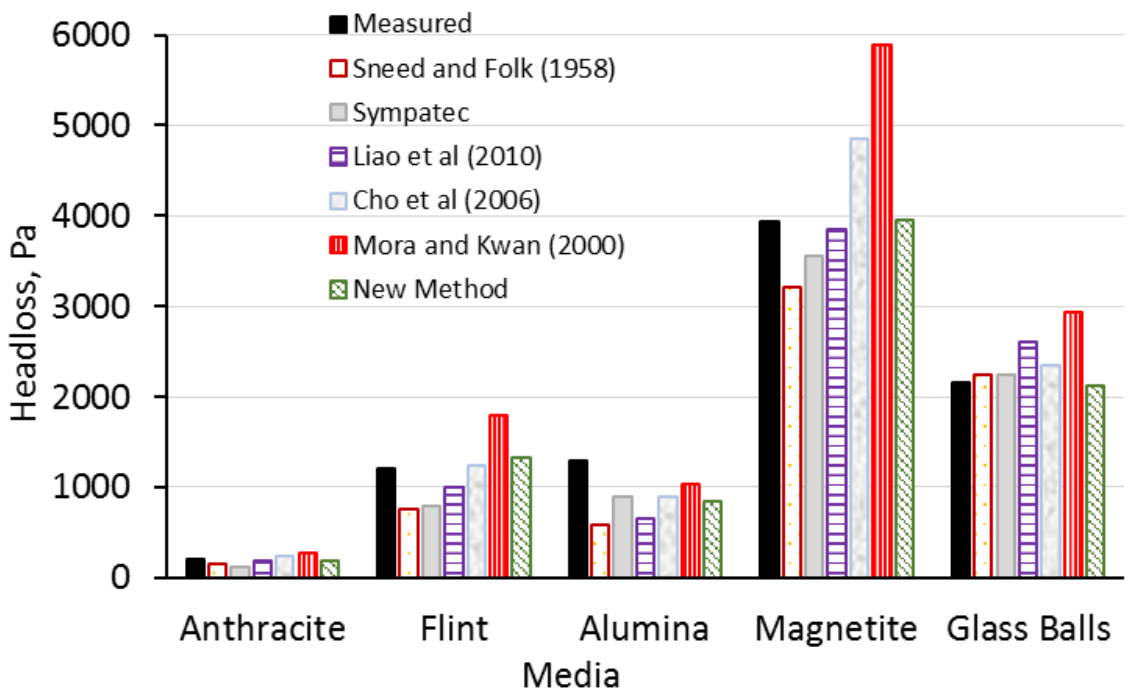

Figure 2-3 Measured and calculated headloss from the determined sphericities.

2.4 Conclusions

The use of DIP has greatly increased the options for particle size and shape quantification, but the loss of the third-dimension information in image capture reduces the accuracy of the methods. The new method in this study compensates for the third dimension in DIP by incorporating equivalent area (which is a 3D property) to the 2D projection area of particles (determined accurately by DIP) providing a reliable technique for sphericity measurement of filter media. The sphericity method introduced in this study measured the sphericity of spherical glass spheres as 1.01 ± 0.02 providing a good validation for the method. The sphericities determined by the new method were used to simulate clean bed headloss of the media filters with greater accuracy for all the four-different media studied with the exception of alumina.

Acknowledgements

The authors greatly thank Dr Garry Hoyland, Richard Hartnett and Dr Caroline Huo for their industrial support and advice, and Bluewater Bio Ltd for funding and permitting the use of the company technology to carry out this investigation. Funding from the Engineering and Physical Sciences Research Council (EPSRC) is also gratefully acknowledged.

References

Akgiray, O.¨and Saatçi, a. M. (2001) ‘A new look at filter backwash hydraulics’, *Water Science and Technology: Water Supply*, 1(2), pp. 65–72.

APHA, AWWA and WEF (2005) *Standard Methods for the Examination of Water and Wastewater*. 21st edn, *American Public Works Association*. 21st edn. Washington D.C.

ASTM C136 (2006), "Standard Test Method for Sieve Analysis of Fine and Coarse Aggregates", American Society for Testing and Materials International, , no. C136.

Blott, S. J. and Pye, K. (2008) ‘Particle shape: A review and new methods of characterization and classification’, *Sedimentology*, 55(1), pp. 31–63. .

Boller, M. A. and Kavanaugh, M. C. (1995) ‘Particle characteristics and headloss increase in granular media filtration’, *Water Research*, 29(4), pp. 1139–1149.

BS3406 (1963) *British Standard Methods for Determination of Particle Size Distribution*.

Carter, R. M. and Yan, Y. (2005) ‘Measurement of particle shape using digital imaging techniques’, *Journal of Physics: Conference Series*, 15(1), pp. 177–182.

Cavarretta, I., O’Sullivan, C. and Coop, M. R. (2009) ‘Applying 2D shape analysis techniques to granular materials with 3D particle geometries’, *AIP Conference Proceedings*, 1145(May), pp. 833–836.

Cho, A. G., Dodds, J. and Santamarina, J. C. (2006) ‘Particle Shape Effects on Packing Density , Stiffness and Strength – Natural and Crushed Sands’, *Journal of Geotechnical and Geoenvironmental Engineering*, 132(5), pp. 591–602.

Cleasby, J. L. and Fan, K. S. (1981) ‘Fluidization and expansion of filter media’, *Journal of the Environmental Engineering division of the American Society of Civil Engineers*,107(3), pp. 455–471.

Crittenden, J. C., Trussell, R. R., Hand, D. W., Howe, K. J. and Tchobanoglous, G. (2012) *Water Treatment principle and design*, *MWH’s Water Treatment:*

Principles and Design, Third Edition.

Dharmarajah, A. H. and Cleasby, J. L. (1986) 'Predicting the expansion behavior of filter media', *Journal / American Water Works Association*, 78(12), pp. 66–76.

Haarhoff, J. and Vessal, A. (2010) 'A falling-head procedure for the measurement of filter media sphericity', *Water SA*, 36(1), pp. 97–104.

Jarvis, P., Jefferson, B. and Parsons, S. (2005) 'Measuring floc structural characteristics', *Reviews in Environmental Science and Biotechnology*, 4(1–2), pp. 1–18.

Li, T., Li, S., Zhao, J., Lu, P. and Meng, L. (2012) 'Sphericities of non-spherical objects', *Particuology*. Chinese Society of Particuology, 10(1), pp. 97–104.

Liao, C.-W., Yu, J.-H. and Tarng, Y.-S. (2010) 'On-line full scan inspection of particle size and shape using digital image processing', *Particuology*. Chinese Society of Particuology, 8(3), pp. 286–292.

Mora, C. F. and Kwan, a. K. H. (2000) 'Sphericity, shape factor, and convexity measurement of coarse aggregate for concrete using digital image processing', *Cement and Concrete Research*, 30(3), pp. 351–358.

Polakowski, C., Sochan, A., Bieganowski, A., Ry, M., Földényi, R. and Tóth, J. (2014) 'Influence of the sand particle shape on particle size distribution measured by laser diffraction method, International Agrophysics 28, pp. 195–200.

Richardson, J. F. and Zaki, W. N. (1997) 'Sedimentation and fluidisation: Part I', *Chemical Engineering Research and Design*, 75, pp. S82–S100.

Rodriguez, J. M., Edeskär, T. and Knutsson, S. (2013) 'Particle Shape Quantities and Measurement Techniques - A review', *Electronic Journal of Geotechnical Engineering*, 18(A), pp. 169–198.

Siwiec, T. (2007) 'The sphericity of grains of filtration beds applied for water treatment on examples of selected minerals', *Electronic Journal of Polish AgriculturalUniversities.*10(1).Availableat:http://www.ejpau.media.pl/volume10/issue1/art-30.html.

Slavik, I., Jehmlich, A. and Uhl, W. (2013) ‘Impact of backwashing procedures on deep bed filtration productivity in drinking water treatment’, *Water Research*. 47(16), pp. 6348–6357.

Sneed, E. D. and Folk, R. L. (1958) ‘Pebbles in the Lower Colorado River, Texas a Study in Particle Morphogenesis’, *The Journal of Geology*, 66(2), pp. 114–150.

Soyer, E. and Akgiray, O. (2009) ‘A new simple equation for the prediction of filter expansion during backwashing’, *Journal of Water Supply: Research and Technology - AQUA*, 58(5), pp. 336–345.

Stevenson, D. G. (1997) ‘Flow and filtration through granular media—the effect of grain and particle size dispersion’, *Water Research*, 31(2), pp. 310–322.

Suthaker, S., Smith, D. W. and Stanley, S. J. (1995) ‘Evaluation of Filter Media for Upgrading Existing Filter Performance’, *Environmental Technology*, 16(7), pp. 625–643.

Sympatec (2015) *Fundamentals: Particle Size and Shape Calculation by Image Analysis*.Availableat:http://www.sympatec.com/EN/ImageAnalysis/Fundamentals.htm (Accessed: 4 October 2015).

Wadell, H. (1935) ‘Volume, Shape and Roundness of Quartz Particles’, *The Journal of Geology*, 43(3), pp. 250–280.

Wen, C. Y. and Yu, Y. H. (1966) ‘Mechanics of fluidization’, *Chemical Engineering Progress, Symposium Series*, 62(1), pp. 100–111.

Yu, A. B. and Standish, N. (1993) ‘Characterisation of non-spherical particles from their packing behaviour’, Powder Technology 74, pp. 205–213.

Zou, R.P. Yu, A. B. (1996) ‘Evaluation of the packing characteristis of mono sized non spherical particles’, *Powder technology*, 88, pp. 71–79.

3 Consequences of pH change on wastewater depth filtration using a multimedia filter

Philani Ncube, Marc Pidou, Tom Stephenson, Bruce Jefferson, Peter Jarvis

Cranfield Water Science Institute, Cranfield University, Cranfield, MK43 0AL, UK

Abstract

Different media materials in a multimedia filter have the potential to trap particles of different surface characteristics dependent on the media-suspension particle interactions. However, the removal of particles from wastewater secondary effluent using granular media filtration is relatively poorly understood because of the complexity of the wastewater matrix. Often the wastewater treatment process is liable to undergo pH changes due to removal or addition of chemicals in the treatment chain or from biological instability which in turn may alter the wastewater characteristics. Wastewater contains a mixture of organic and inorganic components, dissolved or particulate which may influence the aggregation and deposition of suspension solids during depth filtration. Changes in wastewater pH has the potential to change the wastewater matrix and media surface properties hence affecting aggregation and deposition in wastewater filtration. This study investigated how pH change affects wastewater filtration by monitoring zeta potential, aggregation and deposition of solids. The wastewater and filter media were also characterised over a range of pH from 1-13. Aggregation and deposition of wastewater solids was found to be most efficient near neutral pH. This was not concurrent with the conditions of lowest net charge in the system.

Keywords

Multimedia; depth filtration; surface charge; zeta potential; aggregation; deposition.

3.1 Introduction

Filtration of wastewater is becoming ever more important as regulations such as the Water Framework Directive requires wastewater discharged to the environment to reach higher water quality standards. Suspended solids present in discharged wastewater may pollute the natural environment through the presence of nutrients, such as phosphorus, that may cause eutrophication in surface waters. Suspended solids also act as a support for survival and transport of viruses and bacteria, which can attach onto particle surfaces (Walshe *et al.*, 2010) and can subsequently pose a risk to human health. Granular media filtration is one of the important tertiary treatments used to remove particulate materials from treated wastewater effluents. Filtration efficiency depends on physicochemical properties of the particulates and the porous medium (size, shape, chemical composition, surface properties), the suspension chemistry (pH, ionic strength, ionic composition), the biotic activity, the hydrodynamic conditions, and the ambient temperature (Bradford and Torkzaban, 2008; Petosa *et al.*, 2010; Yuan *et al.*, 2012). Wastewater treatment is often accomplished by removal or addition of chemicals that may result in a pH change (Shanahan and Semmens, 2015). For example, through the use of ferric sulphate for coagulation, phosphorous or odour removal (Alias and Assari, 2007; Zhu *et al.*, 2012). A pH change may alter the wastewater matrix through reaction with H^+ and OH^- groups, the surface characteristics of wastewater solids and subsequently compromise solids aggregation and deposition on porous media in depth filtration.

Understanding the conditions for optimum removal of suspension solids passing through porous media and the effect of pH change is of practical importance in wastewater secondary effluent polishing. It has been shown before that one of the most important controlling parameters for deposition of solids in depth filters are the electric double layer (EDL) forces and the London-van der Waals forces (Stumm and Morgan, 1996; Tien and Ramarao, 2007). The force balance between repulsive and attractive forces is summarised in the Derjaguin-Landau-Verwey-Overbeek (DLVO) interaction model which has been successfully applied for filtration of drinking water (Bradford and Torkzaban, 2008; Yuan *et al.*, 2012). Because of the nature of wastewater, other forces such as hydrogen bonding,

hydrophobic interaction, capillary forces, steric interactions (Tien and Ramarao, 2007; Bradford and Torkzaban, 2008; Yuan *et al.*, 2012), polymer bridging (Elimelech *et al.*, 1995; Lee *et al.*, 2014) and biotic colloidal behaviour (Yuan *et al.*, 2012) may also play a significant role in aggregation and deposition. This uncertainty in the nature of interactions constitutes a key knowledge gap that exists between drinking water filtration processes and the growing practice of wastewater filtration.

The purpose of this study was to therefore investigate the effect of changing the pH of wastewater and porous media on the aggregation and deposition of solids in a multimedia filter treating real wastewater secondary effluent. The filter was used as it combines media of different density and grain size, with the grain size decreasing in the direction of flow. This enabled the impact of media properties on filtration over a range of pH to be determined. Different media materials also have the potential to trap particles of different characteristics dependent on the media-suspension particle interactions. In addition to altering the wastewater solids characteristics, pH adjustment causes a number of other interactions with the wastewater, such as with the alkalinity (Shanahan and Semmens, 2015), heavy metals (Freeman, 1989; Corbitt, 1998; Fu and Wang, 2011) and the microbes (Shanahan and Semmens, 2015). Extremes of pH from very low to high was investigated as a means of altering the particle surface charge, which was hypothesised to be the driving force for aggregation and deposition through DLVO interactions.

3.2 Materials and Methods

A filtration pilot plant located at the Cranfield Sewage Treatment Works (United Kingdom) filtering real secondary treated wastewater effluent was used for this research. Upstream wastewater treatment comprised preliminary grit removal, primary sedimentation, trickling filters, alum dosing for phosphorus removal and secondary sedimentation.

3.2.1 Filter Equipment Setup

The wastewater secondary effluent from the discharge well was pumped to a mixed holding tank for pH adjustment prior to transfer to the filter rig. The surface charge on the wastewater particles was measured using zeta potential (ZP) following pH adjustment of the wastewater, following a similar approach to that used by Kim and Lawler (2005). Sodium hydroxide and hydrochloric acid of 2 molar (2M) strength was used to adjust the wastewater pH. In this research, a quadruple granular media filter adapted from a FilterClear pressure filtration system (BluewaterBio Ltd, UK) was used to investigate removal performance of each media at different pH. The pilot filter consisted of four columns (clear acrylic Perspex, 74 mm internal diameter and 700 mm height) connected in series, each containing 100 mm media depth of either anthracite, flint, alumina and magnetite respectively; the detailed description of the filter equipment is found in Appendix D.

The media properties were as follows; anthracite (Effective Size (ES)=1.12 mm, Uniformity Coefficient (UC) =1.49, loose bed porosity (ϵ_0) = 0.51, filter grain sphericity (ψ) = 0.54), flint (ES=0.55 mm, UC =1.42, ϵ_0 = 0.52, ψ = 0.64), alumina (ES=0.58 mm, UC =1.13, ϵ_0 = 0.55, ψ = 0.63) and magnetite (ES =0.26 mm, UC =1.54, ϵ_0 = 0.47, ψ = 0.84) respectively. The wastewater in the holding tank was continually mixed by a submersible centrifugal pump to keep the solids in suspension and maintain a uniform influent to the filter through a filter run. The pilot rig was operated indoors at a temperature of 21 ± 3 ^{0}C. The wastewater was pumped from the holding tank to the filter columns by a variable rate peristaltic pump (620 Industrial LoadSure, Watson Marlow, UK) through a flowmeter (SM6000, IMF Electronic Ltd, Germany) to monitor the flow rate.

Online instruments (flowmeter, pressure sensors and turbidity monitors) were connected to the pilot rig and the output analogue signals were logged into a laptop by an analogue-digital data logger. The columns were fitted with pressure transducers (PN2026, IMF Electronic Ltd, Germany) at the bottom and top of each media bed (100 mm apart) to measure the pressure drop across the filter bed. The sampling points were positioned at the influent and effluent of the filter as well as between the columns. The influent and effluent turbidity was monitored by probes placed in the holding tank and the effluent pipe (Turbi-Tech 2000LS and WaterWatch 2310, Partech, UK, respectively). The filter was run at a constant filtration rate of 25 mh^{-1}, as used for the full-scale quadruple media filter. Grab samples were collected on an hourly basis for turbidity, total suspended solids (TSS), pH, ZP and particle size analysis. After the filter cycle, the columns were backwashed individually by an air scour for two minutes followed by high rate water wash for 10 minutes at 60 mh^{-1} using filtered wastewater which enabled at least one third bed expansion.

3.2.2 Solid deposition measurements

Filtration experiments were designed to investigate the particle deposition on media materials at different pH by measuring the removal efficiency (solids, turbidity) of the filter treating wastewater secondary effluent. The TSS was determined using gravimetric analysis Method 290D, (APHA, AWWA and WEF, 2005) and turbidity was measured using a turbidity meter (2100 Lab Turb, Hach, US).

3.2.3 Wastewater Particle Aggregation

Wastewater was flocculated at different pH to understand the effect of different particle surface charge on particle aggregation. The sample used for flocculation studies was collected from the pilot filter influent and partitioned into thirteen samples for flocculation in a jar tester. The wastewater pH was adjusted using either sodium hydroxide or hydrochloric acid just prior to flocculation and particle size analysis. The wastewater pH was measured before and after flocculation; ZP was measured using a zetasizer (Zetasizer Nano ZS, Malvern, UK) from samples extracted before and after flocculation. Wastewater was flocculated on

a jar tester at 30 RPM using a rectangular paddle. Online particle size analysis was carried out using a laser diffraction instrument (Mastersizer 2000, Malvern, UK) measuring floc growth each minute for up to 100 minutes of flocculation following a similar protocol used before in Jarvis *et al.* (2005). The particle sizes were analysed in the classification of National Science Foundation/American National Standards Institute (NSF/ANSI) Standard categories for particles in water: 0-5, 5-15, 15-30, 30-50 and 50-100 μm (NSF/ANSI Standard 42 and 53).

3.2.4 Media and wastewater zeta potential measurement

The surface charge of wastewater solids and media materials was characterised at different pH to assess optimum conditions for aggregation and deposition using ZP as a surrogate for surface charge. A wastewater sample was collected from the pilot filter effluent and partitioned into subsamples of equal volume. The pH of the subsamples was adjusted incrementally between 1 and 13. Each sample was mixed in a closed bottle by shaking vigorously for one minute before being left overnight to stabilise. The following day the turbidity, TSS, pH, ZP and particle size distribution (PSD) were measured on the stabilised samples. The pH was measured using a pH meter (Jenway 3540, Bibby Scientific, UK), ZP by a zetasizer and the PSD by a Spectrex (PC-2200, Spectrex Corporation, California).

The media surface charge characteristics (ZP) were measured for the four-different media. The media were milled to a uniform size range between 0 – 20 μm prior to analysis to enable processing through the zetasizer using a method adapted from Fuerstenau *et al.* (1983). The ZP measured on milled samples was also identical to that seen for the media fines. The media was then suspended in either ultrapure water or wastewater secondary effluent to understand how the wastewater influenced the surface charge on the media compared to a pure system. Here, wastewater was first filtered through a 0.45 μm filter paper to remove the particulate component prior to addition of the media (Schrader, Zwijnenburg and Wessling, 2005; Yun *et al.*, 2011). A single large sample of each media was initially prepared, then the supernatant partitioned into equal

subsamples. The supernatant contained particles that were <3 µm which ensured that the particles were of an appropriately small size for ZP measurement.

3.2.5 DLVO Forces

The DLVO interactions are the combined effect of repulsive electric double layer (EDL) forces (F_{DL}) and attractive London-van der Waals forces (F_v) and were used here to describe aggregation of particles and attachment or deposition on to filter media. The forces were given by Tien and Ramarao (2007) as:

$$F_{DL} = \frac{\varepsilon_r \varepsilon_0 d_p \left(\zeta_p^2 + \zeta_g^2\right) \kappa e^{-\kappa\delta}}{4\left(1 - e^{-2\kappa\delta}\right)} \left(\frac{2\zeta_p \zeta_g}{\zeta_p^2 + \zeta_g^2} - e^{-\kappa\delta} \right) \qquad \textbf{Equation 3-1}$$

and

$$F_v = -\frac{H d_p}{12\delta^2} \qquad \textbf{Equation 3-2}$$

In this work the particle diameter d_p, the particle and media ZP (ζ_p, ζ_g respectively) were measured directly. The constant parameters were evaluated as Debye reciprocal double layer thickness $\kappa = 1.0 \times 10^{8}$ m^{-1}, relative permittivity of water $\varepsilon_r = 80$, permittivity of free space $\varepsilon_0 = 8.85 \times 10^{-12}$ $C^2N^{-1}m^{-2}$, (Stumm and Morgan, 1996), and the surface-to-surface separation, $\delta = 3 \times 10^{-10}$, the Hamaker constant, $H = 1.4 \times 10^{-20}$ kgm^2s^{-2} (Bai and Tien, 1997). The expressions above assumed a suspension particle to be very small compared to media grains such that the particle is modelled as a small sphere near a plane. Attractive forces are conventionally represented as negative hence the minus sign on Equation 3-2. Apart from the adhesive forces, there are other forces acting on particles as the water flows through the porous media, such as the hydrodynamic forces associated with a scouring effect on deposited solids (Bai and Tien, 1997; Ncube *et al.*, 2016). However, such forces were assumed not to vary at any pH investigated since the filter hydraulic loading rate was maintained constant.

3.3 Results and Discussions

3.3.1 Filter performance at different pH

The highest level of filter performance occurred at the wastewater pH range 6-8, peaking at neutral pH as shown by the highest solids load retention (Figure 3-1a). There was reduced solid load removal at pH less than 6 and above 8 (Figure 3-1a). The solid load retention was also found to vary significantly in the ZP range from -11 to -13 mV, however retention remained stable, but low, for ZP from -11 to +0.2 mV (Figure 3-1b). Therefore, the filter removal effectiveness seemed more dependent on pH and less so on ZP; since in the pH range 3.5 to 10 the ZP was stable at about -13 mV while solid load retention varied significantly. The solids deposition was highest close to the neutral pH where ZP was -13 mV.

The solids retention of each of the media layers closely matched that of the overall filter, with high solids retention realised around neutral pH (at ZP of -13 mV), and lower retention for pH <6 and >8 (Figure 3-2). The solids retention in the four media materials varied in the same way with pH irrespective of the media material. Therefore, the surface properties of the four-different media (anthracite, flint, alumina, and magnetite) seemed to have little influence on the selectivity of particle removal from the wastewater. However, the different media materials have an obvious practical benefit because of the different media sizes and densities that enable the filter bed to stratify such that the filter has a tapered void after backwash. Small media of high density forms the bottom filter layer while progressively larger media of lower density overlays one another producing a filter of ideal media structure.

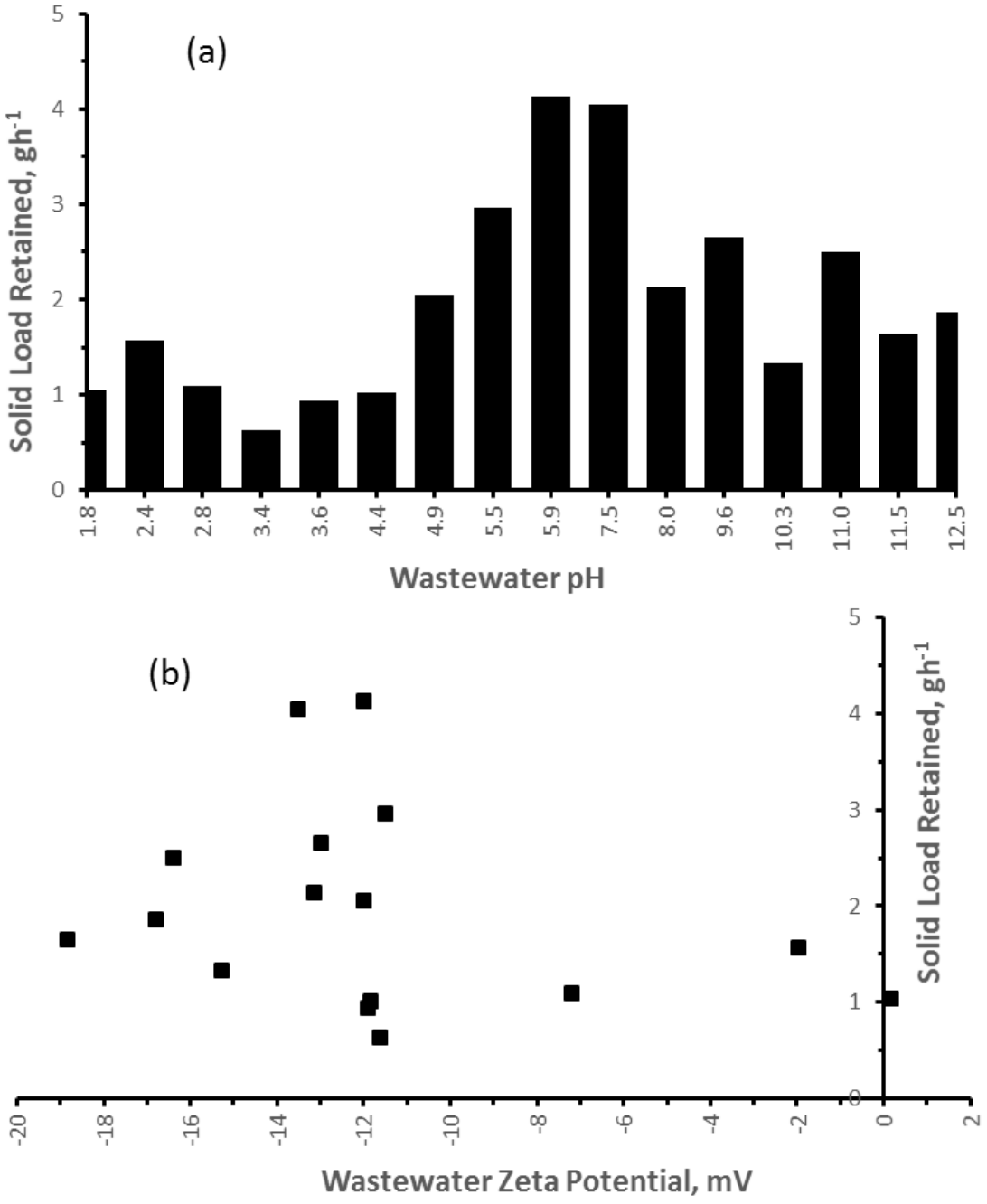

Figure 3-1 Solid load retention at different (a) wastewater pH, (b) wastewater ZP.

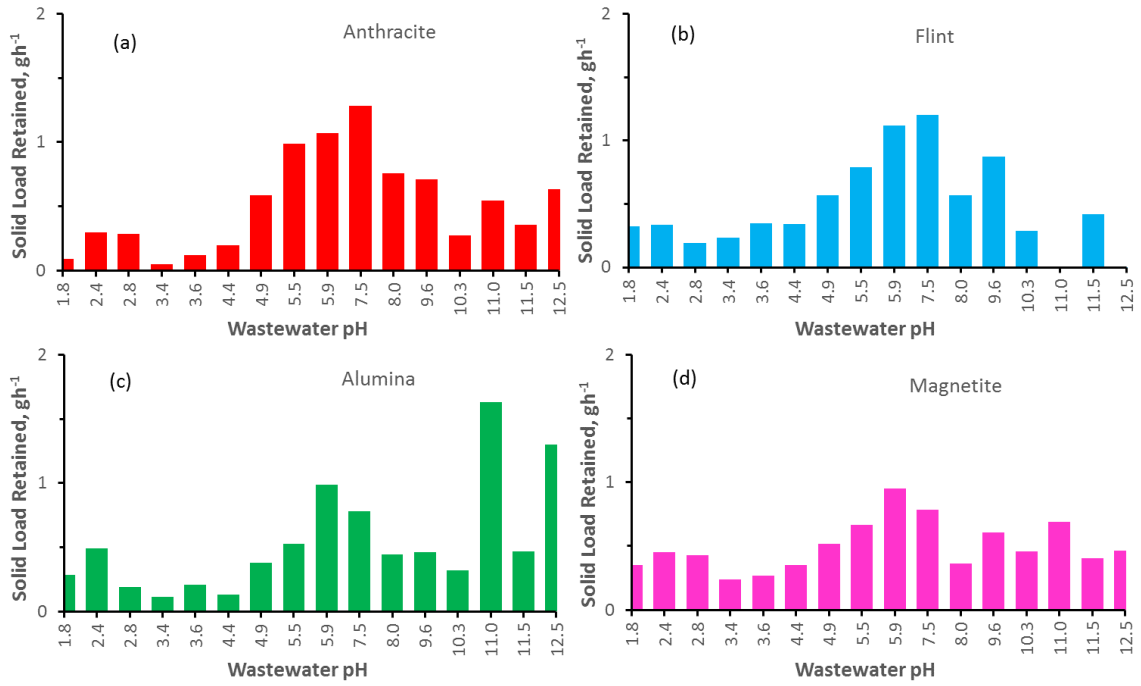

Figure 3-2 Solids load retention as a function of wastewater pH for the media (a) anthracite, (b) flint, (c) alumina and (d) magnetite.

The filter headloss increased with filtered water volume, with the rate of increase changing with wastewater pH (Figure 3-3a). The filter runs fed with high pH wastewater developed more headloss than those at low pH (Figure 3-3a and b). This corresponded to low solid load retention (2.4g) at low pH (pH 2-4), with increasing retention (11.4g) around neutral pH (Figure 3-3c). At higher pH, the headloss development was less related to the solids retention (as shown in Figure 3-1a). Fewer solids were retained at pH 10.3, 11.5 and 12.5 than at neutral pH yet the headloss developed was much greater than for the lower pH ranges (Figure 3-3c). Therefore, pH change influenced solids retention and headloss development with changes in pH likely causing changes in the wastewater solids characteristics, as discussed in the next section.

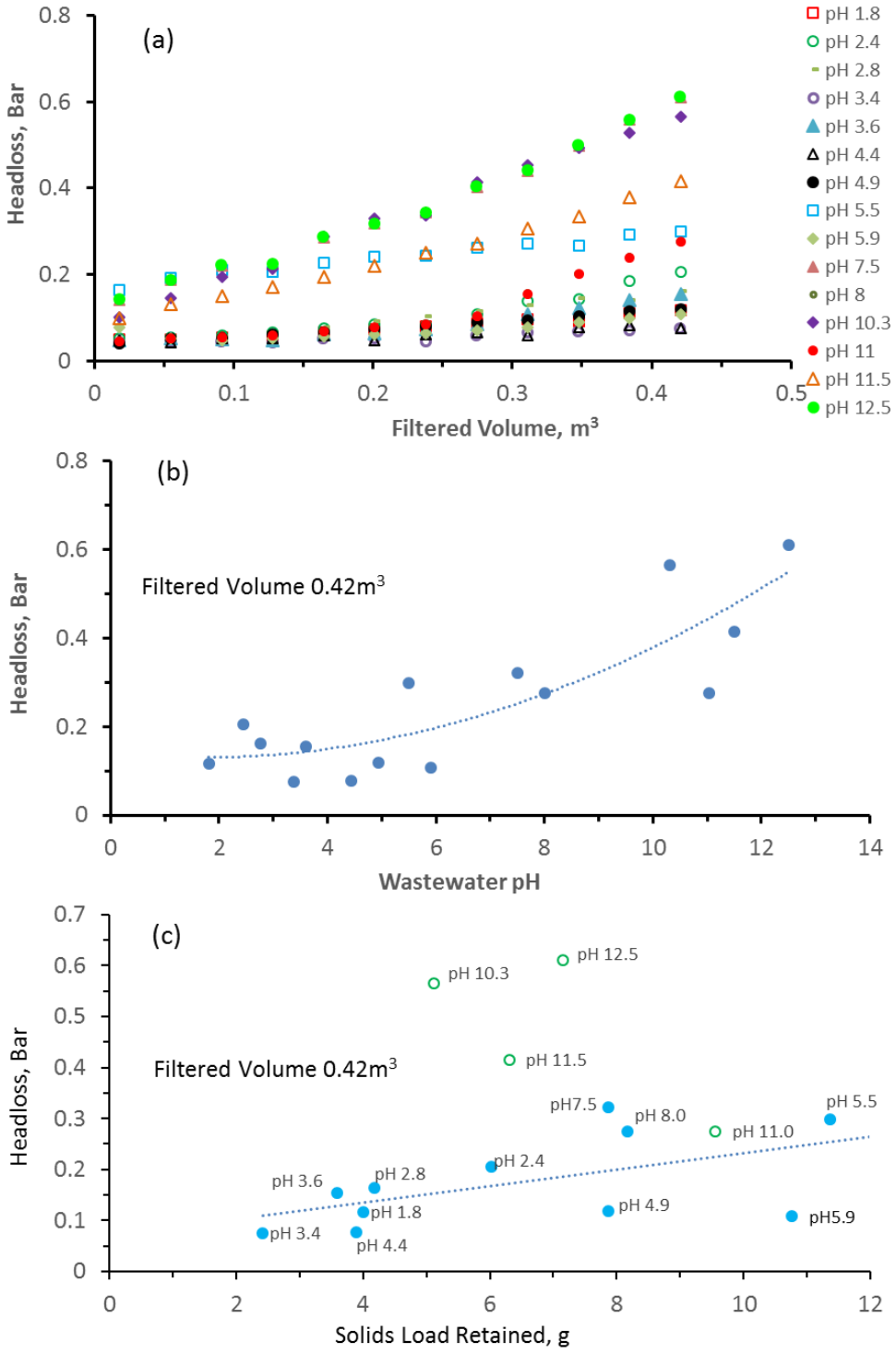

Figure 3-3 (a) Headloss development with filtered wastewater volume at different pH. (b) The filter headloss when filtered wastewater reached 0.42m³ at different wastewater pH. (c) Headloss development with solids load retained, blue dots are for <9 pH while green is >9 pH where there is precipitation. Open circles are for pH > 9. The dotted line is the best fit through the points.

3.3.2 The characteristics of wastewater secondary effluent at different pH

Retention of solids in the filter is a function of both the interactions of the particle with the filter media and the solids loading onto the filter. Therefore, to understand more about the filter performance, the characteristics of wastewater were investigated at the different pH tested. At the environmental wastewater pH (7.6±0.1), the influent TSS was 46±3 mgL^{-1} while the turbidity was 24.8±0.3 NTU. There were small changes in both TSS and turbidity for samples adjusted to low pH but a more significant increase was observed as the pH was increased above 9 (Figure 3-4a). Both the TSS and turbidity rose steeply between pH 9 and 11.5; these then dropped with further pH increase beyond 11.5. The rise in TSS and turbidity was attributed to hydroxide or carbonate precipitation; the various metals in wastewater had different minimum solubility pH, hence precipitation was observed over a range of pH (Freeman, 1989; Stumm and Morgan, 1996; Fu and Wang, 2011).

At pH >9, the solids retention was lower than at neutral pH (Figure 3-1a) although the solids concentration onto the filters was high (Figure 3-4a). The low solids retention was most likely due to hydroxide precipitates not being easily filterable as they are weaker than biological solids and fragment under high shear forces (Freeman, 1989). Beyond pH 11.5, the TSS and turbidity dropped as the hydroxides became more soluble again due to their amphoteric nature (Fu and Wang, 2011). The amphoteric character of hydroxides means that they can go back into solution at high pH. This presents problems in metal removal from mixed metal suspensions since the ideal precipitation pH of one metal may put another back into solution (Baltpurvins, Burns and Lawrance, 1996; Fu and Wang, 2011).

The surface charge of wastewater solids was measured using zeta potential to determine its influence on solids retention in the filter. At the different pH investigated, the wastewater was predominantly negatively charged. The zeta potential moved from close to 0 mV at pH 2 to -17 mV at pH 13, with a ZP of -13.9±0.2 mV at the normal wastewater pH (7.6±0.1) and an isoelectric point (IEP)

at pH 1.80±0.02 (Figure 3-4b). This result was consistent with results reported previously for treated wastewater with ZP of -14 mV at pH 7.2±0.2 (Yun *et al.*, 2011) and an IEP at pH 2-3 for bacterial flocs (Montgomery and Consulting Engineers Inc, 1985), and a ZP of -12.5 to -15 mV for a secondary wastewater sample between the pH range 4-8 (Schrader, Zwijnenburg and Wessling, 2005).

The effect of the different ZPs on particle size and concentration was then examined by measuring the wastewater floc size. The pH change resulted in alteration of the PSD in the wastewater due to a change in the balance of particle aggregation, breakage and concentration in the wastewater as well as other bio-chemical factors (Figure 3-4c). For small particles between 5-15 µm, the lowest count was 5,800 particles/mL at the normal wastewater pH, increasing to up 9000 particles/mL at both extremes of pH (Figure 3-4c). Conversely at the normal wastewater pH, larger particle size classes registered their highest counts at neutral pH while the lowest particle counts were seen at the extremes of pH (Figure 3-4c). It was apparent that particles were aggregating or fragmenting from one size class to another as the total particle count in the system remained consistent across all pH (minimum = 9.6 $x10^3$, average = 10.4 $x10^3$ and maximum = 11.4$x10^3$ particles mL^{-1}). It would therefore seem that the hydroxide precipitates enmeshed and aggregated with existing particles at pH >9 hence this caused no significant change in particle count but caused a significant increase in TSS. Jar tester flocculation of wastewater (Appendix E) showed large particle size distributions for pH > 9.

The relatively low number of small particles and the higher number of large particles at the natural wastewater pH when compared to the extremes of pH indicated optimum aggregation at that pH. Optimal filter deposition was also found around the pH range 6-8 or neutral pH region (Figure 3-4a), consistent with aggregating/larger particles being easier to remove by filtration than stable, smaller ones (Burton, Tchobanoglous and Stensel, 2003). Therefore, better particle aggregation and deposition (Figure 3-4c and Figure 3-1a) was observed under conditions when the ZP was -13.9±0.2 mV rather than under conditions of near zero surface charge (the IEP was at pH 1.8±0.2). These results were

contrary to what would be predicted from DLVO theory, where optimum particle aggregation would be expected near the IEP where the wastewater particles would have minimum repulsion. The non-congruency between the ZP and PSD measurement suggested that there was some other mechanism responsible for the aggregation of particles in wastewater other than DLVO interactions. Based on similar findings, Zita and Hermansson (1994) found DLVO theory alone could not explain aggregation in wastewater flocs in municipal wastewater. Their observations suggested that biological mechanisms and interactions were more important. The present research has extended this further to show that the mechanisms in wastewater filtration were also strongly influenced by non-charge driven processes.

The complex nature of wastewater, with considerable amounts of dissolved organic matter and a varied consortium of particles and organisms promote other interactions. In addition, as wastewater biosolids are usually characterised as being highly porous, loosely connected aggregates with an irregular structure (Jarvis *et al.*, 2005a), the primary constituent particles in wastewater flocs can be at separation distances where the DLVO interactions may be less significant and long range structural forces dominate. Such forces were dominant in promoting aggregation at natural pH, where the wastewater is unaltered in its environmental state. These forces are hydration, hydrophobic and steric interactions which act over longer ranges (Elimelech *et al.*, 1995). Studies have shown microbes forming bacteria-floc interfaces or secretions that sterically aggregate wastewater flocs (Zita and Hermansson, 1994; Sheng, Yu and Li, 2010) or bio-polymer bridging, floc forming bacteria (such as filamentous or saprophytes) bridge particles together (Lee *et al.*, 2014). Additionally, low or high pH may inactivate microbes and alter the organic materials due to reactions with H_3O^+ or OH^- ions, hence altering the structure of the wastewater, therefore inhibiting the formation of biological flocs in comparison to the neutral pH condition. Aggregation of particles is a desirable feature in depth filtration, it upgrades small particles, which are difficult to remove, to larger particles which are easier to remove in a filter (Bradford and Torkzaban, 2008). Furthermore, particles attached onto filter grains can aggregate with particles in the flow if conditions are conducive. The

resultant charge interactions between the filter media and the particles being filtered were then investigated to determine whether DLVO forces were of importance in the subsequent capture of particles.

3.3.3 Filter media zeta potential

To understand further the interaction between the wastewater suspension solids and the media materials during filtration, the surface charge of the media was also analysed at different pH. The results were broadly in line with previous analysis of similar systems. The anthracite suspensions in deionised water had an IEP at pH 5.7 (Figure 3-5a), previously measured as pH 3-6 for material derived from pulverised coal sourced from various locations (Siffert and Hamieh, 1989). Flint is a mineral silicon oxide and its IEP was determined to be at pH 1.4 (Figure 3-5b) which is in close agreement with values measured previously at pH 1.8-2.5 (Kosmulski, 2014) and less than pH 2 (Kim and Lawler, 2005). Alumina was measured with two IEP's at pH 3.3 and 8 (Figure 3-6c). Other studies have measured IEPs at pH 8 or 9 (Sprycha, 1989), at pH 8.6 and 5.4 (Gulicovski, Čerović and Milonjić, 2008) and in the range pH 2-5 (Chera *et al.*, 2007). It was thought that the presence of impurities or surfactants in the alumina used in this study were the reasons why the mineral had multiple IEPs (Chera *et al.*, 2007; Gulicovski, Čerović and Milonjić, 2008). The magnetite suspensions had an IEP at pH 2 (Figure 3-5d). This was different to previous studies that have determined the IEP at pH 6 (Sun *et al.*, 1998) and at pH 5 (Erdemoğlu and Sarikaya, 2006). This was likely to have been due to the differences in the mineral purity of the magnetite through inclusion of surfactants or heavy metals (Erdemoğlu and Sarikaya, 2006).

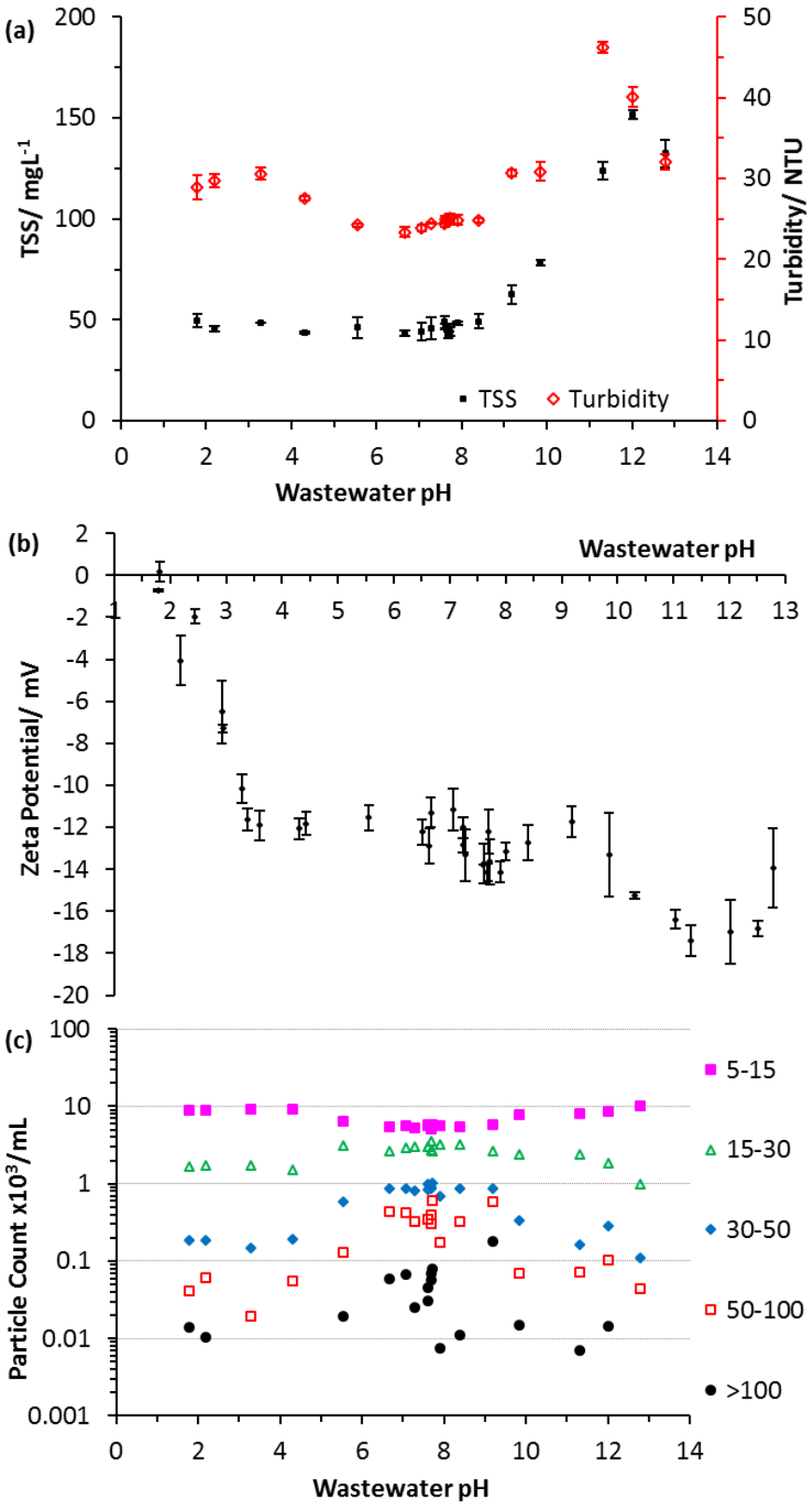

Figure 3-4 The characteristics of a sample of wastewater secondary effluent at different pH. (a) TSS and turbidity with pH. (b) ZP at different pH, (c) PSD measured using a laser diffraction instrument at different pH.

When the media were suspended in filtered wastewater, the IEP moved to a similar value to that observed for the wastewater alone (IEP at pH 2, 1.7, 2 and 2.3 for anthracite, flint, alumina and magnetite respectively) (Figure 3-5). In other words, the ZP of the media in wastewater closely matched that of wastewater (Figure 3-4b). This concurs with previous research which has shown how organic compounds present in the system may influence the characteristics of suspension particles (Yun *et al.*, 2011). This occurs because organic matter adsorbs onto particles altering the surface properties, thus changing the ZP of the particle to match that of the organic matter (Petosa *et al.*, 2010; Chera *et al.*, 2007; Erdemoğlu and Sarikaya, 2006; Yun *et al.*, 2011). This finding has implications for the consideration of aggregation and deposition processes in wastewater as the organic matter alters media surface charge. In the filtration experiments (Figure 3-2), there were no differences in solids deposition in different media materials. From these results, it can be concluded that for wastewater granular media filtration, the media surface charge itself is not important for deposition due to its immediate transformation to match that of wastewater.

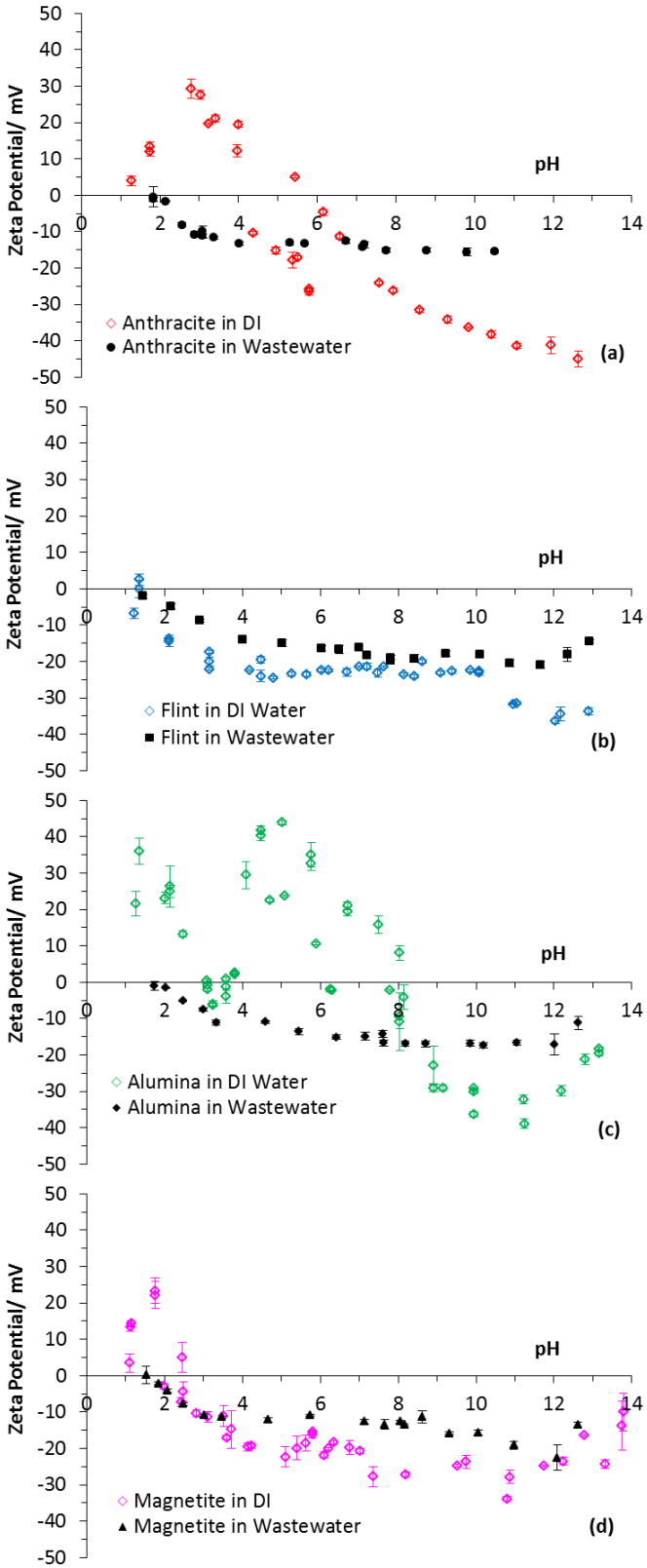

Figure 3-5 The zeta potential of (a) anthracite, (b) flint, (c) alumina and (d) magnetite with changing pH, in a suspension of either de-ionised water or filtered wastewater secondary effluent.

3.3.4 Particle Attachment

Using the ZP measurements, the EDL force (Equation 3-1) and the van der Waals force (Equation 3-2) between particles and media was used to further assess the contribution of DVLO forces to particle deposition. Using the media and wastewater ZP the EDL force was calculated to be 2.7-16.1 $x10^{-11}$ N for median sized particles in the wastewater being filtered (d_{50} size = 32 µm) across the pH range 2.8-12 (Figure 3-6a). The van der Waals force between particles of the median size (32 µm) and the media was calculated as -4.15 x 10^{-7} N (Figure 3-6b). Similar trends were observed in the EDL force and van der Waals force for the 10%tile (16 µm) and 90%tile (70 µm) particle sizes (Figure 3-6a and b). The magnitude of the attractive van der Waals force was 10^4 times greater than the repulsive EDL force, which would imply that all particles were strongly attracted to the media surface at all pH investigated with the implication that solid removal would be uniform at all pH. However, although the DLVO interactions were stable at different pH, the solid load retention varied greatly in the filtration test at different pH (Figure 3-1a and Figure 3-2).

The differences in the particle capture at different pH must therefore have been explained by other phenomena. Wastewater characteristically has a high concentration of organic matter components that may have biological activity (Yu, Gregory and Campos, 2011) as well as producing irregular shaped flocs (Jarvis *et al.*, 2008). These factors may give rise to the dominance of other forces that hold particles together in aggregates or cause attachment following deposition of solids on filter media (Petosa *et al.*, 2010). The long-range forces and biotic activity that were thought to account for differences in particle aggregation would similarly account for differences in deposition of the solids on the porous media and particles already deposited at different pH. Based on this study, such forces appear more effective near the neutral pH based on the PSD (Figure 3-4c) and solid load retention (Figure 3-1a) at different pH. The wastewater biotic conditions were unaltered around the neutral pH whereas low or high pH may have been biocidal.

Many previous studies have used model suspensions to investigate the removal efficiency of particles under different chemical conditions in depth filtration where interactions can be explicitly explained by DVLO interactions. Tufenkji *et al.* (2004) explained the removal of Cryptosporidium parvum oocysts in quartz sand filter at different ZP using the DLVO forces. Likewise, other researchers (Elimelech *et al.*, 1995; Bai and Tien, 1997; Kim and Lawler, 2006) found similar results, with high removal observed at low pH values when the ZP was close to zero. In this body of work, the DLVO interaction explained the observed changes in removal efficiencies; such studies were carried out in conditions where the concentration of organic matter and biological activity were low, typical of filtration in drinking water treatment.

However, in this study, little removal was observed at low pH when the product of the ZP for the media and suspension particles was small, high removal was seen around neutral pH, and low removal was also seen at pH greater than the neutral pH. Therefore, in wastewater filtration, DLVO interactions did not adequately explain differences in aggregation and deposition of wastewater solids alone, rather other mechanisms such as longer range interactions, bio-polymer bridging and biotic activity were the important mechanisms. The dependence of removal efficiency on wastewater pH implies that caution has to be taken when the treatment processes alters the wastewater pH such as when dosing acids, bases or coagulant to avoid impacting wastewater filtration performance (Schrader, Zwijnenburg and Wessling, 2005). Therefore, in wastewater granular media filtration, high solid removal would be achieved when the wastewater pH is in the range 6 to 8, which is close to the neutral pH. Processes such as chemical dosing with ferric sulphate for phosphorous removal lowers the pH to acidic conditions and hydroxide precipitation to remove heavy metals using lime ($Ca(OH)_2$) raises pH to alkaline conditions (Freeman, 1989). Consequently, due to the sensitivity of filtration to pH, conditioning to neutral prior to filtration would be necessary to achieve optimal solids removal.

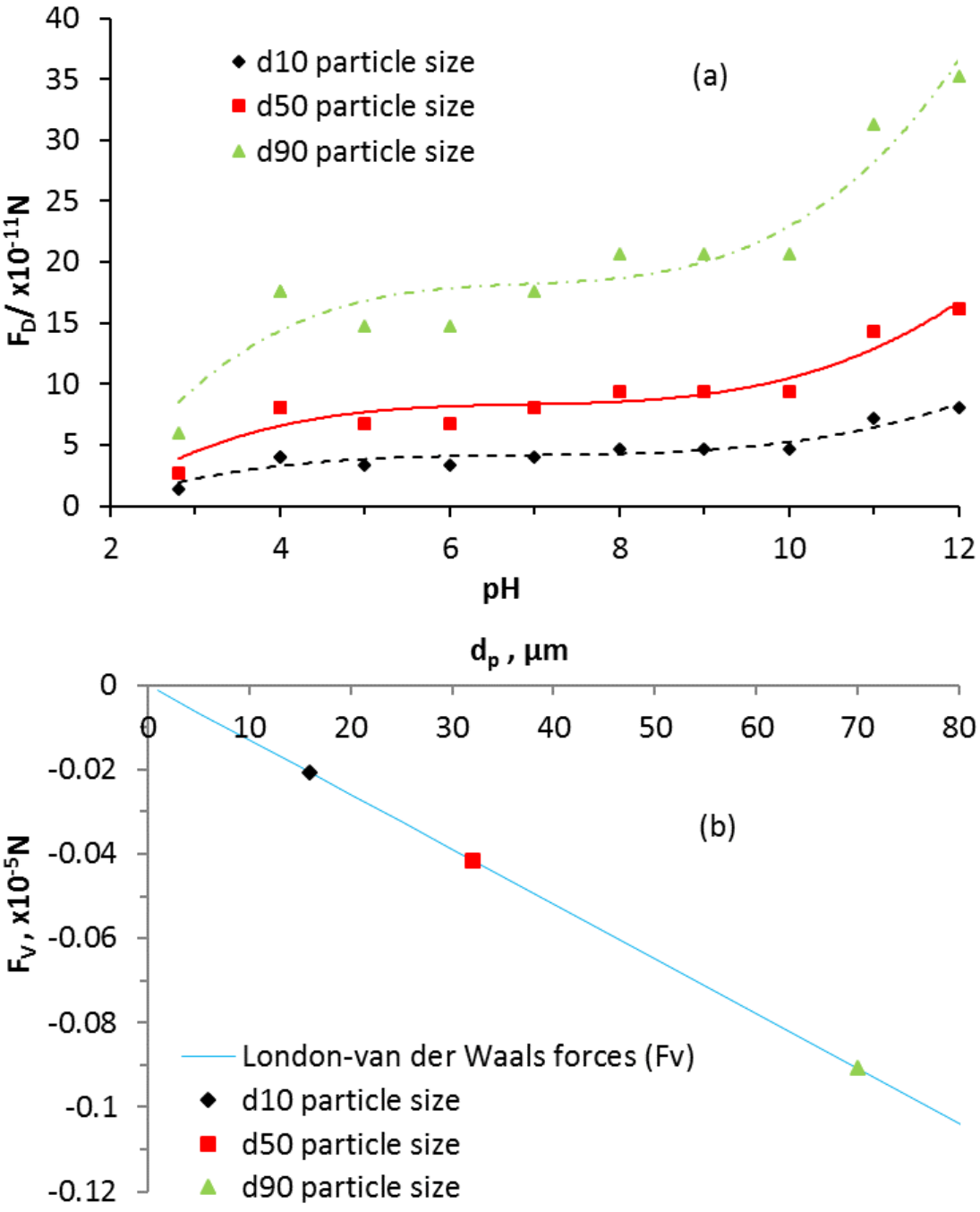

Figure 3-6 DLVO forces between media and suspension particles (a) electric double layer force (b) van der Waals force.

3.4 Conclusions

This study investigated the removal of solids at different pH from wastewater secondary effluent using a pilot scale quadruple media filter. The wastewater solids were found to be negatively charged (negative ZP) over a wide range of pH with an isoelectric point at pH 2. The different media materials were also found to match the wastewater ZP when suspended in wastewater which means that the media surface characteristics were not of significance in solids removal from wastewater. The implication is that the media material in a clean bed may have their individual surface charge/properties but this change immediately on contact with wastewater during filtration.

The wastewater solids aggregation and deposition was not solely dependent on DLVO interactions being favourable, but other forces associated with the organic material were significant in particle-particle or particle-media interactions. The long-range interactions such as hydration, hydrophobic and repulsive steric interactions, bio-polymer bridging and biotic activity were also thought to be responsible for wastewater aggregation and deposition in granular media filters. These forces were more effective around the neutral pH where the wastewater matrix was unaltered.

Each of the four media materials were found to remove wastewater solids, and effective retention by all media layers enabled solids to be distributed such that the entire depth of filter was used for solid retention. Consequently, the filter will have a high solid holding capacity and slow headloss development since solids were distributed throughout the depth of filter. The quadruple media filter hence has a capacity to operate efficiently in depth filtration of wastewater secondary effluent.

Acknowledgements

The authors greatly thank Dr Garry Hoyland, Richard Hartnett and Dr Caroline Huo at Bluewater Bio Ltd for all the industrial support and Bluewater Bio Ltd for funding and the use of the company technology to carry out this investigation. Funding from the Engineering and Physical Sciences Research Council (EPSRC) is also gratefully acknowledged.

References

Alias, S. and Assari, F. (2007) ‘The use of alum, ferric chloride and ferrous sulphate as coagulants in removing suspended solids, colour and COD from semi-aerobic landfill leachate at controlled pH’, *Waste Management & Research*, 25(6), pp. 556–565.

APHA, AWWA and WEF (2005) *Standard Methods for the Examination of Water and Wastewater*. 21st edn, *American Public Works Association*. 21st edn. Washington D.C.

Bai, R. and Tien, C. (1997) ‘Particle Detachment in Deep Bed Filtration’, *Journal of Colloid and Interface Science*, 186(2), pp. 307–17. doi: 10.1006/jcis.1996.4663.

Baltpurvins, K. A., Burns, R. C. and Lawrance, G. A. (1996) ‘Heavy metals in wastewater: Modelling the hydroxide precipitation of copper(II) from wastewater using lime as the precipitant’, *Waste Management*, 16(8), pp. 717–725.

Bradford, S. a. and Torkzaban, S. (2008) ‘Colloid Transport and Retention in Unsaturated Porous Media: A Review of Interface-, Collector-, and Pore-Scale Processes and Models’, *Vadose Zone Journal*, 7(2), p. 667.

Burton, F. L., Tchobanoglous, G. and Stensel, H. D. (2003) *Wastewater engineering: treatment and reuse*. 4th edn, *Wastewater Engineering, Treatment, Disposal and Reuse. Techobanoglous G, Burton FL, Stensel HD (eds). Tata McGraw-Hill Publishing Company Limited, 4th edition. New Delhi, India*. 4th edn. Boston: McGraw-Hill. Available at: http://www.lavoisier.fr/notice/fr097556.html.

Chera, L., Palcevskis, E., Berzins, M., Lipe, and Jansone, I. (2007) ‘Dispersion of nanosized ceramic powders in aqueous suspensions’, *Journal of Physics: Conference Series*, 93, p. 12010.

Corbitt, R. A. (1998) ‘Standard Handbook of Environmental Engineering’, *second ed. McGraw Hill, New York, Chap 6.*, p. 1314. Available at: https://books.google.com.pe/books?id=iwhSAAAAMAAJ.

Elimelech, M., Gregory, J., Jia, X. and Williams, R. A. (1995) *Particle deposition and aggregation: measurement, modelling and simulation*, *Particle deposition and aggregation*.

Erdemoğlu, M. and Sarikaya, M. (2006) 'Effects of heavy metals and oxalate on the zeta potential of magnetite', *Journal of Colloid and Interface Science*, 300(2), pp. 795–804.

Freeman, H. M. (1989) *Standard Handbook of Hazardous Waste Treatment and Disposal*. 1st edn. Edited by H. M. Freeman. McGraw-Hill Professional.

Fu, F. and Wang, Q. (2011) 'Removal of heavy metal ions from wastewaters: a review.', *Journal of Environmental Management*, 92(3), pp. 407–18. doi: 10.1016/j.jenvman.2010.11.011.

Fuerstenau, D. W., Rosenbaum, J. M. and Laskowski, J. (1983) 'Effect of surface functional groups on the flotation of coal', *Colloids and Surfaces*, 8(2), pp. 153–173.

Gulicovski, J. J., Čerović, L. S. and Milonjić, S. K. (2008) 'Point of Zero Charge and Isoelectric Point of Alumina', *Materials and Manufacturing Processes*, 23, pp. 615–619.

Jarvis, P., Jefferson, B. and Parsons, S. (2005) 'Measuring floc structural characteristics', *Reviews in Environmental Science and Biotechnology*, 4(1–2), pp. 1–18.

Jarvis, P., Jefferson, B. and Parsons, S. a. (2005) 'Breakage, regrowth, and fractal nature of natural organic matter flocs', *Environmental Science and Technology*, 39(7), pp. 2307–2314.

Jarvis, P., Parsons, S. A., Henderson, R., Nixson, N. and Jefferson, B. (2008) 'The practical application of fractal dimension in water treatment practice - the impact of polymer dosing', *Separation Science and Technology*, 43(7), pp. 1785–1797.

Kim, J. and Lawler, D. F. (2005) 'Characteristics of Zeta Potential Distribution in

Silica Particles', *Bull. Korean Chem. Soc*, 26(7), pp. 1083–1089.

Kim, J. and Lawler, D. F. (2006) 'Aspects of particle attachment in filtration', *Water Science and Technology: Water Supply*, 6(4), pp. 125–134.

Kosmulski, M. (2014) 'The pH dependent surface charging and points of zero charge. VI. Update', *Journal of Colloid and Interface Science*, 426, pp. 209–212.

Lee, C. O., Boe-Hansen, R., Musovic, S., Smets, B., Albrechtsen, H. J. and Binning, P. (2014) 'Effects of dynamic operating conditions on nitrification in biological rapid sand filters for drinking water treatment', *Water Research*. 64(m), pp. 226–236.

Montgomery, J. M. and Consulting Engineers Inc (1985) *Water Treatment Principles and Design*. New York: John Wiley & Sons.

Ncube, P., Pidou, M., Stephenson, T., Jefferson, B. and Jarvis, P. (2016) 'The effect of high hydraulic loading rate on the removal efficiency of a quadruple media filter for tertiary wastewater treatment', *Water Research*, 107, pp. 102–112.

Petosa, A. R., Jaisi, D. P., Quevedo, I. R., Elimelech, M. and Tufenkji, N. (2010) 'Aggregation and deposition of engineered nanomaterials in aquatic environments: Role of physicochemical interactions', *Environmental Science and Technology*, 44(17), pp. 6532–6549.

Schrader, G. A., Zwijnenburg, A. and Wessling, M. (2005) 'The effect of WWTP effluent zeta-potential on direct nanofiltration performance', *Journal of Membrane Science*, 266(1–2), pp. 80–93.

Shanahan, J. W. and Semmens, M. J. (2015) 'Alkalinity and pH effects on nitrification in a membrane aerated bioreactor: an experimental and model analysis.', *Water research*. 74, pp. 10–22.

Sheng, G.-P., Yu, H.-Q. and Li, X.-Y. (2010) 'Extracellular polymeric substances (EPS) of microbial aggregates in biological wastewater treatment systems: A review', *Biotechnology Advances*, 28(6), pp. 882–894.

Siffert, B. and Hamieh, T. (1989) ‘Effect of mineral impurities on the charge and surface potential of coal: Application to obtaining concentrated suspensions of coal in water’, *Colloids and Surfaces*, 35(1), pp. 27–40.

Sprycha, R. (1989) ‘Electrical double layer at alumina/electrolyte interface’, *Journal of Colloid and Interface Science*, 127(1), pp. 1–11.

Stumm, W. and Morgan, J. J. (1996) *Aquatic Chemistry: Chemical Equilibria and Rates in Natural Waters*. 3rd edn, *Environmental science and technology*. 3rd edn. New York: John Wiley & Sons, Inc,.

Tien, C. and Ramarao, B. V. (2007) *Granular Filtration of Aerosols and Hydrosols*. 1st edn, *Granular Filtration of Aerosols and Hydrosols*. 1st edn. Oxford, UK: Elsevier Ltd. Available at: http://www.scopus.com/inward/record.url?eid=2-s2.0-84882052006&partnerID=tZOtx3y1.

Tufenkji, N., Miller, G. F., Ryan, J. N., Harvey, R. W. and Elimelech, M. (2004) ‘Transport of Cryptosporidium oocysts in porous media: Role of straining and physicochemical filtration’, *Environmental Science and Technology*, 38(22), pp. 5932–5938.

Walshe, G. E., Pang, L., Flury, M., Close, M. E. and Flintoft, M. (2010) ‘Effects of pH, ionic strength, dissolved organic matter, and flow rate on the co-transport of MS2 bacteriophages with kaolinite in gravel aquifer media’, *Water Research*. 44(4), pp. 1255–1269.

Yu, W., Gregory, J. and Campos, L. C. (2011) ‘Breakage and re-growth of flocs: Effect of additional doses of coagulant species’, *Water Research*. 45(20), pp. 6718–6724.

Yuan, H., Shapiro, A., You, Z. and Badalyan, A. (2012) ‘Estimating filtration coefficients for straining from percolation and random walk theories’, *Chemical Engineering Journal*. 210, pp. 63–73.

Yun, H., Zonghai, J., Xuejin, Z. and Dangcong, P. (2011) ‘The Effect of Dissolved Organic Matter on Zeta Potential During the Coagulation Process’, *2011 International Conference on Computer Distributed Control and Intelligent*

Environmental Monitoring, pp. 1402–1405.

Zhu, G., Zheng, H., Chen, W., Fan, W., Zhang, P. and Tshukudu, T. (2012) 'Preparation of a composite coagulant: Polymeric aluminum ferric sulfate (PAFS) for wastewater treatment', *Desalination*, 285, pp. 315–323.

Zita, A. and Hermansson, M. (1994) 'Effects of ionic strength on bacterial adhesion and stability of flocs in a wastewater activated sludge system', *Applied and Environmental Microbiology*, 60(9), pp. 3041–3048. Available at: http://www.scopus.com/inward/record.url?eid=2-s2.0-0028141679&partnerID=tZOtx3y1.

4 The impact of filter bed depth and solids loading using a multimedia filter

Philani Ncube, Marc Pidou, Peter Jarvis

Cranfield Water Science Institute, Cranfield University, Cranfield, MK43 0AL, UK

Abstract

Design and operation of tertiary wastewater filters is not always well understood because of the inherent complexities of filtering a complicated wastewater matrix. The basis of design for filtration systems has usually originated from the principles used in drinking water filtration systems, however the water matrices are different. For example, wastewater usually contains more solid particles with a high biological content and there may be greater diurnal and seasonal variation in suspended solids. As such, there is some uncertainty in the performance of tertiary granular filtration system when different concentrations of solids are loaded onto the filter. Single, dual, triple and quadruple media filters were used in this research to understand how the filter depth, media type and solids concentration influenced filter performance through assessment of parameters such as solids retention, filtrate quality and headloss development. Such an understanding facilitates appropriate design and operation of purpose built wastewater filters. The filter performance was improved by making the filter deeper, however the top 0.1 depth of the filter retained the most solids. The size of the particles exiting the filter reduced with an increase in filter depth. Further increases in filter depth beyond 0.5 m for a quadruple filter produced marginal performance improvements whilst the headloss developed more quickly, reducing filter run times and throughput. An increase in the influent solids concentration had an impact on the particle removal in the filters, where for each suspended solid influent concentration increase of 10 mgL^{-1}, the removal efficiency reduced by an average factor of 0.92 while solids retention increased by a factor 1.2.

Keywords Solids concentration; wastewater; depth filtration; headloss

4.1 Introduction

More stringent discharge requirements for treated wastewater has become ever more important to improve water quality. In addition, the growing demand for water reuse in water stressed regions has driven the need for tertiary treatment of wastewater (Hamoda, Al-Ghusain and AL-Mutairi, 2004; Elfaki, Hawari and Mulligan, 2015; Yu *et al.*, 2015). There are many different forms of tertiary treatment of wastewater, of which granular media filtration is a common choice due to its simplicity and its historical performance in drinking water treatment systems (Tebbutt, 1971; West, Rachwal and Cox, 1979; Slavik, Jehmlich and Uhl, 2013; Yu *et al.*, 2015). However, the process design of granular filters is challenging as it involves a trade-off between various factors, such as the type and size of the filter media, the depth of media, the hydraulic loading rate, the headloss through the filter bed, the backwash hydraulics as well as the solids loading rate (Montgomery and Consulting Engineers Inc, 1985; Lawler and Nason, 2006; French, 2012).

Many design engineers recommend a rule-of-thumb empirical guideline for filter design stipulating the ratio of the filter depth to media size (L/d_m) being between 1000-1200 (Montgomery and Consulting Engineers Inc, 1985; Lawler and Nason, 2006; Tobiason *et al.*, 2011; French, 2012). Drinking water filters designed by this guideline have generally operated reliably and applications in wastewater have followed (Lawler and Nason, 2006; French, 2012). However, wastewater has a higher solids concentration and the quality of discharged effluent is usually lower than that required for drinking water, hence wastewater tertiary filters usually use a coarser media to facilitate feasible operation.

Lawler and Nason (2006) examined a number of operational full-scale filters used for water and wastewater filtration, and demonstrated that these filters had L/d_m ratios ranging from 850 to 1517. They recommended an L/d_m ratio of 1000 as a rationale design guidance while providing a safety margin to moderate against process fluctuations. Lawler and Nason (2006) set-out to introduce theory into filter design by using the Yao *et al.* (1971) model of the efficiency of a packed bed and empirically determined a collection efficiency of 25% for particles of

minimum removal (1-2 μm in diameter). The filter coefficient of 25% collection efficiency was then used as a basis for filter depth design (Lawler and Nason, 2006). The Lawler and Nason (2006) design criterion therefore has a theoretical basis in that it considers the temperature and filtration velocity parameters that are intrinsic to the contact efficiency η calculated by Tufenkji and Elimelech (2004).

The influent solids concentration is also known to influence the performance of depth filtration (Boller and Kavanaugh, 1995; Hamoda, Al-Ghusain and AL-Mutairi, 2004; Elfaki, Hawari and Mulligan, 2015). However, this aspect has received limited attention in wastewater filtration. From the few studies that have been carried out, mixed observations have been seen in filter performance as influent solids concentration increases (Horan and Lowe, 2007). For example, in one study, the effluent quality was found to be dependent on the influent solid concentration; the filters achieved a 70% solid removal for an influent solid concentration of 35-40 mgL^{-1} and a 32% solid removal for an influent solid concentration of 95 mgL^{-1} (Horan and Lowe, 2007). Hamoda *et al.* (2004) reported no significant change in effluent quality with changing influent concentration while Dawda *et al.* (1978) concluded that the variability of influent concentration on a full scale experiment complicated the interpretation of filter performance studies such that different filter runs could not be objectively compared. Tebbutt (1971) concluded that low solids removal in filtration tests were due to low concentrations of wastewater of 10-20 mgL^{-1} in the suspended solids. It is therefore important to establish stronger relationships between solids loading onto filtration systems and filter performance.

The wastewater filter influent quality and characteristics also play an important role in the specific mass deposit and the deposit morphology, consequently determining the filter headloss development and run duration. Therefore, there is uncertainty regarding the filter depth design and the effect of the influent suspension concentration on the output quality. The aim of this study was to determine how the filter depth, media type and the filter influent concentration influenced the effluent quality particle removal characteristics and the headloss

development using mono, dual, triple and quadruple filter media configurations treating wastewater secondary effluent. The quadruple media filter used in this study uses large media in the upper layers and small media in the lower layers hence achieving both a high throughput and a filtrate of high quality (Ncube *et al.*, 2016). Separation of the filter layers has been achieved by using large media of low density and smaller media of high density such that the bed stratifies and segregates following backwash.

4.2 Materials and Methods

4.2.1 Filtration tests

The investigation was carried out using a pilot plant located at a small sewage treatment works (STWs) in the United Kingdom filtering real secondary treated wastewater effluent. The works treats 450 m^3d^{-1} of municipal wastewater using preliminary screening and grit removal, primary sedimentation, alum dosing, trickling filters and secondary sedimentation. Secondary effluent from the STWs discharge well was pumped to a mixed holding tank from where the feed was transferred to the filter rig 7.2Appendix D). The quadruple media pressure filter design was adapted using the same media layers as used in a commercial filter system (FilterClear, BluewaterBio, UK). In pressure filters, pump pressure provides the head in the same way as the water head does in gravity filters.

Each column was loaded with a different media at a predetermined depth in the range 0.02 - 0.32 m. The media specifications were as follows: anthracite (Effective Size, ES=1.12 mm, Uniformity Coefficient, UC =1.49, clean bed porosity, ε_0 = 0.51, media sphericity, ψ = 0.54), flint (ES=0.55 mm, UC =1.42, ε_0 = 0.52, ψ = 0.64), alumina (ES=0.58 mm, UC =1.13, ε_0 = 0.55, ψ = 0.63) and magnetite (ES =0.26 mm, UC =1.54, ε_0 = 0.47, ψ = 0.84) respectively. A standard method, American Society for Testing and Materials (ASTM) C136-2006) was used to obtain the media PSD and uniformity coefficient. The loose bed porosity ε_0 was determined by method ASTM C1252-2006 and the media sphericity ψ was determined by calculations based on clean bed headloss measurement and the Kozeny-Carmen equation.

Online instruments for flowrate, pressure and turbidity were connected to the filter rig and the output analogue signals were logged onto a laptop by an analogue-digital data logger. The columns were fitted with pressure transducers (PN2026, IMF Electronic Ltd, Germany) to measure the pressure drop across the filter bed. Sampling points were positioned at the influent and effluent to each column. The influent and effluent turbidity was monitored by probes placed in the holding tank and the effluent pipe (Turbi-Tech 2000LS and WaterWatch 2310, Partech, UK, respectively). The influent turbidity was adjusted between 5 and 35 NTU for different filter runs by strategically positioning the suction pump in the discharge well to obtain different concentrations of solids in the holding tank. The filter was run at a constant flow rate of 25 mh^{-1} (the rate used in the full-scale unit); the tapered void media bed structure enabled operation at higher hydraulic loading rate than typically used in depth filtration processes. Grab samples were collected on an hourly basis for TSS, turbidity and particle size analysis. After the filter cycle terminated at 7 hours to limit to daytime operation, the columns were backwashed individually by an air scour (2 minutes) followed by high rate (60 mh^{-1}) water wash (10 minutes) using the filtrate.

4.2.2 Performance Measurements

The total suspended solids (TSS) were determined on grab samples by gravimetric analysis Method 290D, 20 (APHA, AWWA and WEF, 2005). Turbidity was measured in the laboratory using a turbidity meter (2100 Lab Turb, Hach, US). The PSD of suspension particles was measured using a laser diffraction particle sizer (Spectrex PC-2200, Spectrex Corporation, California) within 10 minutes of sampling. The grab samples were diluted with distilled water by a factor proportional to the solid concentration to minimise the effect of shielding of particles by those on the same laser path, an effect which is more prevalent at high concentrations. Dilutions were chosen as x12 for turbidity <15 NTU, x18 for 15-20 NTU, x24 for 20-25 NTU and x30 for 25-35 NTU to bring the particle concentration into the correct range for the particle sizing instrument.

4.2.3 Filter Depth Modelling

The Lawler and Nason (2006) design criterion was based on empirical observations of filter performance and filter theory. Based on the Yao *et al.* (1971) model (7.2Appendix B), the solution of the first order filtration relation for a packed bed is:

$$C_L = C_0 \exp(-\lambda L) \quad \text{and} \quad \lambda = \frac{3(1-\varepsilon)\eta\alpha}{2d_m} \qquad \textbf{Equation 4-1}$$

where C_0 and C_L is the influent and effluent solid concentration in mgL^{-1} respectively, L is the filter of depth in m, λ is the filter coefficient in unit m^{-1} which with the filter cycle stage, d_m is the media diameter in unit m and the dimensionless quantities, ε is the filter bed porosity, α is the attachment efficiency and η is the transport coefficient. Lawler and Nason (2006) designed the filter for 25 % collection efficiency of 1-2 micron particles, therefore from Equation 4-1:

$$1-\frac{C_L}{C_0} = 1-\exp\left[-\frac{3}{2}(1-\varepsilon)\alpha\eta\left(\frac{L}{d_m}\right)\right] = 0.25 \qquad \textbf{Equation 4-2}$$

Such that

$$\frac{3}{2}(1-\varepsilon)\alpha\eta\left(\frac{L}{d_m}\right) = \ln(0.75) = 0.29 \qquad \textbf{Equation 4-3}$$

The attachment efficiency α depends on the conditioning of the suspension (taken as 1 in this case) and the contact coefficient η was calculated from the Tufenkji and Elimelech (2004) model for a particle size of minimum removal (≈1.5 μm), based on the media bed characteristics and applied filtration velocity. This approach utilised both a theoretical and empirical approach to determine the filter depth L based on media bed characteristics and Equation 4-3.

4.3 Results and Discussions

4.3.1 Impact of filter depth on performance

This section presents the results and discussion of the effect of depth on the performance of filters of both single media and multimedia configurations. A single media anthracite filter is considered first followed by multimedia configurations of anthracite with flint, alumina and magnetite.

4.3.1.1 Anthracite media filter

The removal efficiency of the anthracite media filter improved as the filter media was made deeper Figure 4-1a). However, the corresponding filter coefficients for the filters were found to decrease from 5.6 to 1.8 m^{-1} as the filter depth increased from 0.02 to 0.42 m for filters operated at 25 mgL^{-1} TSS (Figure 4-1a). As the filter bed becomes deeper, the overall filter coefficient decreases exponentially, subsequently additional depth has proportionally less impact on solids removal efficiency. The filter coefficient dropped markedly in the first 0.10 m depth of the filter showing the high removal of solids that occurs in the top of the filter bed in single media filters such as the anthracite filter. This is in agreement with other researchers who have shown that solids removal was mainly concentrated in the top part of the filter (Boller and Kavanaugh, 1995; Yu *et al.*, 2015).

The filter coefficient calculated using the Lawler and Nason (2006) design criterion (Equation 4-2) was also plotted for comparison (Figure 4-1a). The design criterion filter coefficient coincide with experimentally values at depth near 0.1 m, slightly higher for lower depth and lower as the depth becomes greater than 0.1 m. Thus, the design criterion implies a slightly higher removal close to the filter surface and lower removal at depth. The results of this study show that wastewater solid particles penetrate the filter more and removal at depth is better than predicted by the Lawler and Nason (2006) design criterion. Above a depth of 0.1 m, the anthracite filter coefficients approach a constant value, consequently the filter depth would have to increase significantly to improve solids removal. For example, the filter depth would have to increase by four times from 0.1 to 0.4 m for the removal efficiency to double from 23% to 49%.

Thus, the benefit of increasing filter depth diminish as the filter becomes deeper. This is because, in single media filters, the media size increases with depth due to gravity stratification at backwash, big media grains have less surface area for contact compared to the collective surface area of many small grains. Additionally, reduction in particle concentration reduces the number of collision or contacts and hence the capture of particles. These results agree with previous work that has shown that single media filters generally over-utilise the top section of the filter for solids retention and under-utilise the rest of the filter depth for solid removal and storage (Veerapaneni and Wiesner, 1997; Williams *et al.*, 2007). Designing a filter with different media size and density improves removal, as discussed in the next section.

The modelled filter depths using the rule-of-thumb guideline and the Lawler and Nason (2006) design criterion are shown in Figure 4-1b based on the anthracite media characteristics described in section 2.3 (above). Here, the anthracite filter would be designed at 1.1 m depth by the guideline and 0.96 m depth by Lawler and Nason (2006) criterion for the filter operated at 25 mh^{-1} hydraulic loading rate. Based on the guideline design, the filter would be designed deeper in comparison to the Lawler and Nason (2006) criterion up to the hydraulic loading rate of 35 mh^{-1}, while Lawler and Nason (2006) designs the filter deeper thereafter. The two design criterions coincided at 35 mh^{-1} hydraulic loading rate, which is much higher than hydraulic loading rates typically used in practice. Thus, for all practical filtration rates, the rule-of-thumb guidelines filters are conservatively designed, hence liable to higher headloss. Deepening a filter moderates for loss in performance as hydraulic loading rate increases, however as the study shows, the depth should increase by four times to double solids removal with consequences on the headloss development (as discussed later in the chapter).

The regression fit of the percentage turbidity removal with filter depth yields a relationship of: % Removal = $79.24L^{0.53}$ (R^2=0.97). Using this equation for a filter operated at 25 mh^{-1} to extrapolate performance (Figure 4-1b), an anthracite filter of 1.1 m depth (rule-of -thumb guideline) would have a removal efficiency of 82% while at 0.96 m depth (the Lawler and Nason (2006) design) would achieve 78%

removal efficiency. Both designs would achieve acceptable filter performance for tertiary wastewater filtration, where well-performing wastewater filtration systems have removal efficiencies of about 75% or better (Hamoda, Al-Ghusain and AL-Mutairi, 2004). This extrapolation shows that an anthracite filter of 0.9 m depth is needed to achieve 75% removal efficiency, thus a slightly lower than Lawler and Nason (2006) design depth. Many water and wastewater filters typically operate at filtration rates around 5 mh^{-1} (Williams *et al.*, 2007). Operating at this hydraulic loading rate will require a filter of 0.5 m depth using the Lawler and Nason (2006) design criterion, while the guideline will still design the filter at 1.1 m. The rule-of-thumb guideline make no reference to the hydraulic loading rate while the Lawler and Nason (2006) criterion does. Therefore, many filters designed using the rule-of-thumb guideline may be over-designed in depth at typical hydraulic loading rates used for wastewater depth filtration.

While deeper filters achieve higher solids retention, there was a downside with respect to headloss development in comparison to shallow filters (Figure 4-1a and Figure 4-2). The headloss obtained by anthracite filters of different depth on filtering the same volume of wastewater, 170 m^3m^{-2} at a turbidity of 11.3±0.3 NTU and a suspended solids concentration of 26.0±0.7 mg/L, increased almost exponentially with filter depth over a 7-hour filter run (Figure 4-2b). The filter of 0.42 m depth developed a headloss of 1.04 Bar while 0.32 m filter depth developed a headloss of 0.40 Bar, and at 0.22 m depth a headloss of 0.13 Bar was developed (Figure 4-2b), this was a result of the deeper filter offering more resistance to flow and also retaining more solids.

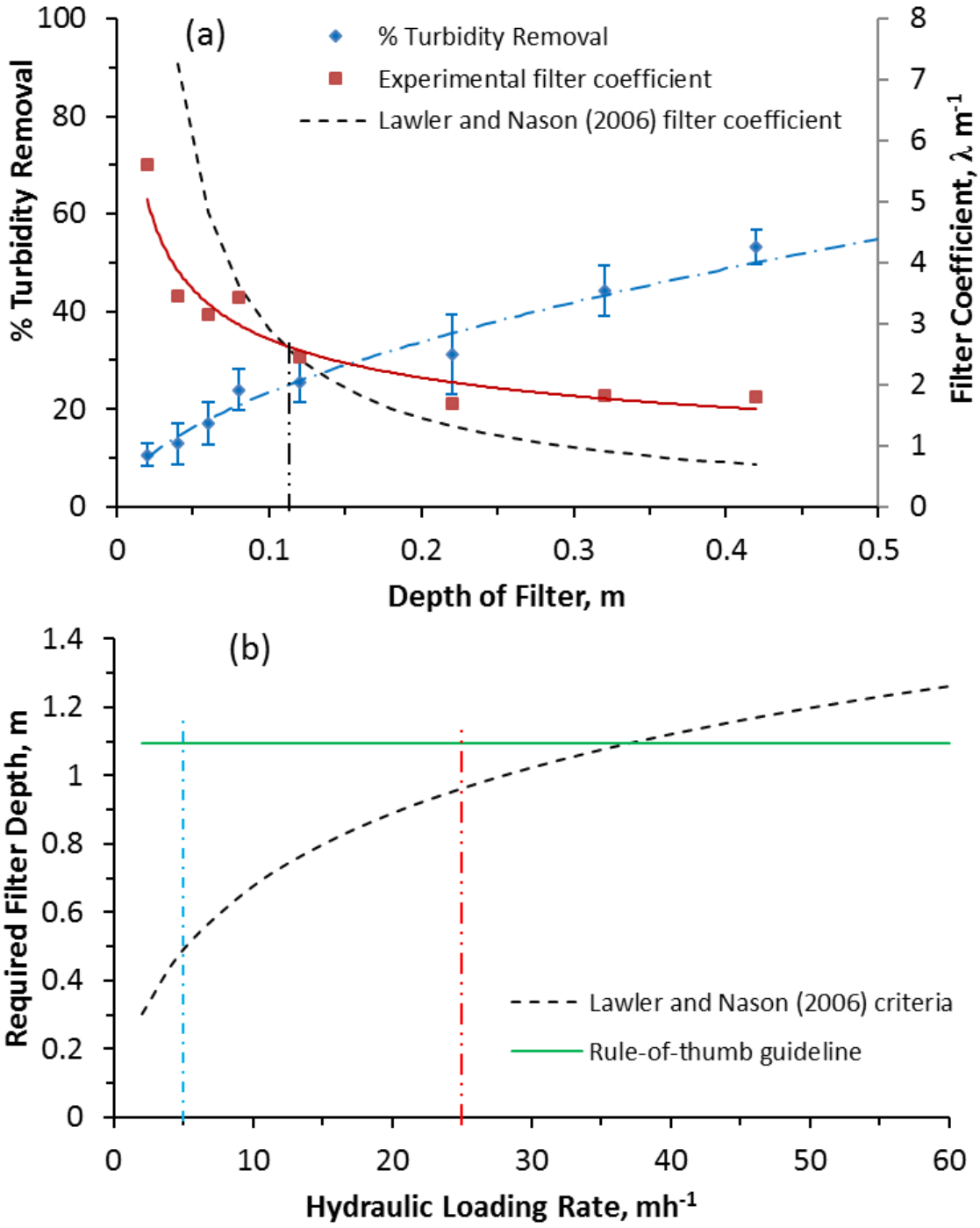

Figure 4-1(a) Anthracite % turbidity removal efficiency, filter coefficients calculated from performance data and modelled filter coefficients for filters of different depths operated at 25 mh^{-1} hydraulic loading rate. The vertical dotted line shows the 0.11m depth where the modelled and experimental filter coefficients coincide; (b) The rule-of-thumb guideline and Lawler and Nason (2006) design criterion for filter depth at different hydraulic loading rate, the blue and red dotted lines indicate the 5 mh^{-1} and 25 mh^{-1} filtration rates respectively.

A deep filter may sometimes be desired to improve effluent quality as increasing the depth of the filter also increases the filter surface area hence improving the solids retention capacity of the filter. The rapid development of headloss as filters became deeper is a major constraint in their operation as the maximum head on full scale plants is usually quite limited. For example, for a headloss of 1.04 Bar seen at 0.42 m depth filter after processing 170 m^3m^{-2} wastewater, an equivalent water head of 10.6 m is needed, which is unlikely to be available on most sites at the tertiary treatment stage, where a water head of 3-5 m is typical (Boller and Kavanaugh, 1995; Williams *et al.*, 2007). Therefore, the filters will have to backwash on a regular basis. A pressure filter can otherwise solve the headloss limitation; a pressure filter can be used as it generates a high head by the force of a pump, enabling them to attain long filter runs before a terminal head is reached. Rapid headloss development usually results from solids being loosely packed (Veerapaneni and Wiesner, 1997), pressure filters pack solids compactly and makes greater usage of void space for solids retention.

4.3.1.2 Multimedia filters

The single media anthracite filter had the lowest removal efficiency for equal depth of filter bed in comparison to filters of multimedia configurations (Figure 4-3a). The filter performance improved with each additional media material. As an illustration, for filters of a combined depth of 0.24 m treating 170 m^3m^{-2}, the anthracite single media filter, anthracite-flint dual media filter, anthracite-flint-alumina tri-media filter, and anthracite-flint-alumina-magnetite quadruple media filter had solids load retentions of 5.81g, 8.63g, 10.96g and 11.33g respectively (Figure 4-3a) resulting in specific mass deposits of 5.64 $kgTSS.m^{-3}$, 8.38 $kgTSS.m^{-3}$, 10.64 $kgTSS.m^{-3}$ and 11 $kgTSS.m^{-3}$. A multimedia filter does not need to be very deep to achieve acceptable effluent quality. For example, for a quadruple filter operated at 25 mh^{-1}, a 75% removal efficiency was achieved by a 0.40 m deep filter in comparison to 50% achieved by same depth of a single media anthracite filter (Figure 4-3 b and a Figure 4-1). However, this comparison was constrained by differences in media size since anthracite was larger than the other media materials.

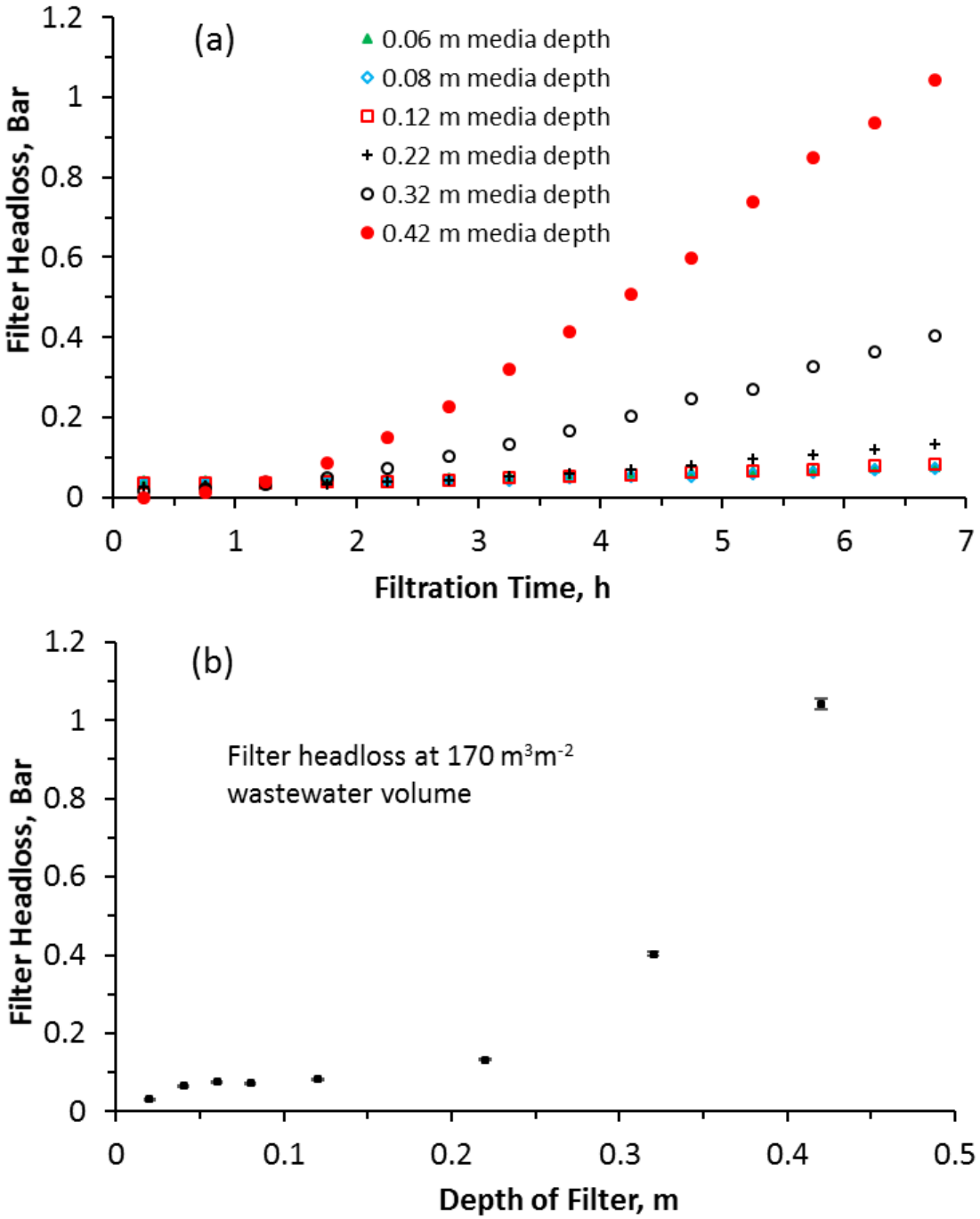

Figure 4-2 (a) Headloss development of anthracite filters of different depths filtering 26 mgL^{-1} influent wastewater concentration with similar operation conditions; (b) Headloss of each filter after filtering 170 m^3m^{-2} wastewater.

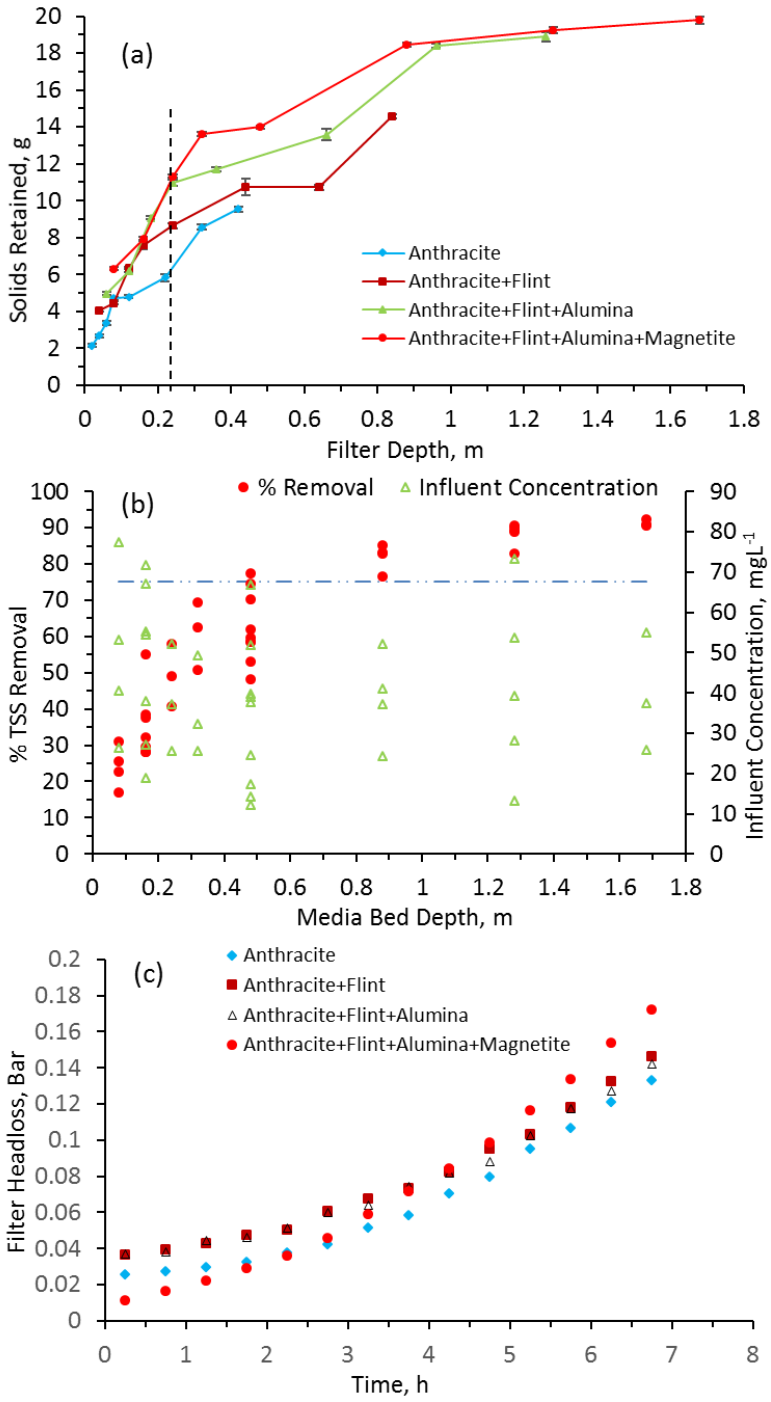

Figure 4-3 (a) Solids load retention of single media and multimedia filters of different depths after processing 170 m^3m^{-2} wastewater, dotted line indicates a 0.24 m filter depth. Each point represents a filter run of a filter of a specific depth; (b) the removal efficiency of quadruple filters of different depth for different influent suspended solids concentrations. The dotted line represents a typical removal efficiency of a performing wastewater filter; (c) the filter headloss

developed by multimedia filters of 0.24 m depth in processing 170 m^3m^{-2} wastewater.

The multimedia filter configurations developed comparable headloss to the single media anthracite filter despite them retaining more solids than the anthracite filter of equivalent depth (Figure 4-3c). The comparison of the single media anthracite filter to multimedia configurations show a headloss range of 0.13 to 0.17 Bar, just a small difference between the filters all of 0.24 m depth (Figure 4-3c). The small difference in headloss development occurred despite the quadruple filter retaining almost double the mass of solids. Thus, following 7 hours' filtration of 170 m^3m^{-2} volume of wastewater for the single media anthracite filter and quadruple filter the solids retained were respectively 5.81 and 11.33 g.

For quadruple filters of different depth, the headloss increased exponentially as the filters became deeper (Figure 4-4a). For example, the headloss after filtering 170 m^3m^{-2} wastewater volume ranged from 0.2 Bar for 0.1 m depth filter to 1.3 Bar for 1.7 m depth filter (Figure 4-4a). In reaching the 1 Bar headloss, the quadruple filter (1.5 m depth) retained 19.50 g after filtering 170 m^3m^{-2} of wastewater while the anthracite filter (0.4 m depth) retained 9.54 g for the same volume treated and for the same influent concentration (Figure 4-2, Figure 4-3 and Figure 4-4). Therefore, in addition to a superior solids retention in filters of multimedia configuration, additional media moderates headloss development such that the filter can be run with greater throughput and solids retention.

The multimedia filters removed more particles compared to the single media filter. The characteristics of the particles in the effluent were also found to depend on the depth of the filter. A shallow filter such as the 0.24 m deep had large numbers of particles ranging from 5-100 µm (Figure 4-4b). For example, there were 6045 particles/mL between 5-15 µm decreasing to 340 particles/mL for 50-100 µm (Figure 4-4b). For a deeper filter of 1.28 m depth, fewer particles were seen in these size ranges. For example, there were 5093 particles/mL in the 5-15 µm range and only 47 particles/mL in the 50-100 µm range (Figure 4-4b). Thus, the particle size exiting the filter reduced as the filters got deeper. One apparent anomaly in the data obtained was for particles <5 µm, where these sized particles

were increasingly found as the filter increased in depth. These small particles were seen for filter depths of 0.48 m and above. Explanations for this can be ascribed to a combination of factors. Firstly, the potential for shielding of small particles by larger particles is increased at higher particle concentrations. While sample dilution was carried out on these samples by a factor proportional to the solids concentration, this did not consider differences in the particle size distributions present in the samples. Secondly, at higher solids concentrations, small particles may aggregate into larger ones in the measuring cell due to increased opportunities for particle-particle collisions. Regardless of this, the deeper filters had more attachment sites hence the greater solids retention and improved removal of large particles, which was in good correlation to the solids removal efficiencies observed (Figure 4-3a).

The investigation on filter depth and the media configuration highlighted some important features. The initial layers of the filter retained more solids than the lower layers, which reflected that the filter may not have to be very deep. An ideal depth filter would use the whole filter depth for solids retention. However, filter coefficients decay exponentially with depth since solids retention decreases with depth. The single media filter designed by the rule-of-thumb guideline as 1.1m depth was deeper than was required for wastewater filtration since the initial 0.10 m was the most effective for solids removal while the rest of the depth brings marginal improvement in performance. The benefit of increasing depth from 0.1 m to 1.1 m was counter balanced by the high headloss development as the filter gets deeper. The filter design by Lawler and Nason (2006) also underestimated the measured filter coefficient at depth greater than 0.1 m hence in that respect will conservatively design the depth of filter required for wastewater filtration. This research suggests that shallower filters may be sufficient to achieve the required effluent quality in wastewater filtration, for example a 0.48m quadruple filter can achieve the 75 % solids removal efficiency typical of performing wastewater tertiary filter.

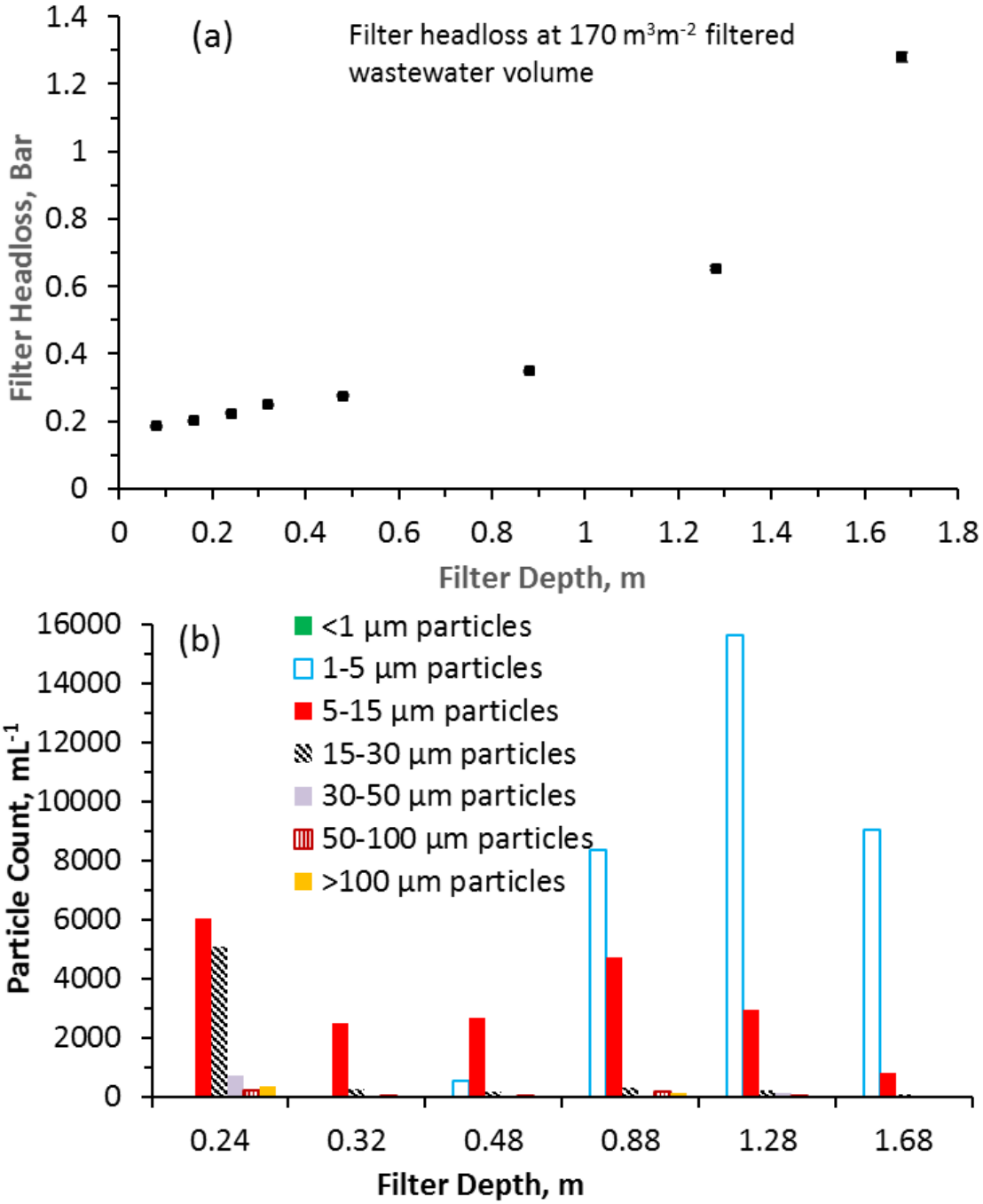

Figure 4-4 Quadruple media filter operational performance. (a) The headloss developed after filtering 170 m^3m^{-2} wastewater for filters of different depth. (b) The concentration of particles of specified size bands exiting filters of increasing depth.

4.3.2 Impact of solids concentration on filter performance

The retention of solids in the filter configurations were investigated at different influent concentrations to represent diurnal changes in the quality of the secondary effluents received by filtration processes from changes in hydraulic loading rate, clarifier performance or other operational parameters. The changes in solids retention with increasing influent concentration (Figure 4-5a), and the percentage solids removal (Figure 4-5b) have been illustrated for similar media bed depths of anthracite media and quadruple media filters.

An anthracite and a quadruple filter of 0.32 m depth were used as an illustration, with other filter depths showing similar observations. The anthracite filter of depth 0.32 m was found to have a solids load retention that increased from 0.79 gh^{-1} to 2.52 gh^{-1} while the % solids removal decreased from 52% to 27% when the influent solids concentration increased from 13.1 mgL^{-1} to 73.2 mgL^{-1} respectively (Figure 4-5a and b). The anthracite filter coefficients were also found to decrease from 1.48 m^{-1}, 1.18 m^{-1} and 0.93 m^{-1} as the influent solids concentration increased from 25 mgL^{-1}, 39 mgL^{-1} and 53 mgL^{-1} respectively (Appendix C, Figure C-1). Thus, the filter effluent quality was seen to deteriorate when the influent concentration increased. In comparison to a single media anthracite filter, the quadruple media filter of a similar total depth had almost double the solids retention (1.45 gh^{-1} compared to 0.79 gh^{-1}) and one and a half times more percentage solids removal (77.4% compared to 52%) compared to the anthracite filter of the same overall depth when filtering wastewater at a concentration of 13.1 mgL^{-1}. The quadruple filter had the potential to retain more solids because of its tapered void structure, where the media size decreased with depth unlike the single media anthracite filter where the media size increased with depth. A decrease in media size with depth results in an increase of collector surface area with depth. This observation illustrated the improvement in solids retention that could be achieved by replacing a single media filter by a multimedia filter of the same total depth. For both the anthracite and quadruple filter of 0.32 m depth, each suspended solid influent concentration increase of 10 mgL^{-1} reduced the removal efficiency by an average factor of 0.9 while the solids retention increased by a factor of 1.2.

As illustrated previously, increasing the filter depth improves filter performance. This occurs since deepening the filter increases the collector surface area for solids removal. A deep filter has a large collector surface area and hence may be affected differently by an increase in influent concentration. To illustrate, the impact of solids concentration was investigated for a quadruple filter of 1.28m depth. The solids load retention increased as the influent solids became more concentrated, changing from 1.18 gh^{-1} to 7.15 gh^{-1} as the influent concentration changed from 13.1 mgL^{-1} to 73.2 mgL^{-1} respectively (Figure 4-6a). Additionally, unlike as was observed in the shallow filters of 0.32m depth (Figure 4-5b), the percentage solids removal efficiency remained stable with increasing influent solids concentration (Figure 4-6b). This is also shown from analysis of the quadruple filter coefficient (λ), which remained constant between 1.3-1.4 m^{-1} from 25 to 53 mgL^{-1} influent solids concentration changes for quadruple filters operated at 25 mh^{-1} (Figure 4-6b). Detailed determination of the filter coefficient is provided in the Appendix C, Figure C-2.

Wastewater treatment works are often challenged to meet a certain discharge limit despite the changing influent solids concentration particularly high concentrations. A buffer capacity would be desired by improving the filter performance. Improvement of effluent quality can be achieved by either making the filter deeper which is not usually operationally viable or using multimedia filter configurations of equivalent depth in place of a single media filter. A deep quadruple filter was also found to moderate the removal efficiency when the influent concentration increased, thus a high effluent quality can be maintained (Figure 4-6b). Alternatively, to achieve high quality effluent standard, filters could be run in series, with an upstream roughing filter followed by a polishing filtration step since filters perform better at low concentrations as observed in this study (Figure 4-5a). At low solids concentration, there is a higher particle to collector ratio than at high concentrations hence increasing chances of particle capture by collectors.

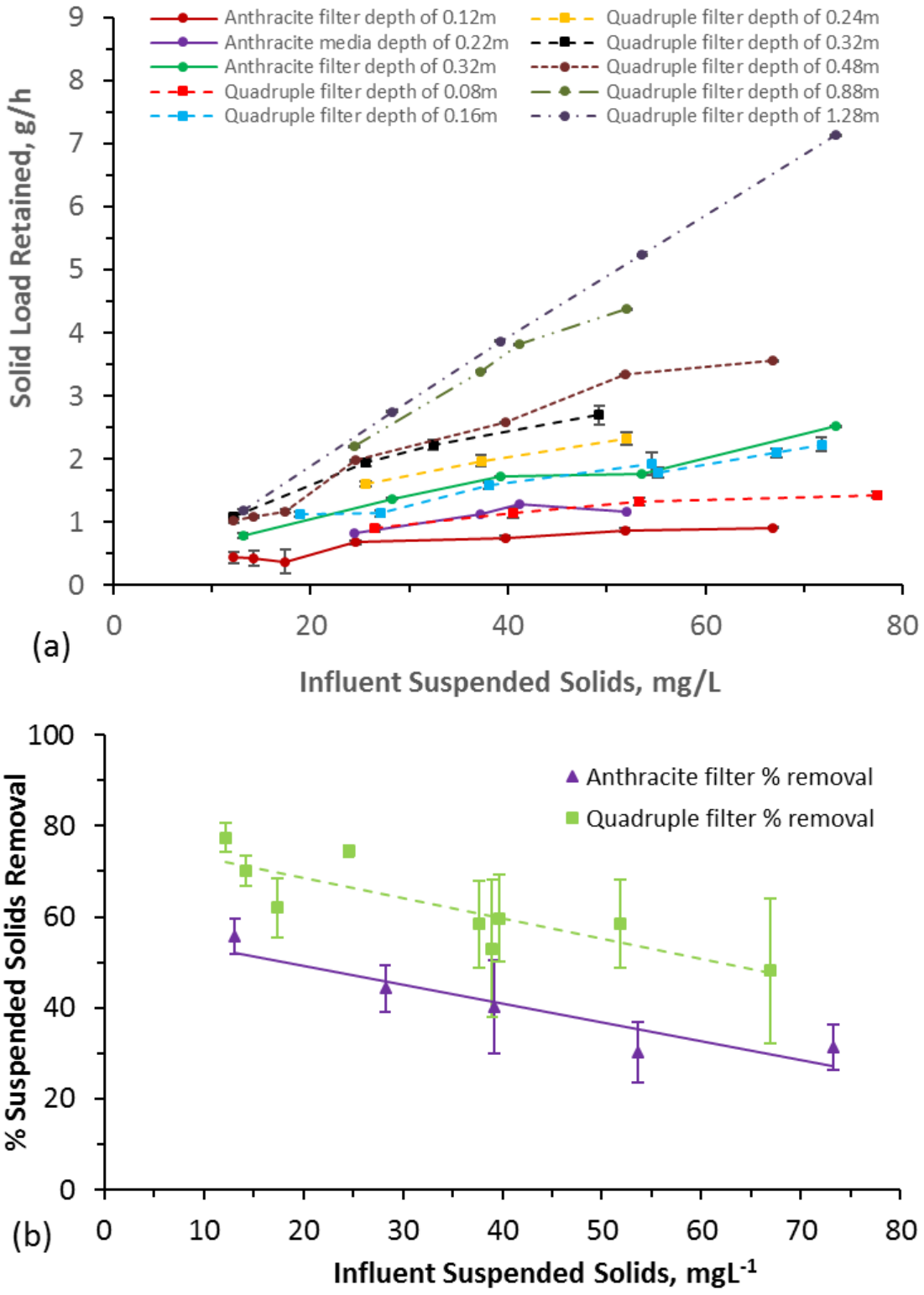

Figure 4-5 (a) The solids load retention with increasing influent solids concentration for anthracite and quadruple media filters of different depths. (b) Average % solids removal of each filter cycle for an anthracite filter and a quadruple media filter both of 0.32m depth.

The filters also developed headloss at different rates when filtering wastewater influents of different concentrations. A filter of 0.48 m depth was chosen to illustrate the changes in headloss with influent concentration, with similar trends observed for other depths. The 0.48 m deep quadruple filter developed headloss gradually at 12.2 mgL^{-1} influent concentration, but the increase was rapid at influent concentrations of 66.9 mgL^{-1} (Figure 4-7a). The solids retained by the filter per unit bed volume was determined as 3.4 kgm^{-3} when the influent solids concentration was 12.2 mgL^{-1} developing a headloss of 0.1 Bar for a filter run of 6.75 hours (Figure 4-7b). At an influent concentration of 66.9 mgL^{-1}, over the same filter run time, the solids retained per unit bed volume was 11.6 kgm^{-3} developing a headloss of 1.7 Bar. The filter headloss increased with solids retention per unit filter volume with greater headloss developed for higher concentration influent solids because of greater solids retention. Consequently, at high influent solids concentration, while the solids load retention was good there was reduced throughput before the available head of the filter. The throughput here refers to the amount of wastewater produced.

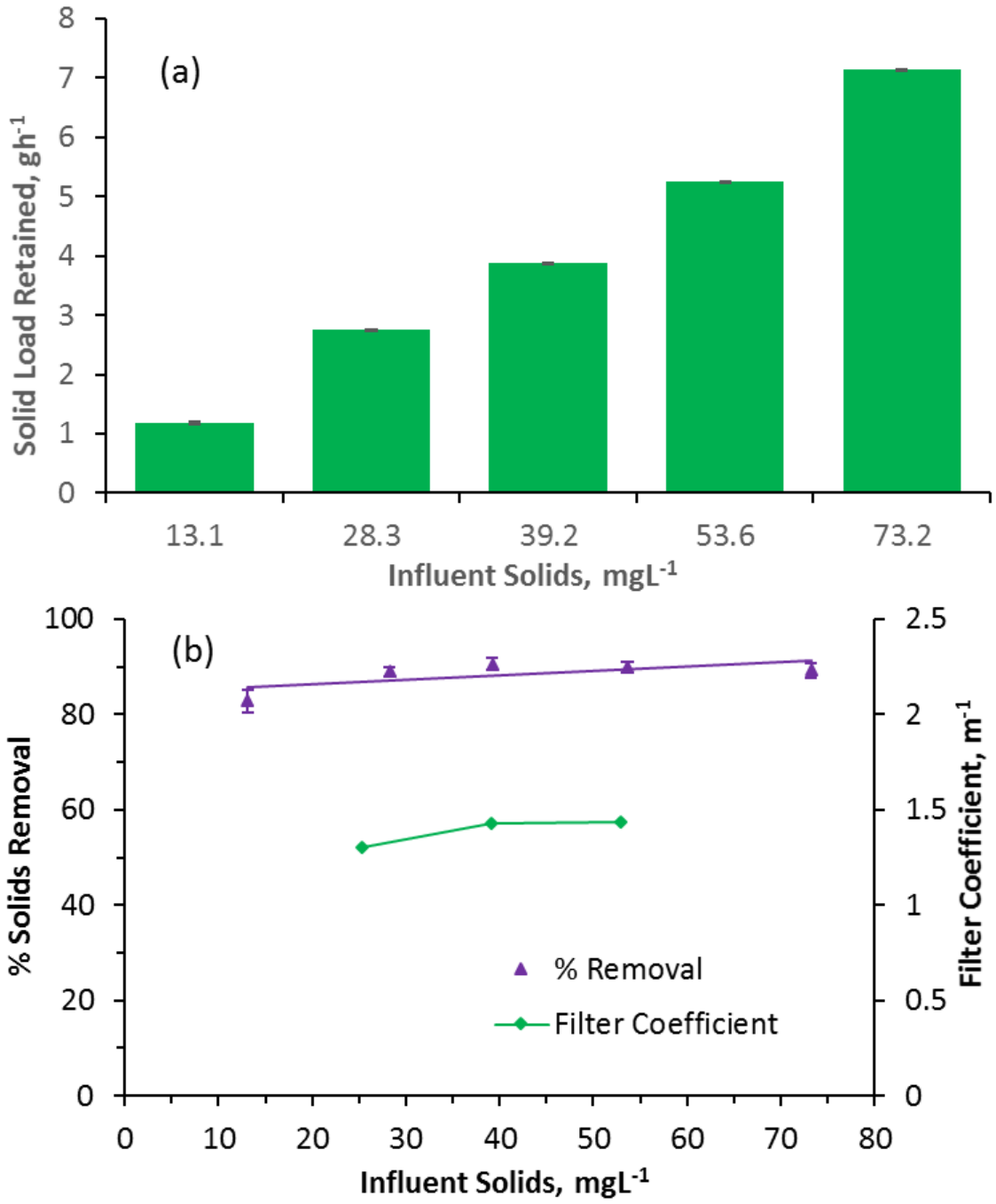

Figure 4-6 (a) Solids load retained at different influent solid concentration for a quadruple filter of 1.28m media depth chosen as an Illustration. (b) % Solids removal efficiency for the 1.28 m depth quadruple filter and the quadruple filter coefficients for filters operated at different influent solids concentrations. The graphs for the calculation of filter coefficients is provided in the Appendix C, Figure C2.

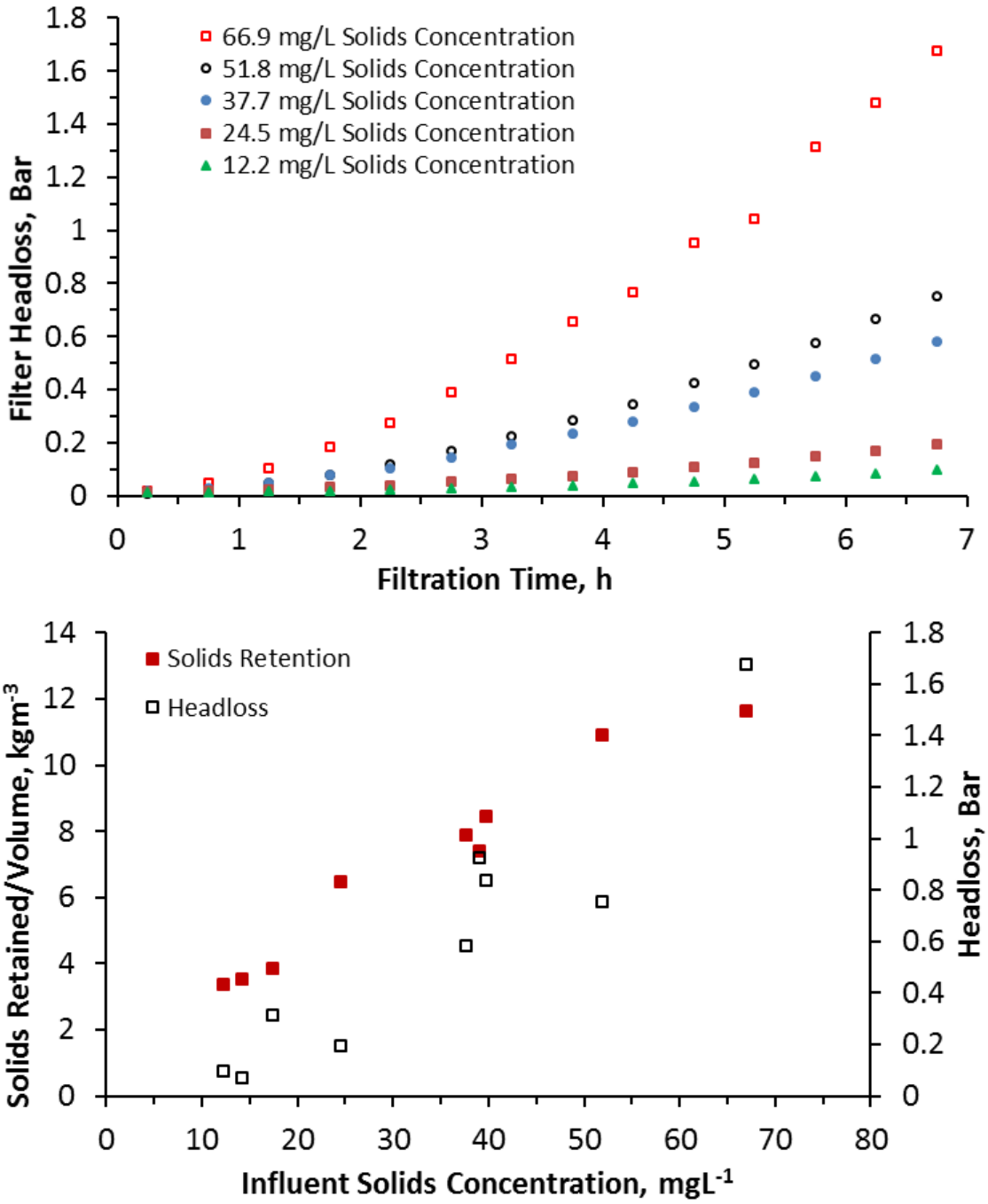

Figure 4-7 (a) Headloss development on a quadruple filter of bed depth 0.48m for influents of different concentrations. (b) Solids retention per filter volume and the headloss developed after 6.75h filtration time for 0.48m depth filter operated at different influent solids concentrations.

4.4 Conclusions

The following conclusions were drawn from the study.

(a) The solids retention and removal efficiency was improved by making the filter deeper but headloss development becomes a limiting factor with increasing depth.

(b) Filters for wastewater filtration can be designed at lower depth than those using the commonly used design criteria to meet desired effluent quality since most of filter removal takes place close to the surface.

(c) Additional layers of filter materials from single, dual, triple to quadruple improved the filter performance for the same depth of filter bed.

(d) Filters of multimedia configuration developed headloss slower than single media filters of equivalent depth and retained more solids by distributing them throughout the depth of the filter.

(e) Increasing the influent concentration increased the solids retention while solids removal efficiency decreased for shallow filters. However, deepening the filter moderated the removal efficiency such that a stable efficiency was observed.

Acknowledgements

The authors greatly thank Dr Garry Hoyland, Richard Hartnett and Dr Caroline Huo for industrial support and advice and Bluewater Bio Ltd for funding and permitting the use of the company technology to carry out this investigation. Funding from the Engineering and Physical Sciences Research Council (EPSRC) is also gratefully acknowledged.

References

APHA, AWWA and WEF (2005) *Standard Methods for the Examination of Water and Wastewater*. 21st edn, *American Public Works Association*. 21st edn. Washington D.C.

Boller, M. A. and Kavanaugh, M. C. (1995) 'Particle characteristics and headloss increase in granular media filtration', *Water Research*, 29(4), pp. 1139–1149.

Dawda, M., Davidson, M. and Middlebrooks, J. (1978) 'Granular media filtration of secondary effluent', *Journal (Water Pollution Control Federation)* , 50(9), pp. 2143–2156.

Elfaki, H., Hawari, A. and Mulligan, C. (2015) 'Enhancement of multi-media filter performance using talc as a new filter aid material: Mechanistic study', *Journal of Industrial and Engineering Chemistry*, 24, pp. 71–78.

French, D. (2012) 'Granular filter media: Evaluating filter bed depth to grain size ratio', *Filtration and Separation*. 49(5), pp. 34–36.

Hamoda, M. F., Al-Ghusain, I. and AL-Mutairi, N. Z. (2004) 'Sand filtration of wastewater for tertiary treatment and water reuse', *Desalination*, 164(3), pp. 203–211.

Horan, N. J. and Lowe, M. (2007) 'Full-scale trials of recycled glass as tertiary filter medium for wastewater treatment', *Water Research*, 41(1), pp. 253–259.

Lawler, D. F. and Nason, J. A. (2006) 'Granular media filtration: Old process, new thoughts', *Water Science and Technology*, 53(7), pp. 1–7.

Montgomery, J. M. and Consulting Engineers Inc (1985) *Water Treatment Principles and Design*. New York: John Wiley & Sons.

Ncube, P., Pidou, M., Stephenson, T., Jefferson, B. and Jarvis, P. (2016) 'The effect of high hydraulic loading rate on the removal efficiency of a quadruple media filter for tertiary wastewater treatment', *Water Research*, 107, pp. 102–112.

Slavik, I., Jehmlich, A. and Uhl, W. (2013) 'Impact of backwashing procedures on

deep bed filtration productivity in drinking water treatment', *Water Research*. 47(16), pp. 6348–6357.

Tebbutt, T. H. Y. (1971) 'An investigation into tertiary treatment by rapid filtration', *Water Research*, 5(3), pp. 81–92.

Tobiason, J., Cleasby, J., Logsdon, G. and O'Melia, C. (2011) 'Granular Media Filtration', in Edzwald James (ed.) *Water Quality & Treatment: A Handbook on Drinking Water*. 6th edn. Massachusetts: American Water Works Association, American Society of Civil Engineers, McGraw-Hill, p. 10.1.

Tufenkji, N. and Elimelech, M. (2004) 'Correlation Equation for Predicting Single-Collector Efficiency in Physicochemical Filtration in Saturated Porous Media', *Environmental Science and Technology*, 38(2), pp. 529–536.

Veerapaneni, S. and Wiesner, M. R. (1997) 'Deposit Morphology and Head Loss Development in Porous Media', *Environmental Science & Technology*. ACS, 31(10), pp. 2738–2744.

West, J., Rachwal, A. J. and Cox, G. C. (1979) 'Experiences with high rate tertiary treatment filtration in the Thames Water Authority', *Journal of the Institution of Water Engineers and Scientists*, 33, pp. 45–63.

Williams, G. J., Sheikh, B., Holden, R. B., Kouretas, T. J. and Nelson, K. L. (2007) 'The impact of increased loading rate on granular media, rapid depth filtration of wastewater', *Water Research*, 41(19), pp. 4535–4545.

Yao, K., Habibian, M. T. and O'Melia, C. R. (1971) 'Water and Waste Water Filtration: Concepts and Applications', *Environmental Science & Technology*, 5(11), pp. 1105–1112.

Yu, J., Li, Y., Liu, Z., Zhang, W. and Wang, D. (2015) 'Impact of loading rate and filter height on the retention factor in the model of total coliform (TC) removal in direct rapid sand filtration', *Desalination and Water Treatment*, 54(1), pp. 140–146.

5 The effect of high hydraulic loading rate on the removal efficiency of a quadruple media filter for tertiary wastewater treatment

Philani Ncube[a], Marc Pidou[a], Tom Stephenson[a], Bruce Jefferson[a], Peter Jarvis[a]

[a]Cranfield Water Science Institute, Cranfield University, Cranfield, MK43 0AL, UK

Abstract

It is well known that filtration removal efficiency falls with an increase in flow rate; however, there is limited supporting experimental data on how removal efficiency changes, particularly for filters with multiple layers of media and for wastewater filtration, a practice that is becoming more common. Furthermore, information is not available on the characteristics of particles that are removed at different flow rates. Here a quadruple media filter was operated at hydraulic loading rates (HLRs) between 5 and 60 mh^{-1} with subsequent measurement of total suspended solids, turbidity and particle size distribution (PSD). Samples were collected from the filter influent, effluent and also between media layers. Pressure changes across the filter layers were also measured. The solids removal efficiency of the filter varied inversely with increase in filtration flow rate. However, the multiple media layers reduced the negative impact of increased HLR in comparison to a single media filter. High flow rates also transported solids, such that particle retention and headloss development was distributed across the entire depth of the filter. There was also a progressive decrease in suspension PSD through the filter. The particle hydrodynamic force simulation was consistent with the changes in measured PSD through the filter layers.

5.1 Introduction

Granular media filtration is one of the oldest forms of treatment technology used in the production of potable water and is still widely used due to its reliability and low cost (Burton, Tchobanoglous and Stensel, 2003; Han, Fitzpatrick and Wetherill, 2009; Kim and Lawler, 2012). However, the filtration of wastewater secondary effluent is a relatively recent practice in situations that demand high water quality. This includes tertiary treatment of wastewater for water reuse in water stressed areas (Aronino *et al.*, 2009; Ho *et al.*, 2011; Bloetscher *et al.*, 2014; Christou *et al.*, 2014), or to meet standards for discharge to sensitive water courses and drinking water protected areas (Defra, 2012).

Granular media filtration removes suspended solids and colloidal particles, which includes particulate biochemical oxygen demand (BOD), chemical oxygen demand (COD), microbes and other suspended chemical contaminants from wastewater secondary effluent (Illueca-Muñoz *et al.*, 2008). Removal of solids is also a necessary step for chemical and UV disinfection to be effective in wastewater reclamation (Lazarova *et al.*, 1999; Williams *et al.*, 2007) by reducing shielding of viruses by solid particles (Kirkpatrick and Asano, 1986). In the UK, tertiary filtration of wastewater secondary effluent is usually necessary in environmentally sensitive areas where tight regulatory discharge requirements are needed. Tertiary treatment is therefore becoming more common to safeguard public health as well as to minimise pollution (Langenbach *et al.*, 2010; Ho *et al.*, 2011; Li *et al.*, 2012).

Filtration of wastewater is significantly more challenging than for potable water due to the higher solid loads, much of which is organic in nature. To illustrate, the average influent turbidity to a drinking water works filtration system is typically around 1 NTU with occasional spikes up to 8 NTU (Zouboulis, Traskas and Samaras, 2007). However, secondary effluents typically have turbidity between 5 to 20 NTU (TSS 10-40 mgL^{-1}) (Lander, 1994; Aronino *et al.*, 2009) which causes rapid headloss development in conventional sand filters (Lander, 1994). Aronino *et al.* (2009) observed cake formation on a single media depth filter treating wastewater secondary effluent and while the filter was effective for virus removal,

the headloss build up was rapid. The increase in normalised headloss (NHL) per filtered volume was 1.65 $(m^3m^{-2})^{-1}$ at a filtration rate of 5 mh^{-1} (Aronino *et al.*, 2009). Rapid headloss development shortens the filter runs and hence results in a low product water throughput before backwash is necessary.

One of the reasons for rapid headloss development in conventional mono-media filters is because the backwash cycle leads to media stratification, with small media grains at the top and large grains at the bottom (Baruth, 2005). The stratified arrangement leads to accumulation of the solids in the top layer in the subsequent filter cycle and hence results in underuse of the rest of the filter depth for solid retention. The proprietary tetra mono-media filter is said to promote deep penetration (Severn Trent Services, no date); this is achieved by use of coarse media of uniform size to discourage size stratification and also promote deep penetration of solids (Severn Trent Services, no date; Crittenden *et al.*, 2012). Use of coarse media however has a downside in that it reduces surface area for particle capture. Multimedia filters benefit from the use of both large and small grains, being designed using large grains of low density media and small grains of dense media. Such a design enables the backwash to stratify the filter bed keeping large grains at the top and small grains at the bottom; hence encouraging deep penetration of solids and improved performance at depth. This counters some of the operational problems associated with single media filters offering the opportunity for such filters to operate longer and at increased hydraulic loading therefore retaining more solids. In this research a quadruple media filter was used that consisted of layers of anthracite, flint, alumina and magnetite, moving from large to small grain size from top to bottom.

Previous studies involving granular media filters have investigated hydraulic loading rates (HLRs) up to 25 mh^{-1} (Cleasby and Baumann, 1962; Suthaker, Smith and Stanley, 1995; Williams *et al.*, 2007; Li *et al.*, 2012), rates typical of rapid gravity filters. Pressure filters have the capacity to operate at a higher rate (Tobiason *et al.*, 2011). However, there is a paucity of information on particle capture when pressure filters operate at high HLRs. Operating the filter at higher rates is a cost-effective means to increase throughput for the same area of filter

bed. The aim of this research was to therefore investigate the effect of high hydraulic loading rate on the solids removal efficiency of a quadruple media filter treating wastewater secondary effluent. The contribution of each media layer was evaluated and the change in treated water particle size distribution (PSD) was assessed through each media layer.

5.2 Materials and Methods

5.2.1 Filtration tests

The investigation was carried out using a pilot plant located at a small sewage treatment works (STW) in the United Kingdom, filtering real secondary treated wastewater effluent. The STW treats 450 m^3d^{-1} of municipal wastewater using preliminary screening and grit removal, primary sedimentation, alum dosing, trickling filters and secondary sedimentation. Secondary effluent from the STWs discharge well was pumped to a mixed holding tank from where the feed was transferred to the filter rig (see schematic in 7.2Appendix D). The quadruple media filter pilot plant was adapted using the same media layers as used in a commercial filter system (FilterClear, Bluewater Bio, UK). For this study, the media were separated into different columns and connected in series so that the effect of each layer could be isolated. To investigate possible aggregation during transfer, the filter effluent was flocculated in jar test at 30 revolutions per minute with online size measurement. The particle sizes only increased gradually by 50 % over 2 hours. In the pilot plant, transfer between the layers had a retention time under 2 minutes, hence on this basis aggregation during transfer may be neglected. Wastewater was pumped from a holding tank to the filter columns by a variable rate peristaltic pump (620 Industrial LoadSure, Watson Marlow, UK) through a flowmeter (SM6000, IMF Electronic Ltd, Germany). The filter rig consisted of four clear acrylic perspex columns of 700 mm height and 74 mm internal diameter. The columns were connected using PVC fittings and a clear PVC hose. Filter nozzles (Type KRI, KSHFisher, Germany) were fitted at the base of the columns to hold the filter media in place and evenly distribute the flow

during the backwash cycle. The columns were connected so that the outlet of one column was fed into the inlet of the next.

Each column contained a different media at a depth of 100 mm. The media were, anthracite (effective size, ES =1.12 mm, uniformity coefficient, UC =1.49, loose bed porosity, ε_0 = 0.51, sphericity, ψ = 0.54), flint (ES=0.55 mm, UC =1.42, ε_0 = 0.52, ψ = 0.64), alumina (ES=0.58 mm, UC =1.13, ε_0 = 0.55, ψ = 0.63) and magnetite (ES =0.26 mm, UC =1.54, ε_0 = 0.47, ψ = 0.84) respectively. A standard method was used to obtain the media effective size and uniformity coefficient (American Society for Testing and Materials (ASTM) C136-2006). The loose bed porosity ε_0 was determined by method ASTM C1252-2006 and the sphericity ψ was determined by calculations based on clean bed headloss measurement and the Kozeny-Carmen equation.

Online instruments for flow, pressure and turbidity were connected to the filter rig and the output analogue signals were logged into a laptop by an analogue-digital data logger (D-149, Dataq Instruments, UK). The columns were fitted with pressure transducers (PN2026, IMF Electronic Ltd, Germany) at the bottom and top of each media bed (100 mm apart) to measure the pressure drop across the filter bed. Sampling points were positioned at the influent and effluent to each column. The influent and effluent turbidity was monitored by probes placed in the influent holding tank and the effluent pipe (Turbi-Tech 2000LS and WaterWatch 2310, Partech, UK, respectively). The filter was run at a determined constant flow rate (from 5 to 60 mh^{-1}) for each filter run and grab samples were collected on an hourly basis for analysis. At the end of the filter cycle, the columns were backwashed individually by an air scour (2 minutes) followed by high rate (60 mh^{-1}) water wash (10 minutes) using the filtrate.

5.2.2 Performance Measurements

The total suspended solids (TSS) were determined from grab samples by gravimetric analysis Method 290D (APHA, AWWA and WEF, 2005). Turbidity was measured in the laboratory using a turbidity meter (2100 Lab Turb, Hach, US). During sampling, the opening and closing of the sampling taps was carried out slowly to avoid hydraulic shocks in the system. The PSD of suspension

particles was measured using a laser diffraction particle sizer (Spectrex PC-2200, Spectrex Corporation, California) within 30 minutes of sampling to minimize aggregation. The grab samples were diluted by a factor of 12 to reduce the effect of particle shielding at high concentrations.

5.2.3 Filtration models

Filtration was modelled using colloid filtration theory to show the effect of HLR on the retention of suspension particles by collectors, an approach used in drinking water filtration, but not to our knowledge in wastewater filtration. Filtration models have been defined assuming laminar flow conditions (Tobiason *et al.*, 2011), the flow regime is an important aspect of hydrodynamics signified by Reynolds number. For a fixed porous media bed, the Reynolds number (Re) is calculated by (Tobiason *et al.*, 2011; Crittenden *et al.*, 2012):

$$\mathrm{Re} = \frac{\rho_w u d_{eq}}{\mu} \qquad \textbf{Equation 5-1}$$

Where ρ_w is the water density, u is the superficial velocity, d_{eq} is the media equivalent diameter and μ is the dynamic viscosity. Re < 1 relates to Darcy flow, 1 < Re < 100 is Forchheimer flow, 600 < Re < 800 is transitional flow and 800 < Re is considered fully turbulent flow (Crittenden *et al.*, 2012). In this study HLR of 5-60 mh^{-1} were investigated for which the Reynolds numbers (Equation 5-1) for each media in the respective flow range were anthracite (2.2 < Re < 26.4), flint (0.9 < Re < 11.2), alumina (0.9 < Re < 11.4) and magnetite (0.6 < Re < 6.7). These Reynolds numbers are within the Darcy and Forchheimer flow regimes which are considered steady laminar flow and hence in the range where fundamental filtration models can be applied. These models, however, do not address the hydrodynamic variability in flow and the effect on streamlines introduced by the use of angular media (Crittenden *et al.*, 2012). This was therefore an important element of investigation for this study.

HLR is a major factor affecting both particle deposition and detachment in filtration (Bai and Tien, 1997). The particle deposition rate is calculated from the single collector transport efficiency η and attachment efficiency α (Yao, Habibian and O'Melia, 1971). The contact/transport efficiency is the rate at which approaching suspension particles contact the collector. This has been described analytically (Yao, Habibian and O'Melia, 1971) and through regression analysis of numerical simulation data (Rajagopalan and Tien, 1976; Tufenkji and Elimelech, 2004) and takes into account the suspension hydrodynamics (Crittenden *et al.*, 2012). The retention of particles (attachment efficiency) on collectors has mainly been explained in terms of the adhesive forces such as the double layer forces and the London-van der Waals forces (Stumm and Morgan, 1996; Tien, 2000), however the hydrodynamic conditions also have a strong influence on whether the particles are retained on collectors (Torkzaban, Bradford and Walker, 2007; Williams *et al.*, 2007). Adhesive forces depend on the physicochemical characteristics of the particles and media and are therefore independent of HLR. High HLR increases the hydrodynamic scouring force and can impair the retention of particles in the filter. The quadruple media filter has a tapered void; as such the channels between the collectors narrow down the bed, bringing particles nearer to the collectors hence increasing the chance of being captured. However hydrodynamic forces may also change in each media layer due to different bed porosities among layers. This investigation therefore explored the change in HLR and its direct influence on the hydrodynamic forces in each layer; the model demonstrated how hydrodynamic forces impact on the retention of particles on collectors. It was also of relevance to demonstrate the change in suspension particle size changes through the media layers.

5.2.4 Hydrodynamic Forces

Particles near collectors are subject to hydrodynamic forces. Since the suspension particles are much smaller than the media grain, they can be modelled as small spheres on a collector plane (Bai and Tien, 1997). The hydrodynamic force acting on the particles can be resolved to two components, the hydrodynamic lifting force (F_l) (normal to the plane of the collector) and the

hydrodynamic drag force (F_{Hydro}) (tangential to the collector) (Bai and Tien, 1997; Tien and Ramarao, 2007). The hydrodynamic lifting force is given by (Bai and Tien, 1997):

$$F_l = k_l d_p^3 (\mu\gamma)^{-0.5} \left(3\mu \frac{A_S}{d_m} \frac{u}{\varepsilon_0 - \sigma} \right)^{1.5} \qquad \textbf{Equation 5-2}$$

Where k_l is the coefficient for lifting force, d_p is the suspended particle diameter, d_m is the filter media diameter, μ is the dynamic viscosity, v is the kinematic viscosity, σ is the bulk specific deposit, ε_0 is the clean bed porosity, u is the filtration velocity and the porosity-dependent parameter based on the Happel's flow model, A_S is defined as $2(1-p^5)/w$, and $w=2-3p+3p^5-2p^6$, $p=(1-\varepsilon)^{1/3}$. The lifting force (Equation 5-2) acts in the same plane as the adhesion forces between the particle and the media; it is assumed to be the force causing the particle to drift away from the collector if it detaches (Bai and Tien, 1997; Tien and Ramarao, 2007).

The hydrodynamic drag force on a particle is the component of the hydrodynamic force along the collector plane given by (Bai and Tien, 1997):

$$F_{Hydro} = 2.551 \times 3\pi\mu \frac{A_S}{d_m} d_p^2 \frac{u}{\varepsilon_0 - \sigma} \qquad \textbf{Equation 5-3}$$

The hydrodynamic drag force has an effect of either sliding or rolling the particle along the collector depending on its point of action on the particle. This displacement is resisted by a sliding frictional force (F_f) calculated as (Bai and Tien, 1997):

$$F_f = k_f \frac{6(1-\varepsilon_0)}{d_m} \frac{H d_p}{12\delta^2} \qquad \textbf{Equation 5-4}$$

Where k_f is the sliding friction coefficient, H is the Hamaker constant and δ is the particle-media separation distance. The coefficient k_f may also be the rolling friction coefficient if assumed the mechanism of particle motion instead of sliding (Bergendahl and Grasso, 2003; Tien and Ramarao, 2007). Both the hydrodynamic drag force and the sliding frictional force act tangentially to the collector, such that the net tangential force (F_T) is given by $F_T = F_f - F_{Hydro}$. The

hydrodynamic drag force increases with filtration rate while the frictional force is independent of the filtration rate.

5.3 Results and Discussions

5.3.1 Turbidity and TSS measurement

The wastewater influent to the filter had the following characteristics: TSS = 21±2 mgL^{-1}, turbidity = 10.2±0.9 NTU, temperature = 20±2 °C and pH = 7.6±0.3. The influent particles had a d(0.5) size of 20 µm. Wastewater TSS was linearly correlated to turbidity with a gradient of 2.3 $mgL^{-1}NTU^{-1}$ (root mean square fit of 0.7), this fits well with previously published data for secondary effluent having gradients of 2-2.4 $mgL^{-1}NTU^{-1}$ (Burton, Tchobanoglous and Stensel, 2003). The TSS removal versus turbidity removal efficiency correlates with a gradient of 0.78 (root mean square fit of 0.8). This comparison of removal efficiency shows that TSS removal efficiency was slightly less than turbidity removal efficiency since unlike turbidity, the TSS is insensitive to the contribution of very small particles that might pass through the filter paper. In this study turbidity was chosen over TSS measurement to evaluate the removal of suspended solids since turbidity can better detect small changes in solids concentration, particularly for the small particles in the system. Williams *et al.* (2007) also found the removal of turbidity to be a representative measure of particle and bacteria removal and hence a good indicator of the overall filter performance.

5.3.2 Overall filter performance

Throughout the study, the influent wastewater turbidity was kept at 10.2±0.9 NTU to facilitate comparison between filter runs. The average effluent turbidity increased from 1.9±0.1 NTU at 5.0 mh^{-1} to 6.8±0.5 NTU at 62.7 mh^{-1} in a five hour filter run; resulting in removals of 80 and 40% respectively for the quadruple filter (Figure 5-1a). The turbidity removal efficiency decreased almost linearly with increasing HLR. The turbidity removal results were compared with literature wastewater filtration removal for increasing HLR (Figure 5-1a). To facilitate comparison, the gradients of linear regression fits were used to measure change in percentage removal per unit change in HLR (measured as $\%m^{-1}h$). For single

media sand filters the suspended solid removal efficiency reduced by 4.4 $\%m^{-1}h$ for an initial influent turbidity of 35 NTU when the HLR changed from 5 to 10 mh^{-1} (Li *et al.*, 2012). A separate study saw reductions of 3.9 $\%m^{-1}h$ for an initial turbidity of 10 NTU when the HLR increased from 5 to 15 mh^{-1} (Yu *et al.*, 2015). An anthracite-sand dual-media filter reduced by 1.25 $\%m^{-1}h$ for an initial turbidity of 6.5 NTU and the HLR increased from 12.2 to 24.4 mh^{-1} (Williams *et al.*, 2007). In the present study, the quadruple-media filter had turbidity removal reducing by 0.67 $\%m^{-1}h$ for an initial influent turbidity of 10.2 NTU with HLR increasing from 5 to 60 mh^{-1}. Hence the increase in HLR had a greater impact on the filter removal efficiency for single media filters than for dual media filters. The impact was even less for the quadruple filter. Therefore, the smallest deterioration in effluent quality with increasing HLR was seen for the quadruple filter, even though the HLR was also over a much wider range. This comparison shows that increasing the number of filter layers buffers the effect of the increased HLR hence giving more robust filter performance.

In this study, the removal efficiency of the top (anthracite) layer decreased quickly from 58 to 40% between 5 mh^{-1} and 10 mh^{-1}, a reduction of 3.5 $\%m^{-1}h$ (Figure 5-1b), a value close to the literature values seen for a single media filter (4.4 $\%m^{-1}h$ in Li *et al.* (2012) and 3.9 $\%m^{-1}h$ in Yu et al. (2015). The quicker change in removal efficiency across a single layer such as may be seen in conventional sand filters (Li *et al.*, 2012; Yu *et al.*, 2015) may be one of the key reasons why there has been reluctance to increase HLRs in conventional mono-media filters. There have been attempts to buffer the effect of increasing HLR on removal efficiency by increasing the coagulant dose (Williams *et al.*, 2007) or changing the filter bed depth (Lawler and Nason, 2006) which works to some extent, but has the downside of quickly raising the filter headloss. In this study, the impact became less abrupt for the combined anthracite and flint layers (2.1 $\%m^{-1}h$), for the combined anthracite, flint and alumina (1.7 $\%m^{-1}h$) and for the quadruple filter (1.2 $\%m^{-1}h$) in the HLR range 5 to 10 mh^{-1}, showing the moderation that the additional layers have when the HLR was increased (Figure 5-1b).

Increasing HLR was observed to significantly affect the particle sizes exiting the filter. Analysis of the 10^{th}, 50^{th} and 90^{th} percentile size showed that while influent particle size was consistent, the effluent particle sizes increased with the HLR (Figure 5-2a). This shows that retention of large particles became harder at high HLRs. Increasing the HLR also had the consequence of raising both the clean bed and filtration headloss due to increased frictional forces (Figure 5-2b). The NHL increase during a filter run is proportional to the mass deposition (specific deposit) and hence is a measure of mass retention (Burton, Tchobanoglous and Stensel, 2003; Mays and Hunt, 2005). The NHL increase was calculated as $(\Delta H-\Delta H_0)/\Delta H_0$ where ΔH is the filtration headloss and ΔH_0 is the clean bed headloss. The increase in NHL rose with filtered volume at all HLRs (Figure 5-2b); however, the rates of change (slopes of fitting lines) did not change significantly (0.0042-0.0164 $m^{-3}m^2$) compared to the large change in HLRs. This was because while high HLR leads to some high solids loading to the filter, the solids removal efficiency reduced at high flow rates (Figure 5-1a) such that fewer solids were retained per filtered volume. Therefore, the rate of increase in NHL remains low at high HLRs making filter operation possible under such conditions.

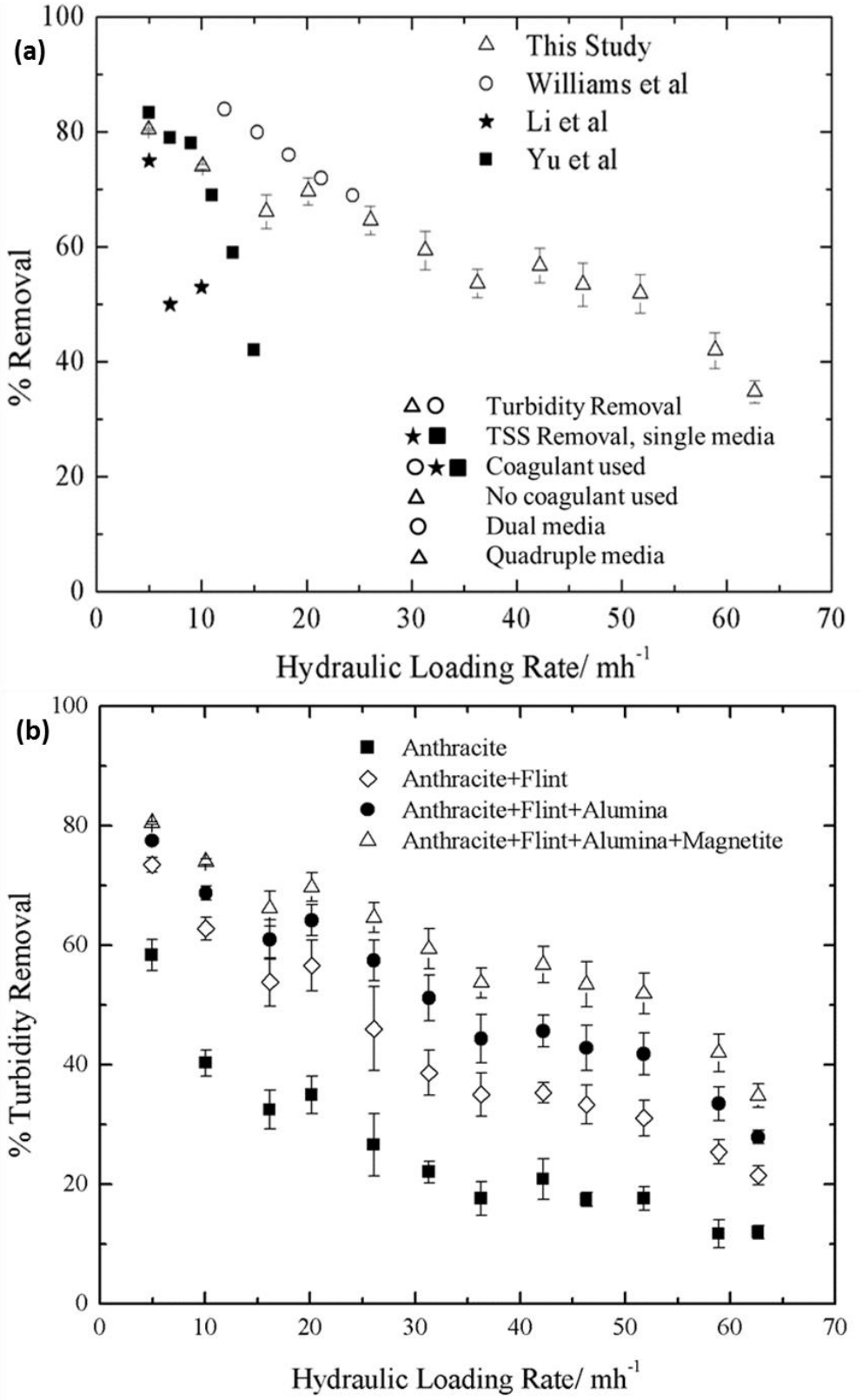

Figure 5-1 (a) Overall turbidity removal efficiency in this study and comparable data from previous studies, (b) d(10), d(50), d(90) particle sizes for both the influent and effluent at different HLRs.

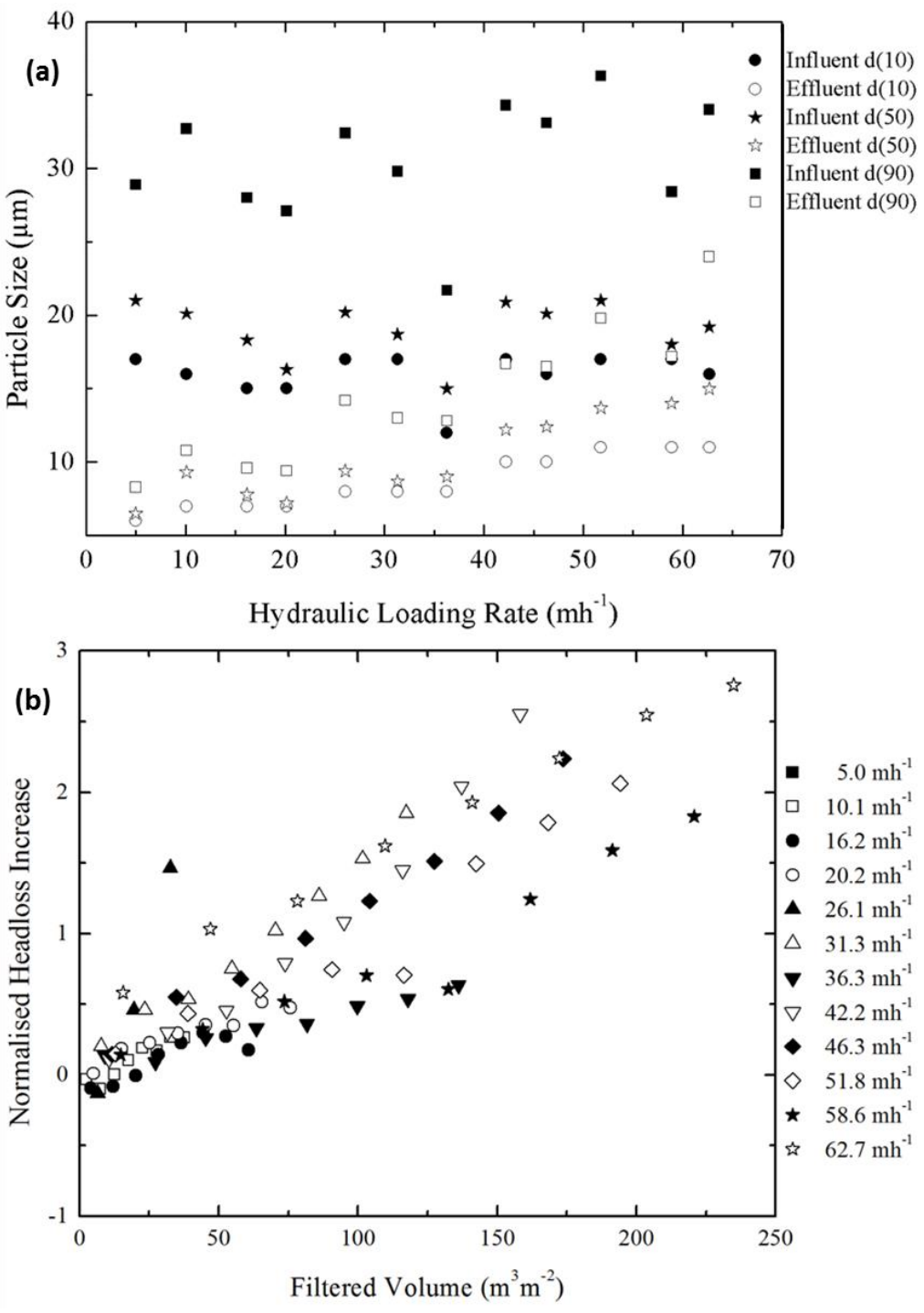

Figure 5-2 (a) The impact of HLR on the average filter turbidity removal efficiency for the quadruple (anthracite, flint, alumina and magnetite) filter, tri-media (anthracite, flint and alumina) filter, dual-media (anthracite and flint) filter and the mono-media (anthracite) filter, (b) Change in NHL increase with filtered volume at different HLRs.

5.3.3 Individual filter layer performance

Each media layer contributed differently to the removal of solids. As wastewater penetrates down through the filter, the larger particles are removed and the overall solids concentration decreases. Therefore, the bottom filter layers receive particles that were not removed upstream or that have been detached from layers above. Solids removed by each layer also depended on the HLR. For example, there was high removal efficiency for anthracite and flint (60% and 40% respectively) at flow rates of 5 mh^{-1} but much lower removal efficiencies of 10% at high HLRs of 60 mh^{-1} (Figure 5-3). Anthracite received a consistent turbidity influent at all different loading rates. The removal efficiency of the anthracite layer demonstrated the profile of a typical single media filter with increasing hydraulic loading (Figure 5-1b). Consequently, the turbidity of the influent to the flint layer increased with HLR (Figure 5-3b). With the increasing turbidity load and HLR, the removal efficiency also decreased.

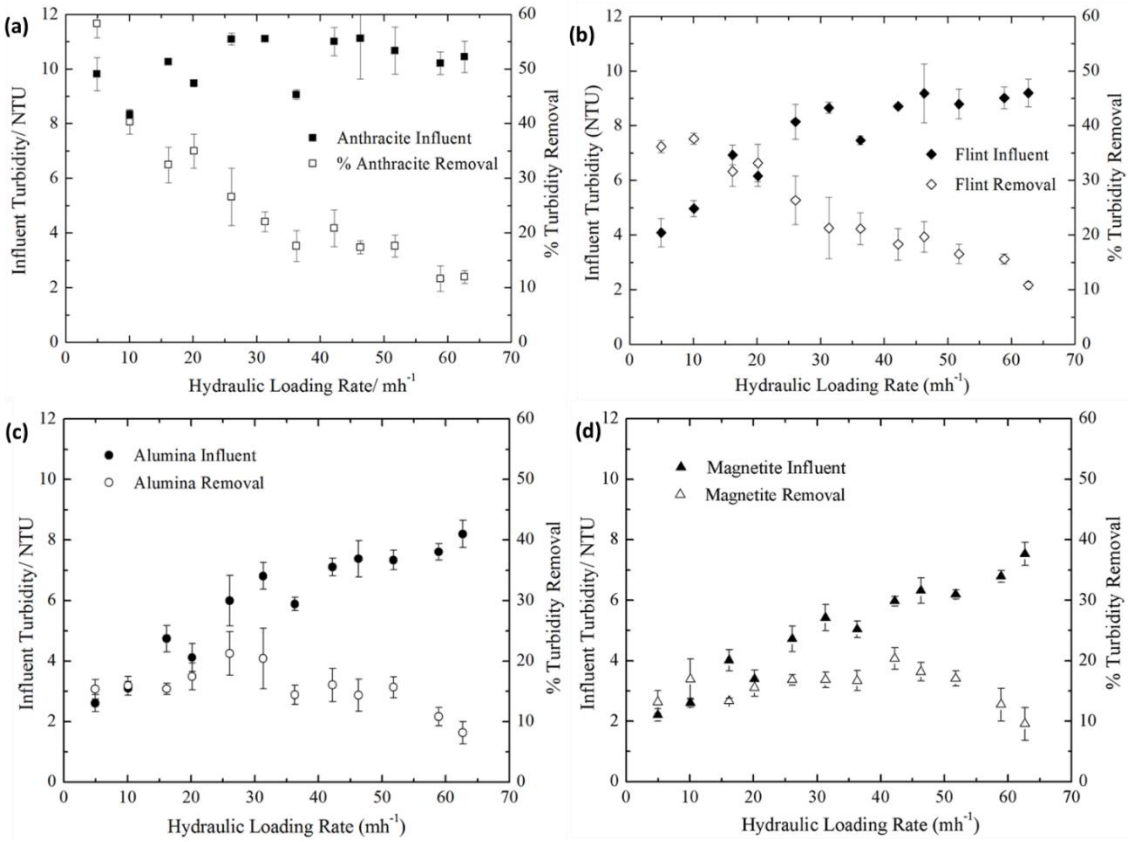

Figure 5-3 Turbidity removal for each media at different HLRs and the turbidity influent to each layer.

In contrast, the bottom two layers (alumina and magnetite) had removal efficiency which started at 15% at low flow rates increasing to a maximum of 20% at 25 mh^{-1} for alumina and 40 mh^{-1} for magnetite before dropping with a further increase in flow rate (Figure 5-3c and d). Although these media had comparatively lower solid removal efficiency, these layers receive much lower suspended solids loads that contained a large number of hard to remove small particles (Williams *et al.*, 2007). The alumina and magnetite turbidity removal efficiency initially improved because of the increased quantity of solids reaching these layers as the HLR increased because of lower removal in upstream media layers. Raising the HLR transported solids deeper into the filter depth, however high HLR also increased hydrodynamic scouring which prevented further improvement in removal efficiency.

The mass accumulation of solids in the filter per unit filter volume, termed specific deposit (Crittenden *et al.*, 2012) was examined for each media at different HLRs. The suspended solids for specific deposit calculation was approximated by multiplying the turbidity measurements by the conversion factor of 2.3 $mgL^{-1}NTU^{-1}$ (as discussed earlier). At low HLRs most solids were retained on the anthracite layer (Figure 5-4). As the HLR increased, the specific deposit also increased due to the increased solid loading rate, but the continued rise was halted by the increased hydrodynamic scouring that limited the retention of solids. In anthracite and flint, the specific deposit rose to a HLR of 25 mh^{-1} and then became constant with further increases in HLR (Figure 5-4a and b). In the alumina layer, the specific deposit increased to a maximum at 30 mh^{-1}, then dropped with increasing HLR (Figure 5-4c). The specific deposit in the magnetite layer continued to increase through the HLRs investigated, a feature that gives the filter added resilience (Figure 5-4d). As the HLR increased, the solids reaching downstream layers increased hence the improved solid retention of downstream layers.

For each filter run, increasing solid retention resulted in an increase in headloss through the filter bed (Veerapaneni and Wiesner, 1997; Mays and Hunt, 2005). The NHL change for the media layers of the quadruple media filter at different HLRs was quite different for each layer (Figure 5-4). The variation of HLR in this study affected the NHL change with solids retention in three main ways: (1) the increased flow resistance due to changes in HLR, (2) the differences in the compactness of solid deposits at different HLR (Veerapaneni and Wiesner, 1997; Mays and Hunt, 2005), and (3) the size of solids reaching each layer. An increase in HLR was coupled by an increase in the flow resistance through the porous media hence an increase in the NHL was observed (Tien and Ramarao, 2007; Crittenden *et al.*, 2012). Research has shown that large particles deposits are more compact than deposits from small particles (Veerapaneni and Wiesner, 1997; Mays and Hunt, 2005) as observed in the anthracite layer (receives large particles) where the NHL remained low (Figure 5-4a). In comparison, the downstream layers (Figure 5-4b, c, d) had higher NHL since they received smaller particles; this was particularly noticeable at the low range of HLR (<15 mh^{-1}) investigated in this work. Anthracite received the largest particles, which were

observed to result in low NHL increase, though the specific deposit was greatest in this layer. While the downstream layers had low specific deposit at low HLRs, the NHL increase was more significant compared to anthracite since these deposits consited of small particles.

Additionally, solids deposited at low HLR have a tendency to form open deposits that occupy more pore space (Veerapaneni and Wiesner, 1997; Mays and Hunt, 2005) and hence result in significant NHL increase for a relatively low specific deposit ((Veerapaneni and Wiesner, 1997; Mays and Hunt, 2005). At high HLR (>40 mh^{-1}), the NHL would be expected to increase. However, this was not seen in this work and may be explained by the differences in compactness of solid deposits (Veerapaneni and Wiesner, 1997; Mays and Hunt, 2005). At high HLR, small solids formed compact deposits which occupied less pore space within the porous media hence moderating the headloss increase. Hence the NHL remained fairly stable while the specific deposit was rising with HLR (Figure 5-4c) in the alumina layer due to the solids being deposited compactly at high HLR. Similar observations were seen in the anthracite, flint and magnetite layers at high HLR where the NHL did not increase appreciably.

The specific deposit and headloss development of the quadruple media filter occurred in all the media layers (Figure 5-4), therefore the entire depth of the filter was utilised for solids storage. High HLR was also seen to increase the deposition of solids in the downstream layers as it caused solids to penetrate deeper into the bed (Kau and Lawler, 1995; Williams *et al.*, 2007). The utilization of the entire filter depth for solid storage ensured a slow headloss development enabling the quadruple filter to be operated at high HLRs, a feature that would not be operationally possible in single media filters.

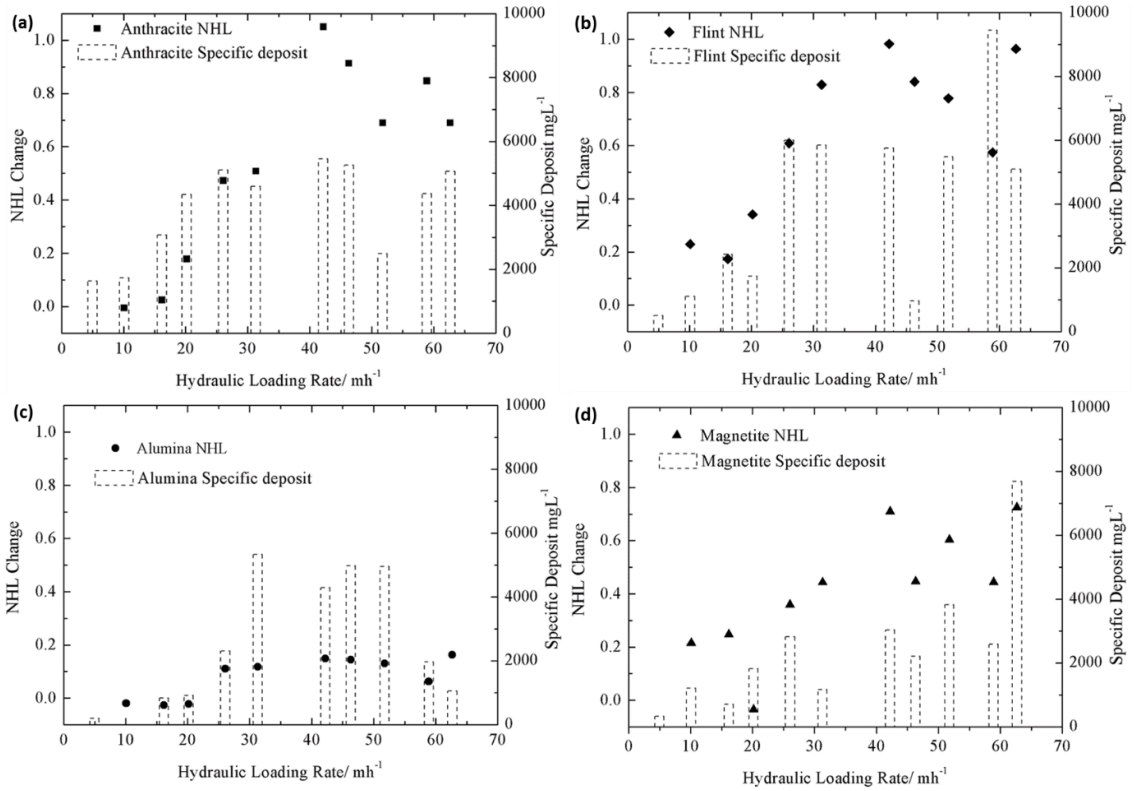

Figure 5-4 NHL change and specific deposit at different filtration rates for the four media.

5.3.4 Particle size analysis

Further support for the changes in the removal efficiencies and headloss development observed in this study were made by examining the changes in the PSDs with filter depth and at different HLRs. The wastewater particle sizes decreased at each stage of the filter for all HLRs; an example of the PSD through each filter layer was shown for the HLR of 5 mh^{-1} (Figure 5-5a). The influent PSD remained unchanged throughout all the filter runs while the effluent sizes were observed to increase when the HLR rose (b). Therefore when the filter was run at higher HLRs, the particle sizes passing through the filter gradually increased, for example, the median particle size d(50) in the filter effluent was 6.5 μm at 5 mh^{-1}, increasing to 15 μm at 60 mh^{-1} (Figure 5-5b).

Analysis of particle size ranges 15-30, 30-50 and 50-100 μm showed reduced removal when the HLR was raised (Figure 5-6b) as a consequence of lower removal efficiency and increased hydraulic scouring. The counting of particle

sizes less than 15 µm in the influent and effluent was inconsistent, the particles appeared to be created; as reflected in Figure 5-5a, small particles were counted in the effluent but appeared to be absent in the influent. Either shear forces led to floc breakage (Jarvis *et al.*, 2005) or large particles had a shielding effect on small particles. Surface erosion on flocs have a potential to rupture them to small fragments (Jarvis *et al.*, 2005) while small particles would be better detected and counted when large particles have been removed. Also, the filter influent was concentrated such that there was a large overlap of particles skewing the particle counting in favour of large particles. Flocculation in the filter can also shift the particle size distribution in polydispersed suspensions such that assessment of filter performance by particle removal becomes challenging (Kim and Tobiason, 2004).

To analyse the trend in turbidity and particle removal efficiency further, comparison was made to removal correlation from drinking water state of the art Tufenkji and Elimelech (2004) clean bed model (commonly called the TE model) (Figure 5-6b) since a wastewater model is currently unavailable.

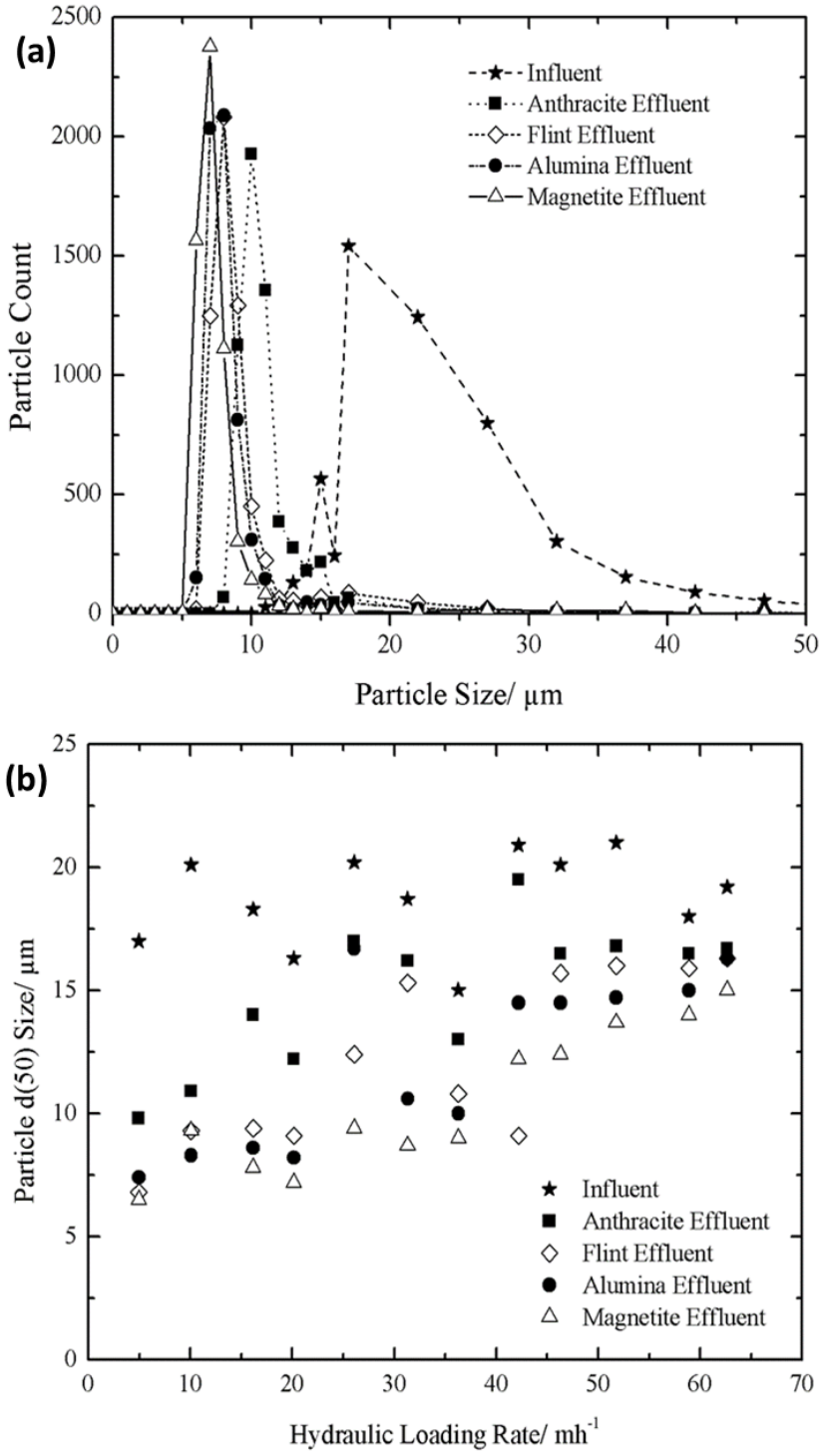

Figure 5-5. (a) Typical PSDs of the wastewater at different stages through the filter (for the 5 mh-1 filter run), (b) The average size of particles passing through each filter stage at different HLRs.

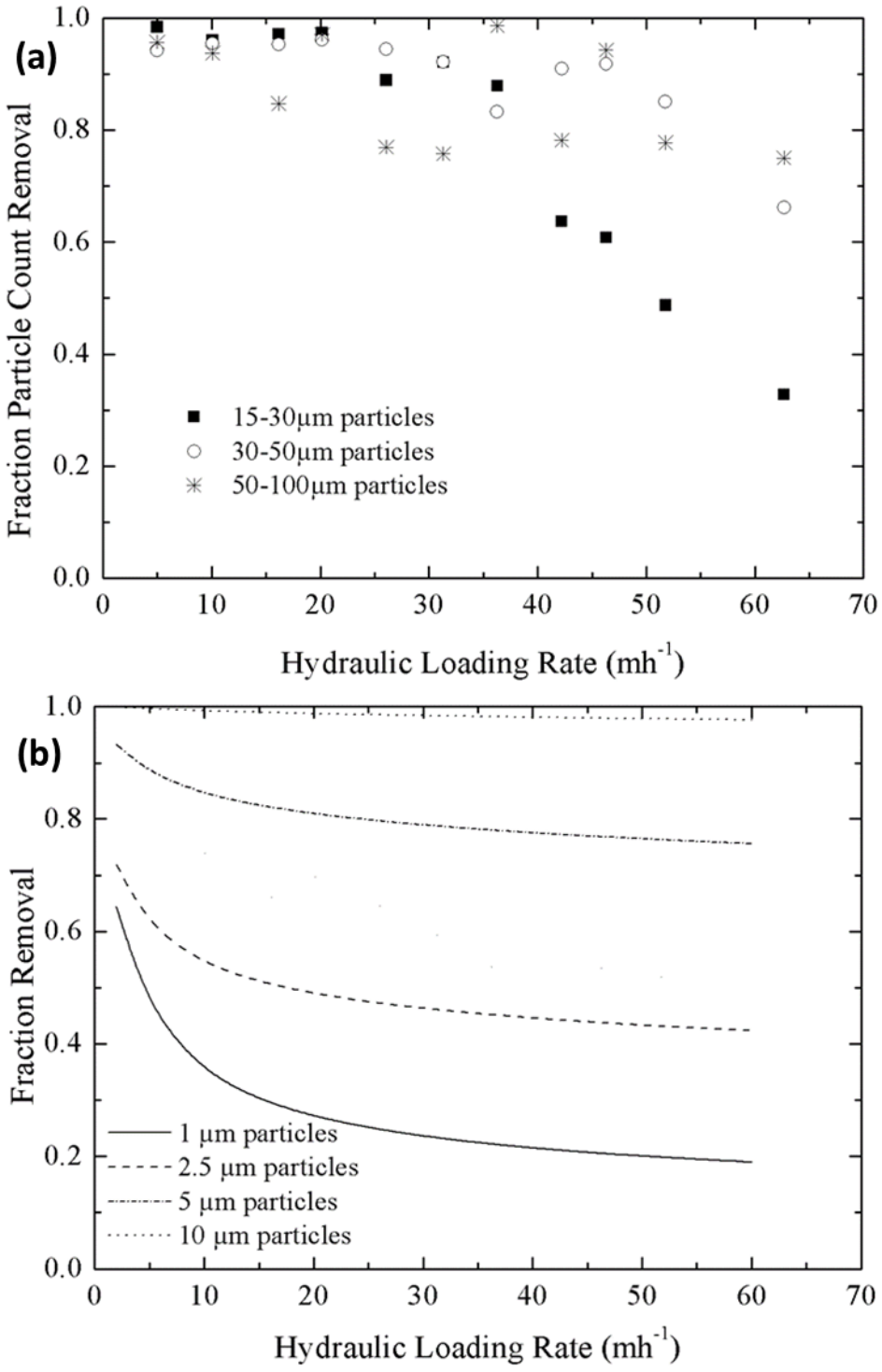

Figure 5-6. (a) Overall removal of 15-30 µm, 30-50 µm and 50-100 µm particles, (b) The TE model plots for the particle sizes 1, 2.5, 5 and 10 µm.

The TE model parameters were assumed as attachment efficiency α = 1, suspension particle density ρ_p = 1.05 kgm^{-3}, ρ_w = 998 kgm^{-3} at temperature T = 20 ^{0}C, the Hamaker constant H = 10^{-20} J and the transport efficiency η was calculated from media characteristics defined in the materials and methods section. The TE model predicts lower removal for particles less than 5 µm, while 10 µm particles are almost completely removed (Figure 5-6b). Removal of average particle sizes (15-30 µm) (Figure 5-6a) was comparable to TE model (Figure 5-6b) at low HLR (20 mh^{-1}), however becomes inconsistent at high HLR. This indicates that the current filter model was consistent at low HLRs but failed to account for the effect of hydrodynamic scouring that occurs at high HLRs. The TE model hence overestimates the removal of large particles by not accounting for particle detachment that occur as a result of hydrodynamic forces (Crittenden *et al.*, 2012). The effect of hydrodynamic forces on the retention of particles is explored further in the next section.

5.3.5 Impact of scouring on filter performance

Further understanding of the filter performance was achieved by analysing the hydrodynamic forces acting on particles in the filter bed as the HLR was changed. An increase in HLR intensified the hydrodynamic scouring on deposited solids with a consequence of reducing particle retention (Tobiason *et al.*, 2011; Crittenden *et al.*, 2012). The modelled net tangential force for a clean bed ($\sigma = 0$) for increasing particle size and HLR shows that large particles are subject to greater hydrodynamic forces and the forces differ in each layer (Figure 5-7a), a similar observation to that made by Bai and Tien (1997). The effect of hydrodynamic force is therefore greater in wastewater filtration where there is usually a much greater proportion of large particles to be filtered than is the case in drinking water filtration.

The frictional force component (F_f) of the net tangential forces acting on a particle attached to a collector does not vary with HLR, however the hydrodynamic drag force (F_{Hydro}) increases with HLR. The net tangential force becomes negative when the hydrodynamic drag force exceeds the frictional force with the

implication that the particle is liable to slide along the collector or get fragmented, hence increasing the chance of detachment. A particle detaches from the collector when the net tangential force exceeds the attachment forces between the particle and collector.

At low HLR, the net tangential force is positive for all particle sizes (Figure 5-7) such that scour plays little to no role in removing particles from collectors hence the high removal efficiency. As the HLR increases, the net tangential force on particles becomes more negative with the effect being much greater on large particles compared to small ones (Bai and Tien, 1997). This is therefore consistent with the observed increase in average particle sizes exiting each media layer (Figure 5-5b) and also the rising influent turbidities to flint, alumina and magnetite layers (Figure 5-3b, c, d) as it became difficult to retain particles at high HLRs. For the same argument, the TE model does not account for scour hence predicted complete removal of particles larger than 10 μm (Figure 5-6b) while observed data showed the removal of 15-30 μm particles to drop at high HLRs (Figure 5-6a). The changes in net tangential force with HLR were also different for each media layer because of the different bed properties (media size and shape and the bed porosity) and the range of particles received by each media layer (Figure 5-7a). Although the surface plots illustrate the forces that would be experienced by a range of particles (0-90 μm), the large particles did not reach the downstream layers as shown by the particle size measurements (Figure 5-5a).

To investigate the effect of the net tangential force acting on particles in relation to the particles observed to leave each filter layer in this study, the critical particle sizes reaching each layer were examined. For average influent particle size (20 μm) to the anthracite layer in this study, the scouring model predicts that these particles would be dislodged at HLR of 27 mh^{-1} (point A1) (Figure 5-7b). Observations were very close to this predicted value, where 15 μm particles were observed to come off the anthracite layer at this HLR (**Error! Reference source not found.**b). For 15 μm particles reaching the flint layer, the model predicted these particles would be dislodged at 38 mh^{-1} (point A2) (Figure 5-7b), identical

to what was observed at this HLR (**Error! Reference source not found.**b). S imilarly, 12 µm particles reaching both alumina and magnetite would potentially be dislodged at 57 mh^{-1} (point A3) and 38 mh^{-1} HLR respectively (Figure 5-7b). The observed results agreed with the model as 12 µm particles were seen to pass through the filter (Figure 5-5b). The anthracite layer reached the critical force first as it was the largest media and received the largest particles (Bai and Tien, 1997). The removal efficiencies of alumina and magnetite were observed to drop for HLR beyond 40 mh^{-1} thus indicating a point where the buffering effect produced by the additional layers began to fall (Figure 5-3c and d), a HLR similar to what the model predicted for flint and magnetite. The specific deposit was also observed to drop after the critical HLR was reached for each layer (Figure 5-4).

The hydrodynamic model was therefore successful in demonstrating the deviation between the TE model and the observed results, the differences arising due to the scouring effect of hydrodynamic forces at high HLRs. Wastewater has a significant number of large particles which are subject to larger detachment forces. The TE model does not account for detachment of retained particles hence may therefore be more appropriate for modelling drinking water filtration where the suspension particles are smaller and low HLRs are usually used.

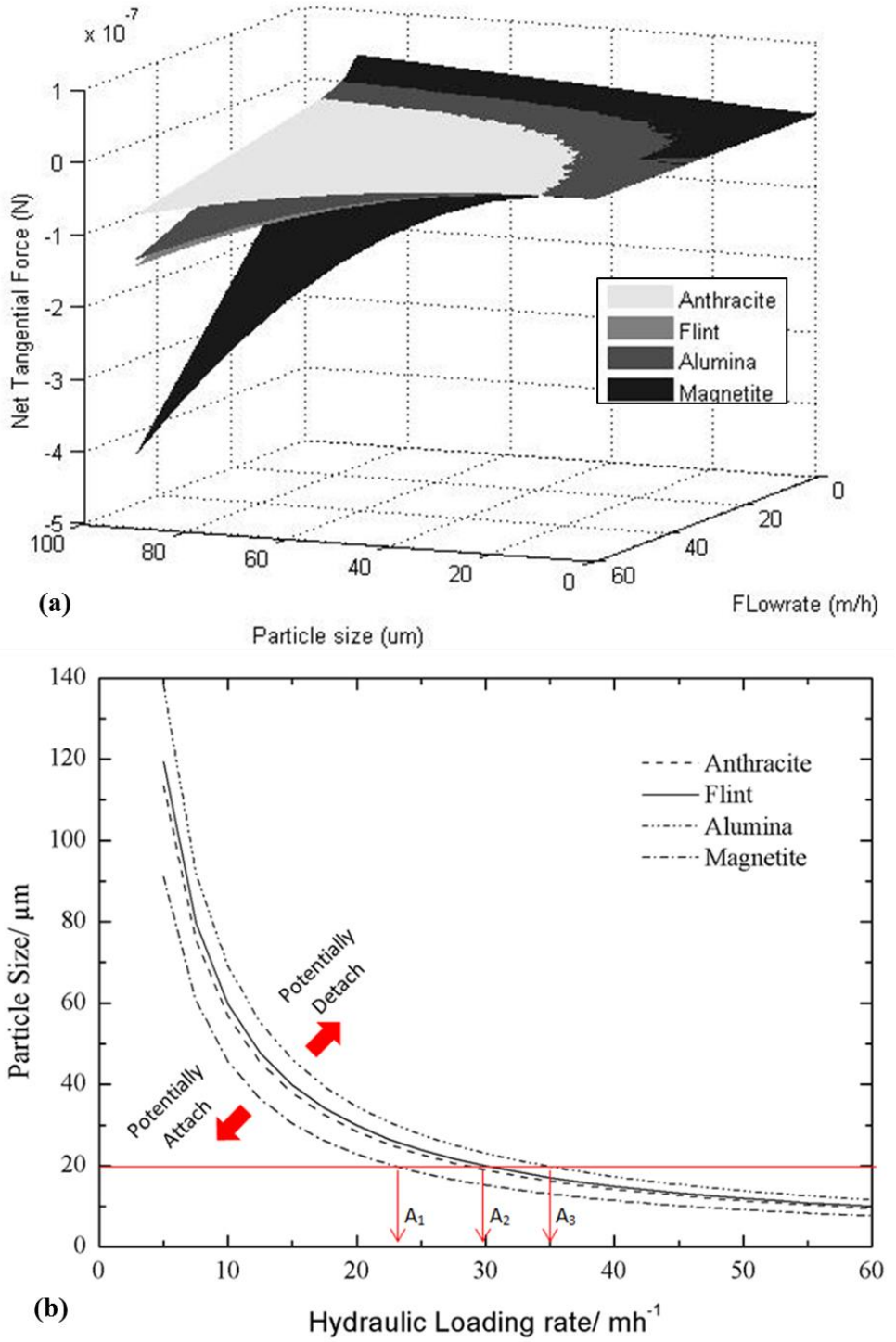

Figure 5-7. Modelled net tangential force (Equation 5-3 and Equation 5-4) in a clean bed (σ = 0) (a) 3D plot for the different particle sizes and HLRs in the four media layers, (b) Plot of the particle sizes and HLR when the net tangential force is zero for the four layers. The values $k_f = 3.79\times10^{-6}$ m, H= 1.4×10^{-20} kgm^{2}s^{-2} and $\delta = 3\times10^{-10}$m (Bai and Tien, 1997), $\mu = 0.000955$ kgm^{-1}s^{-1} and the parameters defined in Materials and Methods were used in the simulation).

5.4 Conclusions

The results from this work have shown that the impact of the increase in HLR for the quadruple media filter was much less than for a single media filter as the system was buffered by the additional layers moderating the loss of performance. High HLR transported solids deeper into the filter bed hence the entire depth of the filter was used for solid storage, ensuring the headloss was distributed to all media layers. The hydrodynamic model successfully explained the observed solids removal and the PSD at changing HLR for the quadruple filter treating wastewater secondary effluent. The hydrodynamic model also explained the deviation of the TE Model from the observed results particularly at high HLR by showing the effects of hydrodynamic scouring on particle retention. The implications of this research are the possibilities of operating the quadruple media filter at high HLR (up to 40 mh^{-1}) to increase the throughput with a moderate impact on the effluent quality.

Acknowledgements

1. The authors greatly thank Dr Garry Hoyland, Richard Hartnett and Dr Caroline Huo for their industrial support and advice and Bluewater Bio Ltd for funding and permitting the use of the company technology to carry out this investigation. Funding from the Engineering and Physical Sciences Research Council (EPSRC) is also gratefully acknowledged.

References

APHA, AWWA and WEF (2005) *Standard Methods for the Examination of Water and Wastewater*. 21st edn, *American Public Works Association*. 21st edn. Washington D.C.

Aronino, R., Dlugy, C., Arkhangelsky, E., Shandalov, S., Oron, G., Brenner, A. and Gitis, V. (2009) 'Removal of viruses from surface water and secondary effluents by sand filtration', *Water Research*, 43(1), pp. 87–96.

Bai, R. and Tien, C. (1997) 'Particle Detachment in Deep Bed Filtration', *Journal of Colloid and Interface Science*, 186(2), pp. 307–17.

Baruth, E. E. (2005) *Water treatment plant design*. 3rd edn. New York: McGraw-Hill.

Bergendahl, J. a. and Grasso, D. (2003) 'Mechanistic basis for particle detachment from granular media', *Environmental Science and Technology*, 37(10), pp. 2317–2322.

Bloetscher, F., Pleitez, F., Hart, J., Stambaugh, D., Cooper, J., Kennedy, K. and Sher Burack, L. (2014) 'Comparing Contaminant Removal Costs for Aquifer Recharge with Wastewater with Water Supply Benefits', *JAWRA Journal of the American Water Resources Association*. Blackwell Publishing Inc., 50(2), pp. 324–333.

Burton, F. L., Tchobanoglous, G. and Stensel, H. D. (2003) *Wastewater engineering: treatment and reuse*. 4th edn, *Wastewater Engineering, Treatment, Disposal and Reuse. Techobanoglous G, Burton FL, Stensel HD (eds). Tata McGraw-Hill Publishing Company Limited, 4th edition. New Delhi, India*. 4th edn. Boston: McGraw-Hill.

Christou, A., Eliadou, E., Michael, C., Hapeshi, E. and Fatta-Kassinos, D. (2014) 'Assessment of long-term wastewater irrigation impacts on the soil geochemical properties and the bioaccumulation of heavy metals to the agricultural products', *Environmental Monitoring and Assessment*. Kluwer Academic Publishers, 186(8), pp. 4857–4870.

Cleasby, J. L. and Baumann, E. R. (1962) ‘Selection of Sand Filtration Rates’, *Journal (American Water Works Association)*, 54(5), pp. 579–602.

Crittenden, J. C., Trussell, R. R., Hand, D. W., Howe, K. J. and Tchobanoglous, G. (2012) *Water Treatment principle and design*, *MWH’s Water Treatment: Principles and Design, 3rd edn*. Chichester: John Wiley & Sons Inc.

Defra (2012) *Waste water treatment in the United Kingdom – 2012 Implementation of the European Union Urban Waste Water Treatment Directive – 91/271/EEC*. London. Available at: https://www.gov.uk/government/uploads/system/uploads/attachment_data/file/69592/pb13811-waste-water-2012.pdf.

Han, S., Fitzpatrick, C. S. B. and Wetherill, A. (2009) ‘The impact of flow surges on rapid gravity filtration’, *Water Research*, 43(5), pp. 1171–1178.

Ho, L., Grasset, C., Hoefel, D., Dixon, M. B., Leusch, F. D. L., Newcombe, G., Saint, C. P. and Brookes, J. D. (2011) ‘Assessing granular media filtration for the removal of chemical contaminants from wastewater’, *Water Research*, 45(11), pp. 3461–3472.

Illueca-Muñoz, J., Mendoza-Roca, J. A., Iborra-Clar, A., Bes-Piá, A., Fajardo-Montañana, V., Martínez-Francisco, F. J. and Bernácer-Bonora, I. (2008) ‘wastewater reuse in europe’, *Desalination*, 222(1–3), pp. 222–229.

Jarvis, P., Jefferson, B., Gregory, J. and Parsons, S. A. (2005) ‘A review of floc strength and breakage.’, *Water research*, 39(14), pp. 3121–37.

Kau, S. M. and Lawler, D. F. (1995) ‘Dynamics of Deep-Bed Filtration : Velocity , Depth , and Media’, *Journal of Environmental Engineering*, 121(1978), pp. 850–859.

Kim, J. and Lawler, D. F. (2012) ‘The influence of hydraulic loads on depth filtration’, *Water Research*, 46(2), pp. 433–441.

Kim, J. and Tobiason, J. E. (2004) ‘Particles in Filter Effluent: The Roles of Deposition and Detachment’, *Environmental Science & Technology*, 38(22), pp.

6132–6138.

Kirkpatrick, W. R. and Asano, T. (1986) ‘Evaluation of Tertiary-Treatment Systems For Waste-Water Reclamation and Reuse’, *Water Science and Technology*, 18(10), pp. 83–95.

Lander, J. (1994) ‘Wastewater rapid-gravity filtration in Severn Trent Water’, *Journal of the Institution of Water and Environmental Management*. Inst of Water & Environmental Management, 8(3), pp. 256–268.

Langenbach, K., Kuschk, P., Horn, H. and Kästner, M. (2010) ‘Modeling of slow sand filtration for disinfection of secondary clarifier effluent’, *Water Research*, 44(1), pp. 159–166.

Lawler, D. F. and Nason, J. a. (2006) ‘Granular media filtration: Old process, new thoughts’, *Water Science and Technology*, 53(7), pp. 1–7.

Lazarova, V., Savoye, P., Janex, M. L., Blatchley, E. R. and Pommepuy, M. (1999) ‘Advanced wastewater disinfection technologies: State of the art and perspectives’, in *Water Science and Technology*, pp. 203–213.

Li, Y., Yu, J., Liu, Z. and Ma, T. (2012) ‘Estimation and modeling of direct rapid sand filtration for total fecal coliform removal from secondary clarifier effluents’, *Water Science and Technology*, 65(9), pp. 1615–1623.

Mays, D. C. and Hunt, J. R. (2005) ‘Hydrodynamic aspects of particle clogging in porous media’, *Environmental Science and Technology*, 39(2), pp. 577–584.

Rajagopalan, R. and Tien, C. (1976) ‘Trajectory analysis of deep-bed-filtration with the sphere-in-cell porous media’, *AIChE Journal*, pp. 523–533.

Severn Trent Services (no date) *Tetra DeepBed Filter, Tertiary Treatment Systems*. Available at: http://www.capitalh2o.com/files/brochures/sts/tetra/Tetra Deep Bed Filter 650_0055.pdf (Accessed: 17 April 2016).

Stumm, W. and Morgan, J. J. (1996) *Aquatic Chemistry: Chemical Equilibria and Rates in Natural Waters*. 3rd edn, *Environmental science and technology*. 3rd edn. New York: John Wiley & Sons, Inc,.

Suthaker, S., Smith, D. W. and Stanley, S. J. (1995) ‘Evaluation of Filter Media for Upgrading Existing Filter Performance’, *Environmental Technology*, 16(7), pp. 625–643.

Tien, C. (2000) ‘Hydrosol deposition in porous media: the effect of surface interactions’, *Advanced Powder Technology*, 11(1), pp. 9–56.

Tien, C. and Ramarao, B. V. (2007) *Granular Filtration of Aerosols and Hydrosols*. 1st edn, *Granular Filtration of Aerosols and Hydrosols*. 1st edn. Oxford, UK: Elsevier Ltd.

Tobiason, J., Cleasby, J., Logsdon, G. and O’Melia, C. (2011) ‘Granular Media Filtration’, in Edzwald James (ed.) *Water Quality & Treatment: A Handbook on Drinking Water*. 6th edn. Massachusetts: American Water Works Association, American Society of Civil Engineers, McGraw-Hill, p. 10.1.

Torkzaban, S., Bradford, S. a. and Walker, S. L. (2007) ‘Resolving the coupled effects of hydrodynamics and DLVO forces on colloid attachment in porous media’, *Langmuir*, *23*(19), pp. 9652–9660.

Tufenkji, N. and Elimelech, M. (2004) ‘Correlation Equation for Predicting Single-Collector Efficiency in Physicochemical Filtration in Saturated Porous Media’, *Environmental Science and Technology*, 38(2), pp. 529–536.

Veerapaneni, S. and Wiesner, M. R. (1997) ‘Deposit Morphology and Head Loss Development in Porous Media’, *Environmental Science & Technology*, 31(10), pp. 2738–2744.

Williams, G. J., Sheikh, B., Holden, R. B., Kouretas, T. J. and Nelson, K. L. (2007) ‘The impact of increased loading rate on granular media, rapid depth filtration of wastewater’, *Water Research*, 41(19), pp. 4535–4545.

Yao, K., Habibian, M. T. and O’Melia, C. R. (1971) ‘Water and Waste Water Filtration: Concepts and Applications’, *Environmental Science & Technology*, 5(11), pp. 1105–1112.

Yu, J., Li, Y., Liu, Z., Zhang, W. and Wang, D. (2015) ‘Impact of loading rate and

filter height on the retention factor in the model of total coliform (TC) removal in direct rapid sand filtration', *Desalination and Water Treatment*, 54(1), pp. 140–146.

Zouboulis, a., Traskas, G. and Samaras, P. (2007) 'Comparison of single and dual media filtration in a full-scale drinking water treatment plant', *Desalination*, 213(1–3), pp. 334–342.

6 Thesis Discussion

Filtration of treated wastewater has been driven by tighter regulation resulting from greater need to protect the environment and to augment dwindling fresh water sources in water stressed area Hamoda, Al-Ghusain and Al-Jasem, 2004). The reuse of treated wastewater has gained significant popularity in recent years as its beneficial potential has been widely recognised. Re-use and recycling of treated wastewater is practised for many different applications but this usually requires high levels of treatment to make it appropriate for use. Tertiary wastewater filtration emerges as a common choice amongst other alternative treatments for polishing treated wastewater due to its relatively simple infrastructure and potential for producing high quality treated wastewater. However, wastewater filtration is challenging because of the nature of the wastewater, as it contains organic matter and high concentrations of solids in comparison to drinking water treatment, where depth filtration is routinely applied. This research has answered some of the questions concerning tertiary wastewater filtration, to improve the understanding of the process science for the removal of wastewater solids.

Because of the organic content of wastewater, a tertiary filter can potentially function as a physicochemical or a biological filter depending on the operation conditions. In this research, the filter was operated at hydraulic loading rate of 5 mh^{-1} up to 60 mh^{-1}, under which biomass growth was very limited, so physical removal processes were dominant. Slow sand filters require a very large filter area to produce a significant throughput. To reduce the footprint of the process, particularly in urban settings, high rate filters of higher hydraulic loading rates (5 - 25 mh^{-1}) in rapid gravity filtration processes has enabled a large throughput on a small filter area (Ncube *et al.*, 2016). High hydraulic loading rates are usually operationally achievable in filters of multimedia due to the substantial increase in headloss of single media filters. Granular media filtration depends on many interrelated factors that complicate filter design and operation, such as media characteristics, filter depth, hydraulic loading rate and suspension concentration which were investigated in this study. This discussion aims to provide new insight

into wastewater filtration bought about by the findings of this research and the benefits to the technology.

A new method was introduced to measure the media sphericity, an important shape parameter used in filter modelling. To simplify derivation of models, spherical media is usually assumed, but real media is irregular in shape, hence shape characterisation is essential for models to be relevant. The new method improved accuracy in sphericity quantification and hence brings accuracy in design and predictions using filter models. As an illustration, the Yao et al (1971) filter coefficient and the Kozeny (1927) headloss expression are calculated respectively as:

$$\lambda = \frac{3(1-\varepsilon)\eta\alpha}{2d} \qquad \textbf{Equation 6-1}$$

and

$$\frac{\Delta p}{L} = \frac{\kappa_k \mu}{\rho_w g \varepsilon^3}\left(\frac{6(1-\varepsilon)}{d}\right)^2 u \qquad \textbf{Equation 6-2}$$

where λ is the filter coefficient in m^{-1} unit, d is the media diameter in m, Δp is the headloss in Pa, L is the filter of depth in m, μ is the dynamic viscosity Nsm^{-2}, ρ_w is the water density in kgm^{-3}, g is the acceleration due to gravity in ms^{-2} and u is the hydraulic loading rate in ms^{-1}, and the dimensionless quantities, ε is the filter bed porosity, α is the attachment efficiency and η is the transport coefficient and κ_k is the Kozeny coefficient.

In these filter formulations, d is the diameter of the spherical media, when the media is of irregular shape, the 3D equivalent diameter and the sphericity determined in (Chapter 2) will improve the accuracy of the evaluation of the models. Thus, the model diameter will be replaced by:

$$d = \psi d_{eq} \qquad \textbf{Equation 6-3})$$

Where Ψ is the media sphericity and d_{eq} is the media 3D equivalent diameter. Thus, the use of the two media characteristics Ψ and d_{eq} in place of the diameter of spherical media diameter d will predict the headloss through filter media beds with fair accuracy (Chapter 2). The media size and sphericity are also important

in determining other filter operation characteristics such as the backwash hydraulics (Akgiray and Saatçi, 2001), which was not investigated in this study.

Another unknown was the role of media surface characteristics in filtration of treated wastewater. The filter media surface characteristics have been known to have an important role in in model filtration systems using glass or silica media and polystyrene microsphere suspensions with removal varying between different media materials of same size (Elimelech *et al.*, 1995; Bai and Tien, 1997; Tufenkji *et al.*, 2004; Kim and Lawler, 2005). This was explained mainly by DLVO forces, due to media having different surface charges and different adsorption characteristics. It was found in this research that in tertiary wastewater filtration, the organic matter altered the media surface characteristics such that the media composition had no selective removal of solids from wastewater (Chapter 3) which may be the case in the absence of organic compounds. The surface charge of the media was altered by changing the pH. Here the media material zeta potential was found to match that of the wastewater at different pH. The implication of this finding being that any media material can potentially be used as a filter material if it satisfies other design criteria, such as the size, porosity, inertness and density characteristics. Thus, media mineral composition was not observed to play any role in its removal capacity while filtering wastewater. The different media materials would however be important for different density in the design of multimedia filters.

Filter performance is efficient if suspension particle aggregation and deposition are optimal, thus when particle-particle and media-particle interactions are favourable (Tien and Ramarao, 2007). Wastewater particle aggregation was found to be optimal around the neutral pH (Chapter 3). At this pH, the particles to be filtered were at their largest size while the concentration of smaller particles was low. Large particles are easier to remove by porous media in comparison to small particles (Tufenkji and Elimelech, 2004; Tien and Ramarao, 2007). With media materials surface properties matching that of wastewater, it was consequently found that particle deposition in the filter was also optimum around the neutral pH. Wastewater secondary effluent are usually around neutral pH

(Wei, Viadero Jr. and Bhojappa, 2008), hence in many cases pH adjustment becomes unnecessary before filtration. Since the media assumes a charge character to match that of the wastewater, determination of conditions for optimal aggregation of wastewater solids should therefore be sufficient in determining conditions of optimal deposition in depth filters.

Apart from the media characteristics, the media bed structure determines filter performance. Filter media size and depth are usually selected based on experience and rules of thumb (Lawler and Nason, 2006). The filter media size for wastewater filtration is usually larger than that in drinking water filters to minimise the headloss through the filter, as wastewater has a higher concentration of solids. The findings from this study showed that most of the solids were retained in the top 0.1 m depth of filter (Chapter 4). The benefits of increasing the bed depth get less and less as the depth increases. However further depth is still essential to provide further removal, to stabilise the hydraulics and structural support to the top layers. Many filters are designed with depths, L of 0.60-1.63 m and the filter depth to media size ratio L/d_m in the range 714-1517 while operating at hydraulic loading rate 9.8-18.6 mh^{-1} (Lawler and Nason, 2006). To achieve the removal efficiency typical of performing filters 75% (Hamoda et al., 2004), the quadruple filter operating at 25 mh^{-1} hydraulic loading rate designed to a depth of 0.50 m or L/d_m ratio 1033 performed with a removal efficiency slightly better than typical performing filters. Considering the filter was operated at a higher hydraulic loading rate, the filter could therefore be designed shallower to operate at the common filtration rate of 10 mh^{-1} to achieve 75% removal.

The quadruple filter had media layers of anthracite, flint, alumina and magnetite moving from the top of the bed to the bottom respectively. It was found in this research that increasing the number of media materials improved filter performance with each addition of media for the same bed depth. The additional media layers also moderated headloss development. Therefore, wastewater tertiary filters could be designed at 0.5 m depth with a high level of removal obtained by using multiple layers of differently sized media. Increasing the

number of media materials is an inventive way to improve performance, better for example than increasing filter depth, which can consequently increase clean bed headloss and headloss development during filtration.

The hydraulic loading rate can be increased to produce a higher throughput for the same filter area, however the filter performance may deteriorate. The quadruple filter had a removal efficiency reducing from 80% to 40% when the hydraulic loading rate increased from 5 to 60 mh^{-1} (Chapter 5). Some previous studies have seen a steep decline in performance with small increases in hydraulic loading rate in single media tertiary wastewater filters (Li *et al.*, 2012; Yu *et al.*, 2015). However Williams et al (2007) showed that using dual media filters reduced the impact of the hydraulic shock. The results from the present research agree with Williams et al (2007) and show that increasing filter layers incrementally from one to four moderates the impact of increasing the hydraulic loading rate. Thus, filters of multimedia configuration can be operated at high hydraulic loading rate with a marginal reduction in performance. It was also demonstrated that solid retention occurred mainly in the top 0.1 m depth of the filter, while increasing the hydraulic loading rate transported and distributed solids deeper into the filter, consequently using the whole filter depth for solids retention.

The high hydraulic loading rate increased the scouring on deposited solids by increasing the hydrodynamic forces, a feature which is not desired in depth filtration particularly in single media filters where media grain size increases with depth and hence the potential to retain the solids downstream reduces. The quadruple filter had a structure with the smallest media at the bottom of filter, hence preserving the capacity to trap the scoured solids downstream. This gives the quadruple filter a capacity to process a large throughput as it maximises the filter void space for solids storage.

The filter throughput that can be achieved is also affected by the suspension solids concentration. High concentrations cause rapid headloss development hence shortening the filter run time. The suspension characteristics are not usually taken into consideration in filter theory, where the suspension is usually assumed to be sufficiently conditioned to produce an attachment when in contact

with media during filtration. Furthermore, synthetic suspension concentrations used to validate models are usually on the low concentration side when compared to that observed in the field. There has therefore been uncertainty as to how suspension concentration affected the performance of tertiary wastewater filters. This study established that the removal efficiency of the quadruple filter decreased as the solids concentration increased while the solids retention increased.

REFERENCES

Akgiray, O.¨and Saatçi, a. M. (2001) ‘A new look at filter backwash hydraulics’, *Water Science and Technology: Water Supply*, 1(2), pp. 65–72.

Bai, R. and Tien, C. (1997) ‘Particle Detachment in Deep Bed Filtration’, *Journal of Colloid and Interface Science*, 186(2), pp. 307–17.

Dabrowski, W., Spaczyńska, M. and Mackie, R. I. (2008) ‘A Model to Predict Granular Activated Carbon Backwash Curves’, *CLEAN – Soil, Air*, 36(1), pp. 103–110.

Elimelech, M., Gregory, J., Jia, X. and Williams, R. A. (1995) *Particle deposition and aggregation: measurement, modelling and simulation*, *Particle deposition and aggregation*.Oxford: Butterworth-Heinemann

Hamoda, M. F., Al-Ghusain, I. and Al-Jasem, D. M. (2004) ‘Application of Granular Media Filtration in Wastewater Reclamation and Reuse’, *Journal of Environmental Science and Health, Part A*, 39(2), pp. 385–395.

Kim, J. and Lawler, D. F. (2005) Characteristics of zeta potential distribution in silica particles. Bulletin of the Korean Chemical Society, 26(7), pp. 1083–1089.

Kozeny, J. (1927) ‘Uber die kapillare Leitung des Wassers im Boden. Sitz. b’, *Sitzungberichte, Abt. Ea, Mathematik, Astronomie, Physik und Meteorologie*, 136a, pp. 271–306. Available at: http://scholar.google.com/scholar?hl=en&btnG=Search&q=intitle:Uber+kapillare+Leitung+des+Wassers+im+Boden#1.

Lawler, D. F. and Nason, J. a. (2006) ‘Granular media filtration: Old process, new thoughts’, *Water Science and Technology*, 53(7), pp. 1–7.

Li, Y., Yu, J., Liu, Z. and Ma, T. (2012) ‘Estimation and modeling of direct rapid sand filtration for total fecal coliform removal from secondary clarifier effluents’, *Water Science and Technology*, 65(9), pp. 1615–1623.

Ncube, P., Pidou, M., Stephenson, T., Jefferson, B. and Jarvis, P. (2016) 'The effect of high hydraulic loading rate on the removal efficiency of a quadruple media filter for tertiary wastewater treatment', *Water Research*, 107. pp. 102-112.

Tien, C. and Ramarao, B. V. (2007) *Granular Filtration of Aerosols and Hydrosols*. *Granular Filtration of Aerosols and Hydrosols*. 1st edn. Oxford, UK: Elsevier Ltd.

Tufenkji, N. and Elimelech, M. (2004) 'Correlation Equation for Predicting Single-Collector Efficiency in Physicochemical Filtration in Saturated Porous Media', *Environmental Science and Technology*, 38(2), pp. 529–536.

Tufenkji, N., Miller, G. F., Ryan, J. N., Harvey, R. W. and Elimelech, M. (2004) 'Transport of Cryptosporidium oocysts in porous media: Role of straining and physicochemical filtration', *Environmental Science and Technology*, 38(22), pp. 5932–5938

Wei, X., Viadero Jr., R. C. and Bhojappa, S. (2008) 'Phosphorus removal by acid mine drainage sludge from secondary effluents of municipal wastewater treatment plants', *Water Research*, 42(13), pp. 3275-3284.

West, J., Rachwal, A. J. and Cox, G. C. (1979) 'Experiences with high rate tertiary treatment filtration in the Thames Water Authority', *Journal of the Institution of Water Engineers and Scientists*, pp. 45–63.

Williams, G. J., Sheikh, B., Holden, R. B., Kouretas, T. J. and Nelson, K. L. (2007) 'The impact of increased loading rate on granular media, rapid depth filtration of wastewater', *Water Research*, 41(19), pp. 4535–4545.

Yao, K., Habibian, M. T. and O'Melia, C. R. (1971) 'Water and Waste Water Filtration: Concepts and Applications', *Environmental Science & Technology*, 5(11), pp. 1105–1112.

Yu, J., Li, Y., Liu, Z., Zhang, W. and Wang, D. (2015) 'Impact of loading rate and filter height on the retention factor in the model of total coliform (TC) removal in direct rapid sand filtration', *Desalination and Water Treatment*, 54(1), pp. 140–146.

7 Conclusions and Further work

7.1 Conclusions

This research investigated the filter media, media bed structure and the operation characterises in wastewater tertiary filtration using multimedia filters. The following conclusions were made:

1. A new method of determining sphericity was introduced, the method was validated as accurate and preserved the 3D property which is lost in the current 2D methods.
2. The zeta potential of different media materials was found to match that of wastewater when suspended in wastewater which means that the media surface characteristics were not of significance in solids removal from wastewater. The wastewater solids aggregation and deposition were both optimal around the neutral pH, where the wastewater matrix was unaltered.
3. The solids retention was mainly on the top 0.1 m depth of the filter. Filter performance improved with filter depth but headloss development became a limiting factor for operation to be feasible. Additional layers of filter materials, successively from one to four improved the filter performance for the same depth of filter bed and moderated headloss development.
4. Increasing the influent concentration increased the solids retention while solids removal efficiency decreased for shallow filters. Making the filter deeper moderated the reduction in removal efficiency such that a stable efficiency was observed, but headloss development became rapid.
5. The increase in hydraulic loading rate reduced the filter removal efficiency, the impact was greater in single media filters than in multimedia configurations, the additional media materials buffered the loss of performance.
6. High hydraulic loading rate transported solids deeper into the filter bed hence the entire depth of the filter was used for solid storage, ensuring the headloss was distributed to all media layers of the quadruple filter. The

high hydraulic loading rate had the advantage of increasing the throughput with a moderate impact on the effluent quality.

7.2 Further Work

At the end of the filter cycle, retained solids were dislodged from the media and washed out of the filter using different backwash strategies. Filter backwash was not investigated on this research and need to be investigated. A concurrent air scour and low rate water wash at 20 mh^{-1} for 2 minutes followed by a high rate water wash at 60 mh^{-1} for 5 minutes was adapted from the full-scale filter with some modification for the pilot filter; the strategy washed the filter adequately.

With further research, suitable backwash flow rates could be determined, that is economic in wash water volume and most importantly result in a clean filter bed. It was also desirable that the filter media bed stratified after the backwash hence retaining the tapered void structure as opposed to intermixing. It is also a challenge to obtain a suitable backwash rate that suitably fluidises all layers, washing all the media adequately and avoiding media washout.

The filter was run with media separated in different columns. Time permitting the filter would have been run with media combined in one column to assess filter performance in one unit. The filter would also have been run longer on a continuous basis with only backwash downtimes. This will also have promoted biomass growth, hence biological activity and treatment.

APPENDICES

Appendix A : Sphericity chart

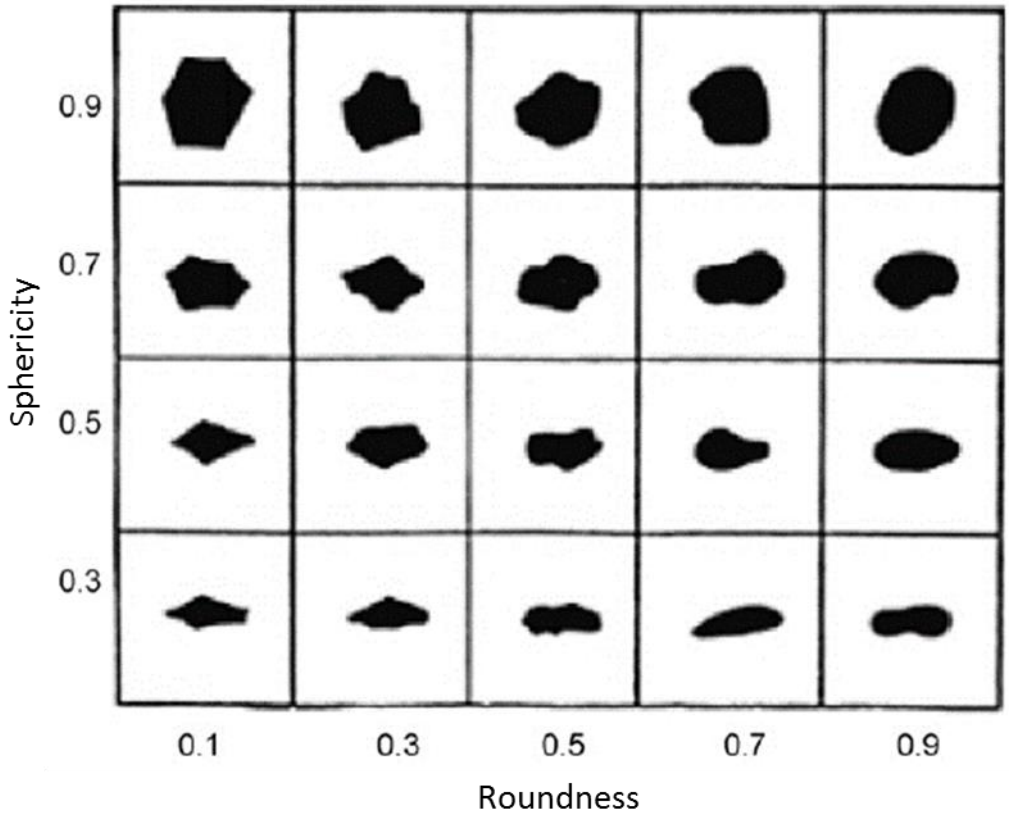

Figure A-1 Chart for sphericity determination by visual comparison extracted from Sneed and Folk (1958).

Appendix B : Filtration Models

B.1 Filtration Kinetics

Based on experimental data Iwasaki (1937) proposed particle removal to be a first order rate relation of concentration C of solids as they are being captured in passing through media length L such that, (Jackson, 1980; Stevenson, 1997; Lawler and Nason, 2006);

$$-\frac{\partial C}{\partial L} = \lambda C \qquad \textbf{Equation B-1}$$

where λ is a measure of filtration efficiency called the filter coefficient. Integration equation B-1 over the entire filter of bed length L, gives

$$C_L = C_0 \exp(-\lambda L) \qquad \textbf{Equation B-2}$$

where C_0 is the initial solid concentration and C_L is the concentration of solids in the effluent of a filter of depth L. The filter coefficient varies with bed depth and filtration time (Jackson, 1980); as well as the characteristics of the filter bed, influent water and filtration rate (Crittenden *et al.*, 2012).

B.2 Filtration Efficiency

The filter coefficient for a clean bed and single collector is the product of rate at which particles traverse the field of impact of the collector (media grains), the transport coefficient (η) and attachment efficiency (α) (O'Melia and Shin, 2001; Lawler and Nason, 2006; Crittenden *et al.*, 2012) such that:

$$\lambda = \frac{3(1-\varepsilon)\eta\alpha}{2d_m} \qquad \textbf{Equation B-3}$$

where d_m is the media diameter, ε is the bed porosity. The attachment efficiency α is the proportion of particles attaching on the grains to the rate at which they strike the grains (Logan *et al.*, 1995); it depends on the chemistry of the suspended solid and the media grains varying from 0 to 1, with 1 being a definite attachment, (O'Melia and Shin, 2001; Tufenkji and Elimelech, 2004). The

dimensionless transport coefficient η is defined as a ratio of rate of contact to rate of approach of suspension particles to the media grains, (O'Melia and Shin, 2001; Zamani and Maini, 2009). Assuming the main components of particle transport, diffusion (η_D), interception(η_I) and gravitational(η_G) are additive (Yao, Habibian and O'Melia, 1971), the transport coefficient is given by (Yao, Habibian and O'Melia, 1971; Elimelech and O'Melia, 1990; Tufenkji and Elimelech, 2004; Crittenden *et al.*, 2012):

$$\eta = \eta_I + \eta_G + \eta_D \qquad \textbf{Equation B-4}$$

The importance of each transport mechanism depends on the system properties. Accurate determination of η can be attained as a numerical solution of the convective-diffusion equation expressed as, (Tufenkji and Elimelech, 2004);

$$\nabla \bullet \left(\overline{U}C\right) = \nabla \bullet \left(\overline{D} \bullet \nabla C\right) - \nabla \bullet \left(\frac{\overline{D} \bullet \overline{F}}{kT} C\right) \qquad \textbf{Equation B-5}$$

where **D** is the particle diffusion tensor, **U** is the particle velocity vector, k is the Boltzmann constant, T is the absolute temperature and **F** is the external force vector.

However the numerically solving of the convective-diffusion equation is not straight forward nor is the alternative method by trajectory consideration for non-Brownian particles (Tufenkji and Elimelech, 2004). The main simplified models predicting the transport coefficient are discussed below. The models assume the suspension particles to be sufficiently conditioned so that the attachment efficiency is nearly 1, (ie α≈1).

Yao Model

The Yao Model predicts the transport coefficient, η of a single collector by means of an analytic approach grounded on theory (Yao, Habibian and O'Melia, 1971;

Logan *et al.*, 1995; Lawler and Nason, 2006; Crittenden *et al.*, 2012) expressed as:

$$\eta = \frac{3}{2} N_R^2 + N_G + 4Pe^{-2/3} \qquad \textbf{Equation B-6}$$

The dimensionless groups N_R , N_G and Pe are defined as follows;

$$N_R = \frac{d_p}{d_m} \quad , \quad N_G = \frac{u_S}{u} = \frac{(\rho_p - \rho_w) g d_p^2}{18 \mu u} \quad \text{and} \quad Pe = \frac{3\pi\mu d_p d_m u}{kT} \qquad \textbf{Equation B-7}$$

where d_p is the diameter of the suspension particle, d_m is the diameter of the media grains, u_s is the Stokes' settling velocity of the suspension particles, u is the superficial velocity, ρ_p is the density of suspension particles, ρ_w is the density of water, g is the acceleration due to gravity, and μ is the water dynamic viscosity. The derivation was based on a mass balance, however did not account for the hydrodynamic interactions and van der Waals forces, (Tufenkji and Elimelech, 2004). The model hence underestimates the transport coefficient by ignoring those transport mechanisms; Logan *et al.* (1995) modelling simulation also confirms this deduction.

RT Model

The RT Model for predicting the transport coefficient was derived by Rajagopalan and Tien (1976) through regression analysis of numerical simulations data of particle trajectories under various filtration conditions, (Rajagopalan and Tien, 1976; Logan *et al.*, 1995; Tufenkji and Elimelech, 2004; Crittenden *et al.*, 2012):

$$\eta = A_S \left(\frac{4}{3} N_A \right)^{1/8} N_R^{15/8} + \left(3.38 \times 10^{-3}\right) A_S N_G^{1.2} N_R^{-0.4} + 4 A_S^{1/3} Pe^{-2/3} \qquad \textbf{Equation B-8}$$

where the dimensionless groups A_S and N_A are defined as:

$$A_S = \frac{2\left(1-p^5\right)}{2-3p+3p^5-2p^6} \quad \text{and} \quad N_A = \frac{H}{3\pi\mu d_p^2 u} \qquad \textbf{Equation B-9}$$

where $p = (1-\varepsilon)^{\frac{1}{3}}$ is a dimensionless porosity coefficient and H is the Hamaker constant. The RT Model analysed the trajectory path of suspended particles near a single collector (media grain); accounting for the interception and gravitational sedimentation in great detail, but adapted the diffusion term from the Yao Model, (Kau and Lawler, 1995). They however incorporated a correction factor, A_S to account for collisions generated by diffusion as proposed by Cookson (1970) to improve the diffusion term. Irrespective of the correction on the diffusion component, the RT Model still has the omission of the hydrodynamic and van de Waals interactions on small particles about a micron (Tufenkji and Elimelech, 2004). Modelling by Logan *et al.* (1995) and Tufenkji and Elimelech (2004) demonstration the RT Model to fit the experimental data for particles greater than 1μm and an overestimate for particles less than 1μm.

The RT Model as expressed in equation B-8 is a modification of the initial publication (Rajagopalan and Tien, 1976): by multiplication of the diffusion term by p^2 factor, in response to communication to the publisher by Rajagopalan et al (1982) in Logan *et al.* (1995); and a modification incorporating the porosity, ε (a variable) which was embedded in the numerals 0.72 and 0.0024 by assuming a value ε = 0.39 representative of porous beds in the original publication (Logan *et al.*, 1995).

TE Model

The TE Model was derived by Tufenkji and Elimelech (2004) using the same approach as in the RT Model but including the consideration of Brownian motion

in the trajectory analysis so producing a more complete depiction of the transport mechanisms. The TE Model was is expressed as (Tufenkji and Elimelech, 2004):

$$\eta = 0.55A_S N_A^{1/8} N_R^{1.675} + 0.22N_R^{-0.24} N_{vdW}^{0.053} + 2.4A_S^{1/3} N_R^{-0.081} N_{vdW}^{0.052} \qquad \textbf{Equation B-10}$$

where N_{vdW} is a dimensionless van der Waals number given by;

$$N_{vdW} = \frac{H}{kT} \qquad \textbf{Equation B-11}$$

The TE Model was found to be in good agreement with values simulated as a numerical result of the convective-diffusion equation over all the particle sizes, (Tufenkji and Elimelech, 2004).

References

Cookson Jr., J. T. (1970) ‘Removal of Submicron Particles in Packed Beds’, *Environmental Science & Technology*, 4(2), pp. 128–134.

Crittenden, J. C., Trussell, R. R., Hand, D. W., Howe, K. J. and Tchobanoglous, G. (2012) *Water Treatment principle and design*, *MWH’s Water Treatment: Principles and Design, 3rd edn* Chichester: John Wiley & Sons Inc.

Elimelech, M. and O’Melia, C. (1990) ‘Effect of particle size on collision efficiency in the deposition of Brownian particles with electrostatic energy barriers’, *Langmuir*, (10), pp. 1153–1163.

Iwasaki, T. (1937) ‘Some Notes on Sand Filtration’, *Water Works Association*, pp. 1591–1602.

Jackson, G. E. (1980) ‘Granular media filtration in water and wastewater treatment, Part 1’, *CRC Critical Reviews in Environmental Control*, 11(1), p. 339.

Kau, S. M. and Lawler, D. F. (1995) ‘Dynamics of Deep-Bed Filtration : Velocity , Depth , and Media’, *Journal of Environmental Engineering*, 121(1978), pp. 850–859.

Lawler, D. F. and Nason, J. a. (2006) ‘Granular media filtration: Old process, new thoughts’, *Water Science and Technology*, 53(7), pp. 1–7.

Logan, B. E., Jewett, D. G., Arnold, R. G., Bouwer, E. J. and Omelia, C. R. (1995) ‘Clarification of Clean-Bed Filtration Models’, *Journal of Environmental Engineering*, 121(12), pp. 869–873.

O’Melia, C. R. and Shin, J. Y. (2001) ‘Removal of particles using dual media filtration: modeling and experimental studies’, *Water Science and Technology: Water Supply*, 1.4, pp. 73–79.

Rajagopalan, R. and Tien, C. (1976) ‘Trajectory analysis of deep-bed filtration with the sphere-in-cell porous media model’, *AIChE Journal*, 22(3), pp. 523–533.

Stevenson, D. G. (1997) ‘Flow and filtration through granular media—the effect of grain and particle size dispersion’, *Water Research*, 31(2), pp. 310–322.

Tufenkji, N. and Elimelech, M. (2004) ‘Correlation Equation for Predicting Single-Collector Efficiency in Physicochemical Filtration in Saturated Porous Media’, *Environmental Science and Technology*, 38(2), pp. 529–536.

Yao, K., Habibian, M. T. and O’Melia, C. R. (1971) ‘Water and Waste Water Filtration: Concepts and Applications’, *Environmental Science & Technology*, 5(11), pp. 1105–1112.

Zamani, A. and Maini, B. (2009) ‘Flow of dispersed particles through porous media - Deep bed filtration’, *Journal of Petroleum Science and Engineering*, 69(1–2), pp. 71–88.

Appendix C : Filter coefficients determination

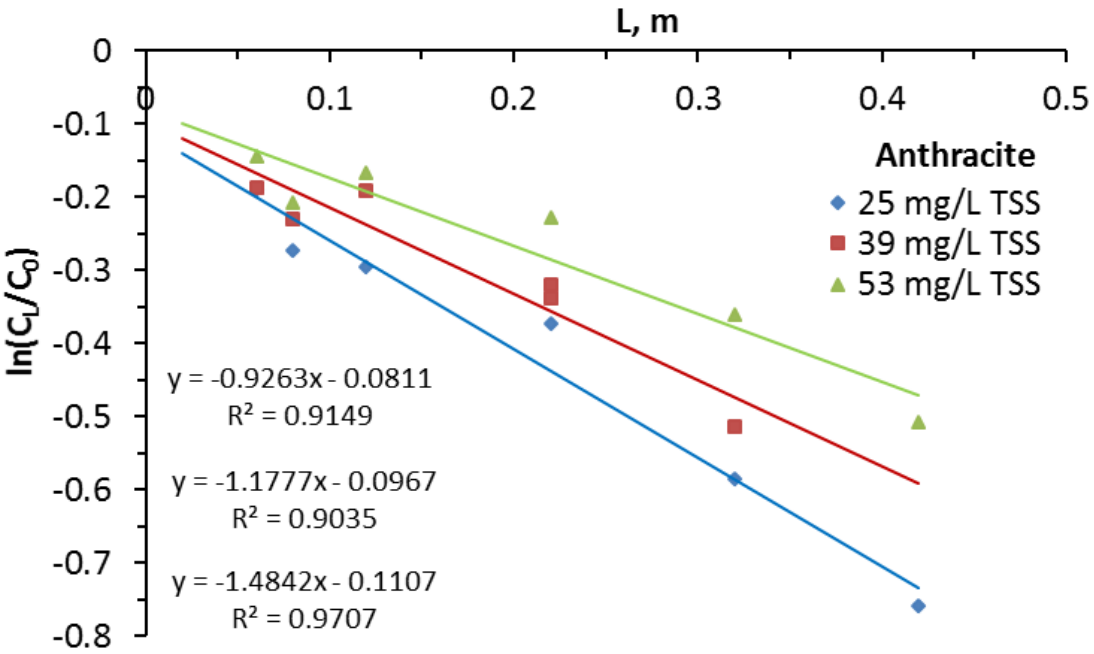

Figure C-1 The plots used to calculate the anthracite filter coefficients at different influent TSS concentrations. The plots are based on Equation 4-1.

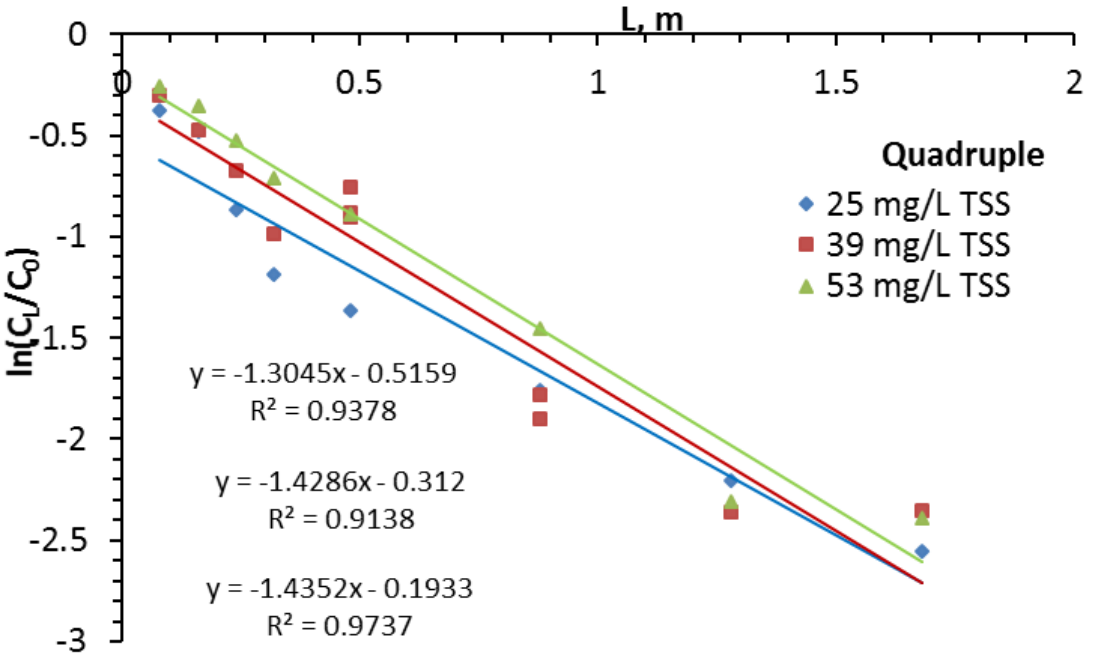

Figure C-2 The plots used to calculate the quadruple filter coefficients at different influent TSS concentrations. The plots are based on Equation 4-1.

Table C-1 Table of filter coefficients determined from the graphs in Figure C-1 and Figure C-2.

	Anthracite		Quadruple	
C_0, mgL^{-1}	Gradient	λ, m^{-1}	Gradient	λ, m^{-1}
25	-1.48	1.48	-1.30	1.30
39	-1.18	1.18	-1.43	1.43
53	-0.93	0.93	-1.44	1.44

Appendix D : Filter Equipment

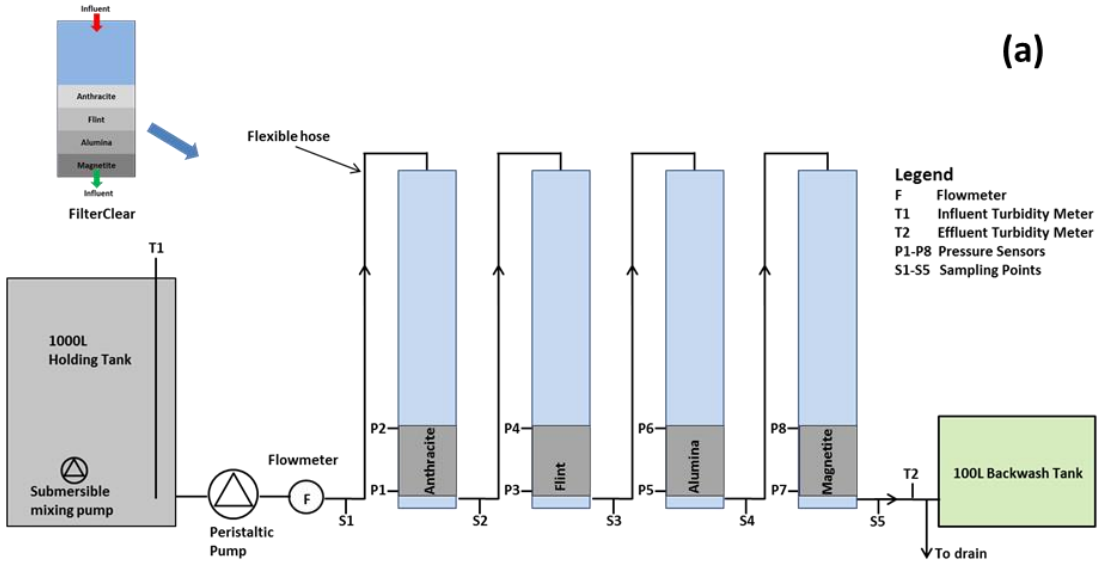

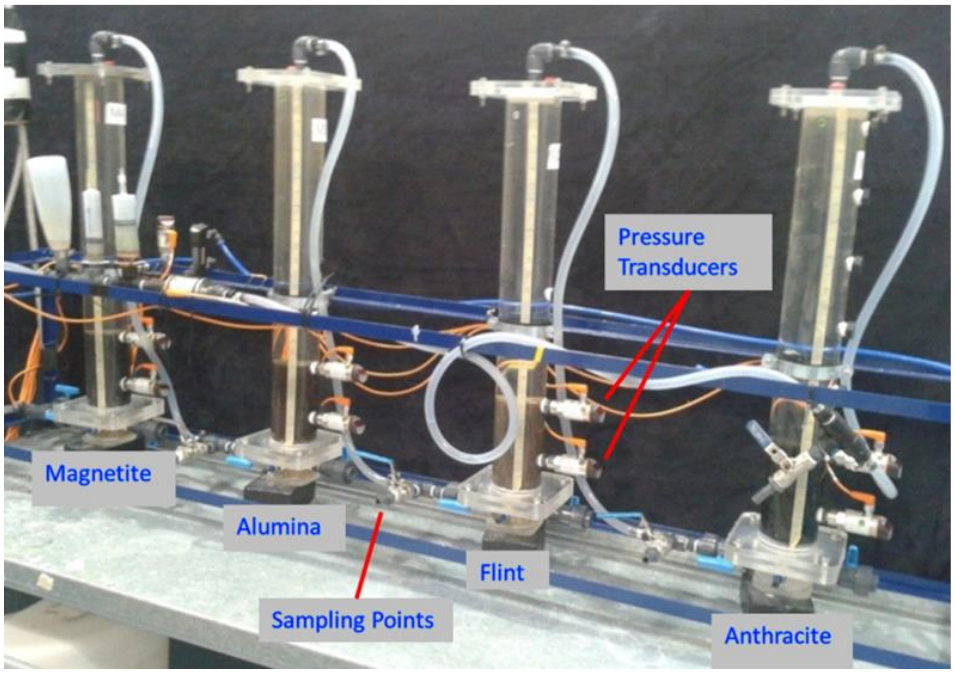

Figure D-1 (a) Schematic and (b) photograph of the pilot filter rig.

Appendix E : Wastewater Jar Tester Flocculation

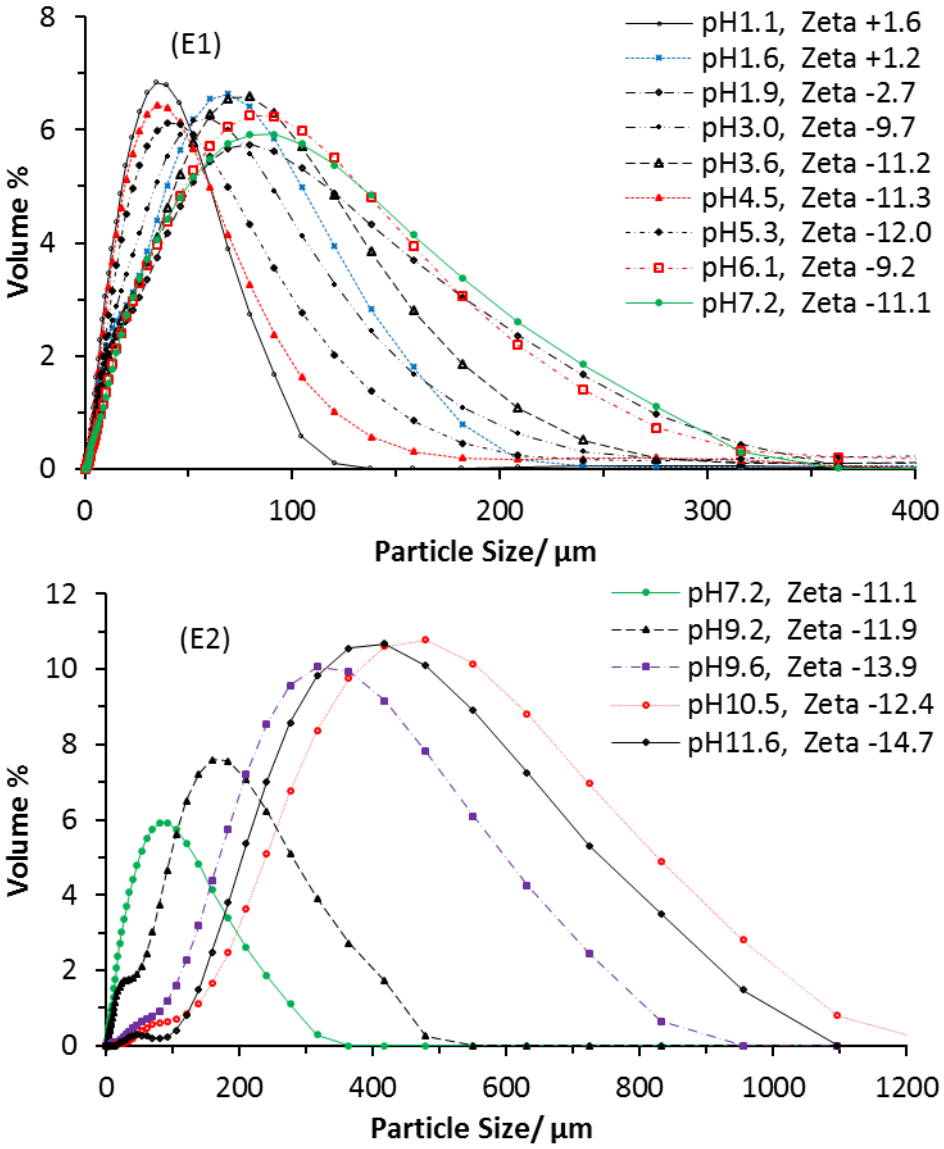

Figure E: Particle size distribution when wastewater is flocculated at different pH in a jar tester.